

Quantum Resolution of Cosmological Singularities using AdS/CFT

Ben Craps,^{1,2} Thomas Hertog^{2,3} and Neil Turok⁴

¹ *Theoretische Natuurkunde, Vrije Universiteit Brussel,
Pleinlaan 2, B-1050 Brussels, Belgium*

² *International Solvay Institutes, Boulevard du Triomphe,
ULB-C.P.231, B-1050 Brussels, Belgium*

³ *APC, Université Paris 7, 10 rue A.Domon et L.Duquet, 75205 Paris, France*

⁴ *DAMTP, CMS, Wilberforce Road, Cambridge, CB3 0WA, UK and
African Institute for Mathematical Sciences, 6-8 Melrose Rd, Muizenberg 7945, RSA*

Ben.Craps@vub.ac.be, Thomas.Hertog@apc.univ-paris7.fr, N.G.Turok@damtp.cam.ac.uk

ABSTRACT

The AdS/CFT correspondence is used to describe five-dimensional cosmology with a big crunch singularity in terms of $\mathcal{N} = 4$ supersymmetric $SU(N)$ gauge theory on $\mathbb{R} \times S^3$ deformed by an unstable potential. In this boundary field theory, a one-loop computation shows that the coupling governing the instability is asymptotically free, so that quantum corrections cannot turn the potential around. The big crunch singularity in the bulk corresponds in the boundary theory to a scalar field rolling to infinity in finite time. We generalize the method of self-adjoint extensions to define consistent unitary quantum evolution in the boundary theory. The quantum mechanical spread of the wave function for the homogeneous mode on the sphere suppresses the creation of high energy particles as the scalar field rolls down the potential and bounces back. This leads to the prediction that a quantum transition from the big crunch to a big bang is the most probable outcome of cosmological evolution, for a specific parameter range. Intriguingly, the instability and approximate scale-invariance of the boundary theory lead to the generation of an approximately scale-invariant spectrum of stress-energy perturbations on the boundary, whose amplitude is suppressed by the asymptotically free coupling. We comment on qualitative differences with holographic descriptions of large black holes, on four-dimensional generalizations and on implications for cosmological perturbations.

Contents

1	Introduction and Summary	2
2	Anti-de Sitter Cosmology	7
2.1	Setup	7
2.2	Boundary Conditions	9
2.3	AdS Cosmologies	10
2.4	Ten-dimensional Viewpoint	12
3	The Boundary Theory: a Double Trace Deformation of $\mathcal{N} = 4$ Super-Yang-Mills Theory	14
4	Unbounded Potentials, Self-Adjoint Extensions and Ultra-Locality	18
4.1	Quantum Mechanics in a $-\lambda x^p/4$ Potential for $p > 2$	18
4.2	Ultralocality and Self-Adjoint Extensions in Quantum Field Theory	21
5	Quantum Evolution of the Homogeneous Component	25
5.1	Complex Classical Solutions and Quantum Mechanics	26
5.2	The Self-Adjoint Extension via Complex Classical Solutions	31
5.3	Dealing with Branch Cuts in $V(x)$ at Complex x	33
5.4	Resolving the Branch Points arising from Renormalization	35
5.5	Complex Solutions for ϕ with a Fixed Coupling	38
5.6	Behavior of the Wavefunction at Large $\bar{\phi}$ and Small t	41
5.7	Complex Solutions for ϕ with a Running Coupling	43
6	Quantum Evolution of the Inhomogeneous Modes	45
6.1	Particle Production Using Complex Classical Solutions	46
6.2	Equations of Motion for Inhomogeneous Fluctuations	48
6.3	Production of $\delta\phi$ Excitations with a Running Coupling	51
6.4	Production of Light Higgs Particles	55
6.5	Production of Massless Gauge Bosons	57
6.6	Backreaction	58
7	Stress-Energy Correlators	59
8	Conclusions	63
A	More on the Bulk Theory	65
B	Renormalization of the Boundary Theory	70
C	The Renormalized Effective Potential $V(\phi)$ in the Complex ϕ-plane	79
D	Complex Classical Solutions in the Infinite Cutoff Limit	81

1 Introduction and Summary

Any theoretical framework for cosmology must ultimately include a resolution of the cosmic singularity, most likely involving quantum gravitational effects. In the absence of such a resolution, many predictions of cosmological models can be traced to a set of *ad hoc* initial conditions that remain unexplained. Central questions include whether the big bang represents a true beginning of time and, if not, what happens to the thermodynamic arrow of time near the big bang. The no-boundary proposal [1] predicts the arrow of time reverses, but an alternative and perhaps simpler possibility is that the physics responsible for resolving the singularity may in fact provide a consistent rule for dynamical evolution across it [2–4]. Whichever of these options is correct has profound implications for cosmology. If the singularity was the beginning, the horizon and flatness problems, and the problem of the origin of the long wavelength density variations, seem to demand an early epoch of cosmological inflation [5]. Whereas if the singularity was not the beginning of time and there was a preceding epoch of slow cosmological contraction before it, non-inflationary solutions of these problems are possible [3, 6, 7]. Furthermore, in a universe where repeated cycles of evolution occur, technically natural mechanisms for slow relaxation of the dark energy density (or cosmological constant) to tiny values become viable [8].

Perturbative string theory breaks down in the simplest models with cosmological singularities, namely time-dependent orbifolds, where large gravitational backreaction leads to divergences in perturbative string scattering amplitudes [9]. Attempts to avoid this conclusion in these and closely related models [10] have so far not led to a reliable description of what happens at cosmological singularities. In M-theory, the proposed setting for the ekpyrotic model [3], the lightest modes are represented by winding M2-branes [11, 12]. Near the singularity, the effective string coupling (in IIA or heterotic frame) vanishes, and the classical string dynamics suggests that the α' expansion should be replaced by an expansion in $1/\alpha'$. But again, fully quantum mechanical calculations have not yet been possible in this regime.

It appears, therefore, that a description of the quantum dynamics near spacelike singularities requires a non-perturbative formulation of string theory, involving a *dual description* in terms of more fundamental variables. Models with two spacetime dimensions have been described using $c = 1$ matrix models [13]. Higher-dimensional models with light-like singularities have been studied in the framework of matrix theory [14], which has led to the suggestion that spacetime may be replaced by non-commuting matrices near a singularity [15]. The quantitative study of the dynamics of this regime is still work in progress, however.

In the present paper, we shall instead work in the framework of the AdS/CFT correspondence [16], which has emerged as an extremely powerful tool for understanding quantum gravity and which provides a non-perturbative definition of string theory in asymptotically anti-de Sitter (AdS) spacetimes in terms of conformal field theories (CFT) on their conformal boundaries. By relaxing the boundary conditions on some of the negative mass squared scalars (satisfying the Breitenlohner-Freedman bound) in supergravity, one can extend the AdS/CFT correspondence to include solutions where smooth, asymptotically

AdS initial data evolve to a big crunch singularity in the future [17, 18]. In this context, a big crunch singularity is simply any spacelike singularity that extends to infinity and reaches the boundary in finite time. As we shall discuss, the dual description of these “AdS cosmologies” involves field theories with potentials that are unbounded below. The cosmological singularity in the bulk corresponds to what appears to be a singularity in the boundary theory, where a scalar field rolls to infinity in finite time. In fact, there is strong evidence¹ that the existence of supergravity solutions with big crunch singularities *requires* boundary conditions that correspond to unstable dual field theories with steep potentials that are unbounded below. The AdS/CFT duality, therefore, relates the problem of cosmological singularities to the problem of understanding the dynamics of (non-gravitational!) field theories of this type.

In earlier work, the dual CFT description has also been used to study the singularity inside black holes, which is analogous to a cosmological singularity [19]. Although some progress in this direction has been made, the fact that the singularity is hidden behind an event horizon clearly complicates the problem. This is because the CFT evolution is dual to bulk evolution in Schwarzschild time, so that the CFT never directly “sees” the singularity. This should be contrasted with the model discussed in the present paper, in which the bulk singularity reaches the boundary in finite time and is thus directly visible in the boundary theory. Other AdS/CFT models of cosmological singularities include [20].

In this paper, we study a class of five-dimensional cosmologies for which the dual field theory is a deformation of $\mathcal{N} = 4$ Super-Yang-Mills (SYM) theory on $\mathbb{R} \times S^3$ by an unbounded double trace potential $-f\mathcal{O}^2/2$, with \mathcal{O} a trace operator quadratic in the adjoint Higgs scalars. The dual field theory has several key properties that allow us to analyze its dynamics quantitatively:

1. The principal advantage of this five-dimensional setup, compared with similar four-dimensional cosmologies studied previously, is that the undeformed dual boundary theory is well-understood. Furthermore, a one-loop computation shows that, because of the “wrong” sign of the deformation, the coupling f that governs the instability is asymptotically free [21], allowing perturbative field theory computations in the regime near the singularity, *i.e.*, for large \mathcal{O} , at least at small ’t Hooft coupling. In particular, we can show that quantum corrections do not turn the potential around, so that it is really unbounded below.
2. As the dual theory evolves towards the singularity, the field evolution becomes *ultralocal* on any fixed length scale, meaning that spatial gradients become unimportant. This means that one effectively has an infinite set of decoupled quantum mechanical systems, one at each spatial point, in the regime near the singularity.
3. Since the conformal boundary has finite spatial volume, the unstable, homogeneous background mode, evolves quantum mechanically. The quantum mechanical spread of its wave function will turn out to be crucial for the suppression of particle creation

¹This is closely related to cosmic censorship in the bulk [17].

as the homogeneous mode rolls down the potential, bounces back from infinity, and rolls back up towards its starting value.

4. As the singularity is approached, the semiclassical approximation becomes increasingly accurate, both for the homogeneous background and for the fluctuations.

The resulting picture is that even an initially localized wave packet spreads to infinite scalar field values with some probability, in an arbitrarily short time. Unless suitable boundary conditions are imposed, probability will be lost. Therefore, to study quantum evolution in this theory at all, one must impose boundary conditions at large \mathcal{O} that restrict the Hilbert space to the subspace on which the Hamiltonian is self-adjoint. In quantum mechanics, this prescription is known as a “self-adjoint extension” of the theory. Because the dual evolution is ultralocal for large \mathcal{O} , we can extend this construction to the boundary field theory by imposing the same self-adjoint extension at each point independently. The semiclassical approximation, which is excellent near the singularity, allows us to implement the self-adjoint extension using classical solutions and the method of images. The relevant classical solutions are generically complex near the singularity as a consequence of the quantum spread in the homogeneous mode. To leading order, therefore, the inhomogeneous modes evolve in a complex classical homogeneous background. The complexity of the background turns out to be essential to the resolution of the singularity, providing an ultraviolet cutoff on quantum particle creation when the wave packet rolls down the potential and bounces back. We shall find that, for a certain range of parameters, backreaction of created particles on the homogeneous mode is negligible for most values of the Schrödinger wavefunction’s argument carrying significant probability.

The resulting construction specifies a consistent rule for unitary quantum evolution in the boundary theory in the presence of bulk cosmological singularities. Evolving the wave packet forward in time, the most probable outcome is that at late times, the homogeneous background nearly returns to its original starting point, with a finite density of particles and an interesting spectrum of spatially inhomogeneous density variations. The quantum evolution in the boundary theory, therefore, predicts a *quantum* transition from a big crunch to a big bang in the bulk as the most probable outcome of cosmological evolution, for a certain range of parameters.

If the ’t Hooft coupling in the boundary SYM theory is small, we have good control over the field theory. However, for small ’t Hooft coupling, the bulk is in a stringy regime. We shall see that the form of the quantum effective potential is still valid at large ’t Hooft coupling, so at least the crucial dynamical feature of unbounded potentials is shared by both regimes. Further analysis is required, though, to fully treat the regime where the bulk is well-described by supergravity.

At first sight our findings seem to indicate that the quantum dynamics of cosmological singularities is rather different from the thermalization process that describes the formation of large AdS black holes in the dual theory. To compare the two situations, we show the Penrose diagram of gravitational collapse to a large black hole in anti-de Sitter space in Figure 1. This is identical to the Penrose diagram of an anti-de Sitter cosmology. Therefore from this point of view, there appears to be little distinction in the classical bulk

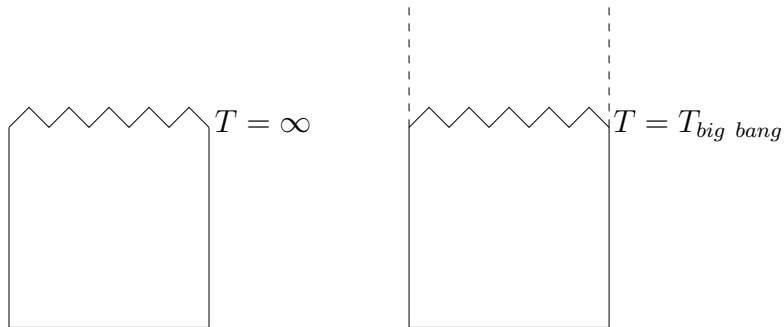


Figure 1: The Penrose diagram of a large black hole in anti-de Sitter space is identical to that of an anti-de Sitter cosmology. In a black hole spacetime, however, time at infinity continues forever whereas in an AdS cosmology the singularity hits the boundary in finite time.

theory between singularities inside black holes and cosmological singularities extending to the boundary in finite time. However the dual (quantum) description of both types of singularities appears to be qualitatively different: as we discussed above, AdS cosmologies are described in terms of unstable conformal field theories with steep potentials \mathcal{V} that are unbounded below (Figure 2, left), whereas black holes are interpreted as thermal states requiring a vacuum state in the dual theory (Figure 2, right).

If one “regularizes” the unbounded potential in Figure 2 (left), for example by adding higher order terms to obtain a potential like the one shown in Figure 2 (right), one finds this changes the evolution in the bulk near the big crunch, in the upper corners of the Penrose diagram. This is because the regularization affects the bulk boundary conditions. In particular one finds this causes the cosmological singularity to turn into a large (stable) black hole with scalar hair [18], where the bulk scalar field turned on is dual to the operator \mathcal{O} in the boundary theory. This is a new type of black hole which does not exist (in a stable form) for the original bulk boundary conditions. It has a natural interpretation in the dual theory as an oscillatory excitation about the global negative minimum of \mathcal{V} [18] (whereas the usual Schwarzschild-AdS black holes correspond to thermal states around the standard vacuum at $\langle \mathcal{O} \rangle = 0$). This new black hole with scalar hair is the natural end state of evolution in the bulk corresponding to a wave packet rolling down a regularized potential.

Considering a series of dual theories where the global minimum is taken to be more and more negative, one finds that the horizon size of the black holes with scalar hair – keeping the mass constant – increases. In the limit where the global minimum goes to minus infinity the hairy black holes become infinitely large and we recover the original cosmological solutions. While for the black hole case (with bounded potentials) it is plausible that the system will eventually thermalize, it is unclear what the very late time behaviour is in the cosmological case (with unbounded potentials). But the two cases may be similar for intermediate times. Indeed one expects that even for boundary conditions corresponding to steep but

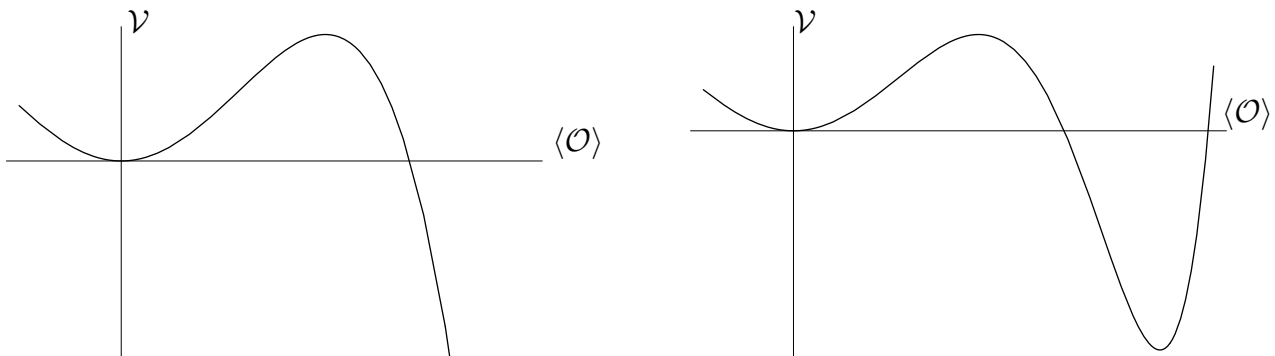


Figure 2: The dual description of AdS cosmologies involves a wave packet rolling down an unstable direction of the field theory potential (left). At first sight this is qualitatively different from the formation of large black holes in AdS, which is described as a thermalization process in a dual theory that has a ground state (right). We argue however that for cosmology the dynamics at intermediate times is relevant, and that this may well be qualitatively similar in both theories, at least for potentials that are sufficiently steep around the global minimum.

bounded potentials a wave packet rolling down the potential will bounce back a number of times before the system thermalizes and settles down. These bounces could presumably be interpreted as “regularized” versions of the big crunch/big bang transitions we will study.

We emphasize, however, that although the dual description in terms of a bounded \mathcal{V} describing the formation of hairy black holes may share some qualitative features with the cosmologies at intermediate times, it does not provide us with a precise and consistent model of singularities. This is because the higher order terms needed to regularize the potential generally lead to a non-renormalizable boundary theory. In contrast, in this paper we focus on a class of five-dimensional cosmologies for which the dual field theory is a renormalizable deformation of $\mathcal{N} = 4$ SYM on $\mathbb{R} \times S^3$ by an unbounded double trace potential $-f\mathcal{O}^2/2$. As we have explained, in this model we are able to develop a consistent and precise description of at least some quantities of interest, described by unitary quantum evolution in the boundary theory in the presence of bulk cosmological singularities.

Although the prime focus of this work is on understanding whether passage across a cosmological singularity is possible, there is another, perhaps even more remarkable consequence of the AdS/CFT dual description of cosmology. Since the boundary theory is unstable, a spectrum of fluctuations is generated by the ekpyrotic mechanism [22]; as the scalar rolls down the potential, the inhomogeneous modes acquire a tachyonic mass squared that becomes increasingly negative in time, causing modes of successively higher momentum to cease oscillating and enter a “growing mode” solution instead. After the big crunch/big bang transition this results in a spectrum of spatially dependent modes which are excited states about the final adiabatic vacuum. But the boundary theory is classically scale-invariant. The quantum theory breaks this symmetry, but only slightly as the coupling f is asymptotically free. As a direct consequence of the approximate scale-invariance of the dual field theory, the stress-energy fluctuations turn out to be approximately scale-invariant.

Furthermore, their amplitude is suppressed by positive powers of f . While we still have to translate these boundary fluctuations into the bulk, it is intriguing that the AdS/CFT duality seems to automatically yield a physical mechanism for producing scale-invariant cosmological perturbations.

The outline of this paper is as follows. In Section 2, we introduce the bulk cosmologies of interest. We review how modifications of the standard AdS boundary conditions allow smooth initial data to evolve into a big crunch singularity, and focus on a specific example for which the dual field theory analysis will be tractable. We also show that the bulk cosmological solution to IIB supergravity is, after a duality taking us to type IIA frame, qualitatively similar to that describing compactified Milne (or colliding orbifold planes) in M-theory. In Section 3, we discuss the dual field theory, an unstable double trace deformation of $\mathcal{N} = 4$ SYM theory, deriving the effective potential both at weak and strong 't Hooft coupling. Section 4 discusses self-adjoint extensions in quantum mechanics, as well as the ultralocality that will allow us to extend this idea to quantum field theory. In Section 5, we discuss the quantum evolution of the homogeneous background, which exhibits a quantum spread because the field theory lives on a finite volume space. We develop a method for implementing self-adjoint extensions in the semiclassical expansion, using complex classical solutions and the method of images. We also explain how this method extends to potentials with branch points, such as the quantum effective potential of interest in this paper. Section 6 focuses on the inhomogeneous modes, in particular on the question whether abundant particle creation may prevent the scalar field from running back up the potential after the bounce. We find that for most of the range of the Schrödinger wavefunction's argument ϕ_f carrying significant probability, the quantum spread of the homogeneous background provides an ultraviolet cutoff on the wavelength of produced particles; provided the spread is sufficiently large, backreaction on the homogeneous mode is suppressed. In Section 7, we calculate the two-point correlator of stress-energy fluctuations in the boundary theory, which in principle determines the spectrum of classical metric perturbations in the bulk. Appendix A contains more details on the bulk theory. In Appendices B and C, we discuss a number of technical details related to the field theory effective potential. Appendix D contains details on complex classical solutions with and without a cutoff in the field theory.

A brief and less technical overview of this work can be found in [23]; a preliminary report was presented in [24].

2 Anti-de Sitter Cosmology

2.1 Setup

Our starting point is $\mathcal{N} = 8$ gauged supergravity in five dimensions [25–27], which is thought to be a consistent truncation of ten-dimensional type IIB supergravity on S^5 . The spectrum of this compactification involves 42 scalars parameterizing the coset $E_{6(6)}/USp(8)$. We concentrate on the subset of scalars that parameterizes the coset $SL(6, R)/SO(6)$. From the higher-dimensional viewpoint, these arise from different quadrupole distortions of S^5 .

The relevant part of the action involves five scalars α_i and takes the form [28]

$$S = \int \sqrt{-g} \left[\frac{1}{2}R - \sum_{i=1}^5 \frac{1}{2}(\nabla\alpha_i)^2 - R_{AdS}^{-2}V(\alpha_i) \right], \quad (2.1)$$

where we have chosen units in which the coefficient of the Ricci scalar is $\frac{1}{2}$, *i.e.*, the 5d Planck mass is unity. The potential for the scalars α_i is given in terms of a superpotential $\mathcal{W}(\alpha_i)$ via

$$V = \frac{1}{R_{AdS}^2} \sum_{i=1}^5 \left(\frac{\partial\mathcal{W}}{\partial\alpha_i} \right)^2 - \frac{4}{3R_{AdS}^2}\mathcal{W}^2. \quad (2.2)$$

\mathcal{W} is most simply expressed as

$$\mathcal{W} = -\frac{1}{2\sqrt{2}} \sum_{i=1}^6 e^{2\beta_i}, \quad (2.3)$$

where the β_i sum to zero, and are related to the five α_i 's with standard kinetic terms as follows [28],

$$\begin{pmatrix} \beta_1 \\ \beta_2 \\ \beta_3 \\ \beta_4 \\ \beta_5 \\ \beta_6 \end{pmatrix} = \begin{pmatrix} 1/2 & 1/2 & 1/2 & 0 & 1/2\sqrt{3} \\ 1/2 & -1/2 & -1/2 & 0 & 1/2\sqrt{3} \\ -1/2 & -1/2 & 1/2 & 0 & 1/2\sqrt{3} \\ -1/2 & 1/2 & -1/2 & 0 & 1/2\sqrt{3} \\ 0 & 0 & 0 & 1/\sqrt{2} & -1/\sqrt{3} \\ 0 & 0 & 0 & -1/\sqrt{2} & -1/\sqrt{3} \end{pmatrix} \begin{pmatrix} \alpha_1 \\ \alpha_2 \\ \alpha_3 \\ \alpha_4 \\ \alpha_5 \end{pmatrix}. \quad (2.4)$$

The potential reaches a negative local maximum when all the scalar fields α_i vanish. This is the maximally supersymmetric AdS state, corresponding to the unperturbed S^5 in the type IIB theory. At linear order around the AdS solution, the five scalars each obey the free wave equation with a mass that saturates the Breitenlohner-Freedman (BF) bound $m_{BF}^2 = -(d-1)^2/4R_{AdS}^2$ [29] in five dimensions,

$$m^2 = -4/R_{AdS}^2. \quad (2.5)$$

Nonperturbatively, the fields couple to each other and it is generally not consistent to set only some of them to zero. However it is possible to truncate this theory further [26] to gravity coupled to a single $SO(5)$ -invariant scalar φ by setting² $\beta_i = \varphi/\sqrt{30}$ for $i = 1, \dots, 5$ and $\beta_5 = -5\varphi/\sqrt{30}$. The action (2.1) then reduces to

$$S = \int \sqrt{-g} \left[\frac{1}{2}R - \frac{1}{2}(\nabla\varphi)^2 + \frac{1}{4R_{AdS}^2} (15e^{2\gamma\varphi} + 10e^{-4\gamma\varphi} - e^{-10\gamma\varphi}) \right], \quad (2.6)$$

with $\gamma = \sqrt{2/15}$.

²There are several inequivalent ways in which this theory can be further truncated to a single scalar as only matter field [28]. An alternative option that was studied in [17, 18] is to take $\beta_i = \varphi/\sqrt{3}$ for $i = 1, \dots, 4$ and $\beta_4 = \beta_5 = -2\varphi/\sqrt{3}$, which corresponds to taking only $\alpha_5 \neq 0$. This choice preserves an $SO(4) \times SO(2)$ symmetry.

2.2 Boundary Conditions

We will work mainly in global coordinates in which the AdS_5 metric takes the form

$$ds_0^2 = R_{AdS}^2 \left(-(1+r^2)dt^2 + \frac{dr^2}{1+r^2} + r^2 d\Omega_3 \right). \quad (2.7)$$

In all asymptotically AdS solutions, the scalar φ decays at large radius as

$$\varphi(r) = \frac{\alpha \ln r}{r^2} + \frac{\beta}{r^2}, \quad (2.8)$$

where α and β generally depend on the other coordinates.

For the dynamics of the theory to be well-defined it is necessary to specify boundary conditions at $r = \infty$ on the fields. This amounts to specifying a relation between α and β in (2.8). For example, one can take $\alpha = 0$, leaving β totally unspecified. This is the usual boundary condition, which preserves the full AdS symmetry group and which has empty AdS as its stable ground state [30, 31]. Alternatively, one can adopt boundary conditions of the form

$$\alpha = -\frac{\delta W}{\delta \beta}, \quad (2.9)$$

where $W(\beta)$ is an essentially arbitrary real smooth function.³ Theories of this type have been called designer gravity theories [33], since their dynamical properties depend significantly on the choice of W . We will see that under the AdS/CFT duality, this function W appears as an additional potential term in the action of the dual field theory.

Boundary conditions of the form (2.9) generically break some of the asymptotic AdS symmetries, but they are invariant under global time translations. The conserved energy associated with this is well-defined and finite [34, 35], but its expression depends on the function W .

This can be seen as follows. When W is nonzero, the scalar field falls off more slowly than usual. This backreacts on the asymptotic behavior of the $g_{r\mu}$ metric components, which causes the usual gravitational surface term of the Hamiltonian to diverge. This divergence is exactly canceled, however, by an additional scalar contribution to the surface terms. The total charge can therefore be integrated (provided one has specified a functional relation between α and β). Hence one arrives at a finite expression for the conserved mass, which generally contains an explicit finite contribution from the scalar field which depends on W . Whether or not the energy admits a positive mass theorem,⁴ however, depends on the choice of the function W .

Below we will be interested in solutions with the following scalar field boundary conditions

$$\alpha_f = f\beta, \quad (2.10)$$

³In general, boundary conditions specified by an arbitrary function W can be imposed in anti-de Sitter gravity coupled to a tachyonic scalar with mass m^2 in the range $m_{BF}^2 \leq m^2 < m_{BF}^2 + R_{AdS}^{-2}$ (see e.g. [32]).

⁴See [36] for recent work on the stability of theories of this type.

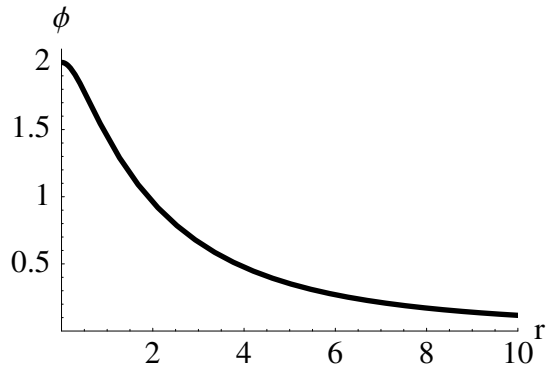


Figure 3: Regular initial data $\varphi(r)$ that evolve to a big crunch singularity for boundary conditions with $f = 0.1$.

where f is an arbitrary constant. The corresponding asymptotic form of the g_{rr} component of the metric is given by

$$g_{rr} = \frac{1}{r^2} - \frac{1}{r^4} - \frac{2f^2\beta^2}{3r^6}(\ln r)^2 - \frac{4f\beta^2}{3r^6} \ln r + \frac{f^2\beta^2}{3r^6} \ln r + O(1/r^6). \quad (2.11)$$

The conserved mass of spherically symmetric configurations with these boundary conditions reads

$$M = 2\pi^2 R_{AdS}^2 \left[\frac{3}{2} M_0 + \beta^2 \left(1 - \frac{1}{2} f \right) \right], \quad (2.12)$$

where M_0 is the coefficient of the $O(1/r^6)$ correction to the g_{rr} component of the metric.

2.3 AdS Cosmologies

We now construct a class of asymptotically AdS big bang/big crunch cosmologies that are solutions of (2.6) with boundary conditions (2.10) on the scalar field, with $f > 0$. This is a straightforward generalization of the four-dimensional cosmologies discussed in [17, 18].

A particularly simple example of an open FLRW cosmology can be found from the evolution of an initial scalar field profile $\varphi(r)$ obtained from an $O(5)$ -invariant Euclidean instanton⁵. Indeed, in Appendix A we show that all boundary conditions (2.10), for $f > 0$, admit precisely one such instanton solution.⁶ The slice through the instanton obtained by restricting to the equator of the four sphere defines time symmetric initial data for a Lorentzian solution with mass $M = -\pi^2 R_{AdS}^2 f^2 \beta^2 / 4$. The instanton, therefore, specifies *negative mass* initial data in this theory.⁷ In Figure 3 we show the initial scalar field profile obtained in this way for $f = 0.1$.

⁵See e.g. [17, 18, 37] for a discussion of similar four-dimensional cosmologies.

⁶Instantons also exist for negative f provided $f < -\mathcal{O}(1)$. However, as we explain below, we do not expect initial data obtained from slicing these instantons across the four sphere to evolve to a big crunch.

⁷As mentioned earlier, the mass of initial data obtained from instantons depends on the asymptotic behavior of the fields. For the AdS-invariant boundary conditions discussed in Appendix A (see eq. A.5)

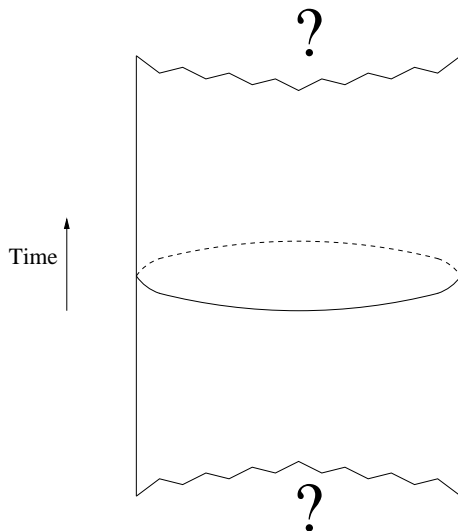


Figure 4: Anti-de Sitter cosmology. To predict what happens at the singularities one must turn to the dual field theory description.

Analytic continuation of the Euclidean geometry yields a Lorentzian solution that describes the evolution of these initial data under AdS-invariant boundary conditions [38]. The origin of the Euclidean instanton then becomes the lightcone emanating from the origin of the Lorentzian solution. Outside the lightcone, the scalar field is constant along four-dimensional de Sitter slices of AdS and the scalar remains bounded in this region. On the light cone we have $\varphi = \varphi(r = 0)$ and $\partial_t \varphi = 0$ (since $\varphi_{,r} = 0$ at the origin in the instanton). Inside the lightcone, the $SO(4, 1)$ symmetry ensures that the solution evolves like an open FLRW universe,

$$ds^2 = -dt^2 + a^2(t)d\sigma_4, \quad (2.13)$$

where $d\sigma_4$ is the metric on the four-dimensional unit hyperboloid. Under time evolution, φ rolls down the negative potential. This causes the scale factor $a(t)$ to vanish in finite time, producing a singularity that extends to the boundary of AdS in finite global time. A coordinate transformation in the asymptotic region outside the light cone between the usual static coordinates (2.7) for AdS_5 and the $SO(4, 1)$ invariant coordinates (see Appendix A) shows that $\beta \sim \beta(t = 0)/(\cos t)^2$. Hence β is now time dependent and blows up as $t \rightarrow \pi/2$, when the singularity hits the boundary.

The boundary conditions (2.10) of interest here break conformal invariance weakly when the logarithm is large, and one cannot obtain the Lorentzian solution by analytic continuation from an $O(5)$ -invariant instanton. Instead one must evolve the initial data numerically. However, when the logarithm is large, our boundary conditions are nearly AdS-invariant except when α becomes large, and causality then restricts its effect. In particular, since

one finds the instanton initial data have exactly zero mass, in line with their interpretation as the solution AdS_5 decays into [17].

the evolution of the instanton data for AdS-invariant boundary conditions has trapped surfaces, a singularity will still form in the central region and the effect of the modification of the boundary conditions on the evolution will only be appreciable in the corners of the conformal diagram where the singularity hits the boundary at infinity. Hence it is reasonable to expect that a singularity must form under evolution with α_f boundary conditions when f is small. This restricts us to positive f since for negative f we find instantons only for $f < -\mathcal{O}(1)$. It would now appear possible, however, for the singularity to be enclosed inside a large black hole instead of extending out to infinity. Since the instanton initial data have slightly negative mass, $MR_{AdS}^{-2} \sim -\mathcal{O}(1)$, these black holes must necessarily have scalar hair. In Appendix A we numerically integrate the field equations to verify whether α_f boundary conditions admit static, spherically symmetric black hole solutions with scalar hair outside the horizon. We find a one-parameter set of spherical hairy black holes, which can be characterized by their conserved mass. However, it turns out that for $f > 0$ the hairy black holes are always more massive than a vacuum Schwarzschild-AdS black hole of the same size. Hence the singularity that develops from the spherical negative mass initial data defined by the instanton cannot be hidden behind an event horizon. It is therefore plausible that it extends all the way to the boundary, cutting off all space.

2.4 Ten-dimensional Viewpoint

$D = 5$, $\mathcal{N} = 8$ supergravity is believed to be a consistent truncation of ten-dimensional IIB supergravity on S^5 . This means that it should be possible to lift our five-dimensional solution to ten dimensions. At the linearized level, the fields which saturate the BF bound correspond to $\ell = 2$ modes on S^5 . Since the field diverges at the classical singularity, one expects that the sphere will become highly squashed.

Even though it is not known how to lift a general solution of $D = 5$, $\mathcal{N} = 8$ supergravity to ten dimensions, this is known for solutions that only involve the metric and scalars that saturate the BF bound [39]. So we can immediately write down the ten-dimensional analog of our cosmologies. The ten-dimensional solution involves only the metric and the self-dual five-form. To describe them, we first introduce coordinates on S^5 so that the metric on the unit sphere takes the form ($0 \leq \xi \leq \pi$)

$$d\Omega_5 = d\xi^2 + \sin^2 \xi d\Omega_4. \quad (2.14)$$

Letting $f = e^{\gamma\varphi}$ and $\Delta^2 = f \sin^2 \xi + f^{-5} \cos^2 \xi$, the full ten-dimensional metric is

$$ds_{10}^2 = \Delta ds_5^2 + f^4 \Delta d\xi^2 + (f\Delta)^{-1} \sin^2 \xi d\Omega_4, \quad (2.15)$$

which preserves an $SO(5)$ symmetry of the five-sphere, as expected. The five-form is given by

$$G_5 = -U\epsilon_5 + 10 \sin \xi \cos \xi f^{-1} * df \wedge d\xi, \quad (2.16)$$

where ϵ_5 and $*$ are the volume-form and dual in the five-dimensional solution and

$$U = -3f^2 \sin^2 \xi + f^{-10} \cos^2 \xi - f^{-4} - 4f^{-4} \cos^2 \xi. \quad (2.17)$$

In the homogeneous region of the asymptotic AdS_5 space, the metric can be written in Robertson-Walker form (2.13). Near the singularity both the potential and the curvature are unimportant in the Friedmann-Lemaître equations, and we have $a(t) \propto (t_s - t)^{1/4}$ and $\varphi(t) = -(\sqrt{3}/2) \ln(t_s - t)$. Therefore, over most of the S^5 near the singularity, the metric approaches

$$ds_{10}^2 = \sin \xi [-(t_s - t)^{-1/2\sqrt{10}} dt^2 + (t_s - t)^{1/2-1/2\sqrt{10}} d\sigma_4^2 + (t_s - t)^{-9/2\sqrt{10}} d\xi^2 + (t_s - t)^{3/2\sqrt{10}} d\Omega_4]. \quad (2.18)$$

Introducing a new time coordinate $T = (t_s - t)^{\mu/4\sqrt{10}}$, where $\mu = 4\sqrt{10} - 1$, this takes a simple Kasner-like form

$$ds_{10}^2 = \sin \xi \left[- \left(\frac{\mu + 1}{\mu} \right)^2 dT^2 + T^{(2\sqrt{10}-2)/\mu} d\sigma_4^2 + T^{-18/\mu} d\xi^2 + T^{6/\mu} d\Omega_4 \right]. \quad (2.19)$$

The anti de Sitter space and four of the dimensions of the S^5 shrink to zero, with Kasner exponents of approximately 0.19 and 0.26 respectively, while the fifth dimension of the S^5 , labelled by ξ , blows up with a Kasner exponent of ≈ -0.77 so the S^5 becomes spindle-shaped. Following the analysis of [40], we can T-dualize the ξ dimension to obtain a homogeneous spacetime solution of type IIA string theory. The duality-invariant dilaton is $2\phi - \sum_i \lambda_i$, where the scale factor of the i 'th spatial dimension is $a_i = e^{\lambda_i}$. Under T-duality, $\lambda_\xi \rightarrow -\lambda_\xi$ and the string-frame Kasner exponent for the ξ dimension becomes $+0.77$. The dilaton was static in the original IIB frame, but in the T-dual theory we have $e^\phi \sim T^{0.77}$ so the string coupling tends to zero at the singularity. The new metric is more isotropic than the original metric, and qualitatively similar to the isotropic cosmological solution to the low energy effective action for string theory in string frame, with $a_i \propto T^{\frac{1}{3}}$ for $i = 1, \dots, 9$, and $e^\phi \propto T$. This background solution in type IIA theory corresponds to the solution to 11-dimensional M-theory in which the M-theory dimension and time form compactified Milne spacetime, with the other dimensions are static [4, 12]. It will be very interesting to see whether we can find an unstable mode within the generalized $AdS^5 \times S^5$ setup which, near the singularity, corresponds precisely to the collapse of the M-theory dimension and which could, once the appropriate boundary deformation is identified, be used to model an end-of-the-world brane collision in 11 dimensions, in the heterotic model.

More generally, it is clear that the cosmological solution we focus on here is only one of many possible cosmologies allowed by generalized boundary conditions on $AdS^5 \times S^5$. The AdS/CFT correspondence can thus be used as a ‘‘laboratory’’ for the study of the nonperturbative counterparts (in both α' and g_s) of a large class of cosmological solutions to the low-energy effective actions for string theories. Every nontrivial solution possesses a spacelike singularity but, by mapping the theories in each case into an unstable dual quantum field theory, it may be possible to resolve many of these singularities and to describe the passage of model universes through them.

3 The Boundary Theory: a Double Trace Deformation of $\mathcal{N} = 4$ Super-Yang-Mills Theory

In the previous section, we have seen that our bulk theory with boundary conditions (2.10) allows smooth, asymptotically AdS initial data to evolve in finite time into a big crunch singularity that extends all the way to the boundary. Now we discuss the dual CFT counterpart of this phenomenon. First, we review that the boundary conditions (2.10) with $f > 0$ correspond to adding an unstable potential to the boundary field theory. Then we argue that, in this particular model, the quantum effective potential shares the property of being unbounded below.

For the usual $\alpha = 0$ boundary conditions on the bulk scalars, the dual field theory is $\mathcal{N} = 4$ super Yang-Mills theory. The bulk scalars that saturate the BF bound in AdS correspond in the gauge theory to the operators $c \text{Tr}[\Phi^i \Phi^j - (1/6)\delta^{ij}\Phi^2]$, where Φ^i are the six scalars in $\mathcal{N} = 4$ super Yang-Mills and c is a normalization factor that will be fixed momentarily. The $SO(5)$ -invariant bulk scalar φ that we have kept in (2.6) couples to the operator

$$\mathcal{O} = c \text{Tr} \left[\Phi_1^2 - \frac{1}{5} \sum_{i=2}^6 \Phi_i^2 \right]. \quad (3.1)$$

According to the AdS/CFT correspondence, this means the following. In the asymptotic behavior (2.8), the function α of the coordinates along the boundary plays the role of a source for \mathcal{O} in the field theory: the field theory action has a term $\int d^4x \alpha(x) \mathcal{O}(x)$. The usual boundary conditions set this source to zero, meaning that the boundary field theory is the undeformed $\mathcal{N} = 4$ super Yang-Mills theory. On the other hand, the function β plays the role of the expectation value of \mathcal{O} in the field theory; different β correspond to different quantum states of the boundary theory.⁸

In general, imposing nontrivial boundary conditions $\alpha(\beta)$ in the bulk corresponds to adding a multi-trace interaction $W(\mathcal{O})$ to the CFT action, such that after formally replacing \mathcal{O} by its expectation value β one has [21, 43]

$$\alpha = -\frac{\delta W}{\delta \beta}. \quad (3.2)$$

Adding a source term to the action can be considered as a special case, where W is a single-trace interaction linear in \mathcal{O} . The boundary conditions (2.10) that we have adopted correspond to adding a double trace term to the field theory action

$$S = S_0 - W(\mathcal{O}) = S_0 + \frac{f}{2} \int \mathcal{O}^2. \quad (3.3)$$

The operator \mathcal{O} has dimension two, so the extra term is marginal and preserves conformal invariance, at least classically (we shall see that conformal invariance is broken quantum mechanically).

⁸For a detailed discussion of the relation between the bulk field and the Yang-Mills operator, see for instance [41]. For issues specific to AdS/CFT in Lorentzian signature, see for instance [42].

In the previous section we have taken the constant f to be small and positive in the bulk. The term we have added to the CFT action, therefore, corresponds to a negative potential. Since the energy associated with the asymptotic time translation in the bulk can be negative, the dual field theory should also admit negative energy states and have a spectrum unbounded below. This shows that the usual vacuum must be unstable, and that there are (nongravitational) instantons which describe its decay. After the tunneling, the field rolls down the potential and becomes infinite in finite time. This provides a qualitative dual explanation for the fact that the function β of the asymptotic bulk solution (2.8) diverges as $t \rightarrow \pi/2$, when the big crunch singularity hits the boundary. Since β is interpreted as the expectation value of \mathcal{O} in the dual CFT, this shows that to leading order in $1/N$, $\langle \mathcal{O} \rangle$ diverges in finite time.⁹

So the big crunch spacetime in the bulk theory corresponds in the boundary theory to an operator rolling down an unbounded potential in finite time. It is important to know whether quantum corrections preserve the unbounded nature of the potential in the boundary theory. While this was unclear for the AdS₄ model that was the main focus of earlier work [17, 18, 44, 45], we shall now argue that for our model we indeed have an unbounded quantum effective potential.

For this purpose, we first briefly summarize the renormalization properties of a double trace deformation (3.3) of $\mathcal{N} = 4$ super-Yang-Mills theory; a more detailed discussion can be found in Appendix B. As explained in [21], the computation of amplitudes at order f^2 involves matrix elements of

$$\frac{f^2}{8} \int d^4x d^4y \mathcal{O}^2(x) \mathcal{O}^2(y). \quad (3.4)$$

From conformal invariance, $\langle \mathcal{O}(x) \mathcal{O}(y) \rangle = v/|x - y|^4$ on flat \mathbb{R}^4 (where the constant v depends on the normalization factor c in (3.1) as well as on N). This leads to a short distance divergence that renormalizes f and survives in the large N limit:

$$\frac{f^2}{2} \int d^4x d^4y \mathcal{O}(x) \mathcal{O}(y) \langle \mathcal{O}(x) \mathcal{O}(y) \rangle \sim \pi^2 f^2 v \ln \Lambda \int d^4x \mathcal{O}^2(x), \quad (3.5)$$

with Λ an ultraviolet cutoff. This leads to a one-loop beta function for f , which does not receive higher loop corrections in the large N limit [21]. As in [21], we now fix the normalization constant c (and thus v) by demanding that the beta function coefficient should be one. At least for small 't Hooft coupling, it is easy to see that $v \sim c^2 N^2$ for large N ; therefore $c = a/N$ with a a numerical constant. The coupling f can then be kept fixed in the large N limit. The existence of a non-vanishing beta function means that the conformal invariance of $\mathcal{N} = 4$ super-Yang-Mills theory is broken quantum mechanically by the double trace deformation.

We will be interested in an approximation to the quantum effective action that is valid for a large range of field values, in particular for large field values. An appropriate frame-

⁹In fact, we shall see later that when we consider our theory on $\mathbb{R} \times S^3$, the expectation value of \mathcal{O} in a state described by a wavepacket diverges well before the center of the wavepacket reaches infinity, so in our deformed theory on a finite volume space it is inappropriate to phrase the dynamics in terms of expectation values. What happens in that case is that the bulk of the wavepacket reaches infinity in finite time.

work is that of [46], where the standard Feynman diagram expansion is resummed and the theory is organized in a derivative expansion and an expansion in the number of loops (see Appendix B). The one-loop effective potential is given by [47]

$$V(\mathcal{O}) = -\frac{f_\mu}{2}\mathcal{O}^2 + \frac{f_\mu^2\mathcal{O}^2 \ln(\mathcal{O}/\mu^2)}{4}, \quad (3.6)$$

where μ is a renormalization scale, f_μ a renormalized coupling, and the counterterms have been chosen such that there is no constant and no linear term in \mathcal{O} , and such that

$$V(\mu^2) = -\frac{f_\mu}{2}\mu^4. \quad (3.7)$$

The renormalization group equation can be obtained by demanding that $V(\mathcal{O})$ be independent of μ :

$$\mu \frac{df_\mu}{d\mu} = -f_\mu^2, \quad (3.8)$$

which shows that the normalization of \mathcal{O} implicit in (3.6) is indeed such that the beta function coefficient is one. In (3.8), we have ignored a contribution from $d/d\mu$ hitting the f_μ^2 in the second term of (3.6), which is justified as long as $|f_\mu \ln(\mathcal{O}/\mu^2)| \ll 1$. Equation (3.8) is solved by

$$f_\mu = \frac{1}{\ln(\mu/\tilde{M})}, \quad (3.9)$$

with \tilde{M} an arbitrary scale (this implements dimensional transmutation). Choosing $\mu^2 = \mathcal{O}$, *i.e.*, the renormalization scale is set by the value of the field \mathcal{O} , the Coleman-Weinberg potential can then be written as

$$V(\mathcal{O}) = -\frac{\mathcal{O}^2}{\ln(\mathcal{O}/\tilde{M}^2)}. \quad (3.10)$$

Now suppose that for some value \mathcal{O}_0 , the coupling is small,

$$0 < f_{\mathcal{O}_0} \ll 1, \quad (3.11)$$

then $\tilde{M}^2 < \mathcal{O}_0$ and (3.10) is trustworthy (*i.e.*, higher order corrections can be ignored) for any \mathcal{O} such that $\mathcal{O} > \mathcal{O}_0$. As a result, we can conclude that in this case

$$V(\mathcal{O}) \rightarrow -\infty \quad \text{for } \mathcal{O} \rightarrow \infty. \quad (3.12)$$

Other quantum corrections are small in the large \mathcal{O} regime we will be interested in, as described at the end of Appendix B.

As was shown in [21], these renormalization properties have a precise counterpart in the bulk theory. First, define a new coordinate $0 \leq u < 1$ by $r = 2u/(1-u^2)$. In terms of this coordinate, the conformal boundary of AdS is at $u = 1$. Near a point on the boundary, the metric takes the form

$$ds^2 = \frac{R_{AdS}^2}{z^2}(-dt^2 + dz^2 + dx^i dx^i), \quad (3.13)$$

where $z = 1 - u \approx 1/r$ and x^i replace the coordinates of the three-sphere (which is approximately flat when zooming in on one point) [48]. With the boundary condition $\alpha = f\beta$, the behavior of the field ϕ near the boundary $z = 0$ is

$$\phi = \beta z^2(-f \ln z + 1). \quad (3.14)$$

It was shown in [49] that the near-boundary (small z) region of the bulk theory corresponds to the UV of the dual field theory. Therefore, to study this UV regime, we introduce a new coordinate

$$\tilde{z} = \frac{z}{\epsilon} \quad (3.15)$$

with $\epsilon \ll 1$; this new coordinate is well-suited to studying the near-boundary (small z) region of AdS. In terms of \tilde{z} , the boundary behavior (3.14) reads

$$\phi = \tilde{\beta} \tilde{z}^2(-\tilde{f} \ln \tilde{z} + 1) \quad (3.16)$$

with

$$\tilde{f} = \frac{f}{1 - f \ln \epsilon} \quad (3.17)$$

and $\tilde{\beta} = (1 - f \ln \epsilon)\beta$. Interpreting ϵ as a ratio of renormalization scales, $\epsilon = \mu/\tilde{\mu}$, and interpreting $f \equiv f_\mu$ and $\tilde{f} \equiv f_{\tilde{\mu}}$ as the coupling defined at the scales μ and $\tilde{\mu}$, respectively, (3.17) implies the following relation between the couplings at different scales:

$$f_{\tilde{\mu}} = \frac{f_\mu}{1 - f_\mu \ln(\mu/\tilde{\mu})}, \quad (3.18)$$

which is consistent with the renormalization group equation (3.8). The reason that this bulk computation (valid for large 't Hooft coupling) agrees with the perturbative field theory computation (valid for small 't Hooft coupling) is the fact that the beta function is one-loop exact for large N [21].¹⁰

In what follows we will mostly concentrate on the steepest negative direction of the effective potential. Fluctuations in orthogonal directions in field space acquire a positive mass and we will see these are suppressed. For the $SO(5)$ -invariant operator we consider, the most unstable direction comes from the $-\Phi_1^4$ term in (3.10) (see (3.1)). We focus on the dynamics of Φ_1 as it rolls along a fixed direction in $su(N)$:

$$\Phi_1(x) = \phi(x)U \quad (3.21)$$

¹⁰To relate our version of the above argument to Witten's, given in Ref. [21], note that our conventions are related to his by $z = r_W, \alpha = -\alpha_W, f = -f_W$. In the original argument, the boundary condition is written as

$$\phi = \beta z^2(-f \ln(\mu z) + 1), \quad (3.19)$$

where μ is an arbitrary scale introduced to define the logarithm. One can choose a different mass scale $\tilde{\mu}$ if one "renormalizes" the field β and the coupling f in such a way that the bulk field ϕ is left invariant:

$$\tilde{\beta}[-\tilde{f} \ln(\tilde{\mu} z) + 1] = \beta[-f \ln(\mu z) + 1], \quad (3.20)$$

which implies the relation (3.18) between the couplings at different scales.

with U a constant Hermitian matrix satisfying $\text{Tr}U^2 = 1$, so that ϕ is a canonically normalized scalar field. The Coleman-Weinberg potential (3.10) for this scalar is then given by

$$V(\phi) = -\frac{\lambda_0}{4} \frac{\phi^4}{\ln\left(\frac{\phi}{NM}\right)} \equiv -\frac{\lambda_0}{4} \frac{\phi^4}{l} \equiv -\frac{\lambda_\phi}{4} \phi^4, \quad (3.22)$$

where

$$\lambda_0 = \frac{2a^2}{N^2}, \quad M^2 = \frac{\tilde{M}^2}{Na}, \quad \lambda_\phi = \frac{\lambda_0}{l} \quad (3.23)$$

with a the numerical constant implicitly defined after (3.5).

4 Unbounded Potentials, Self-Adjoint Extensions and Ultra-Locality

We have seen that our field theory description involves the potential (3.22), which is unbounded below. This implies that the quantum field theory has no ground state. While such unstable theories are usually considered unphysical, we want to explore whether quantum mechanical evolution can be defined for them in a consistent way. A clue is provided by quantum mechanics (as opposed to quantum field theory) with unbounded potentials. As we shall review momentarily, if a potential allows a wavepacket to move off to infinity in finite time, one can nevertheless define unitary quantum evolution by imposing appropriate boundary conditions at infinity. Technically, one restricts the domain of allowed wavefunctions to those on which the Hamiltonian is self-adjoint – this is called a “self-adjoint extension”. In this section, we begin to develop the case that the quantum field theory we are interested in should also possess a self-adjoint extension. In Subsection 4.1, we review unbounded potentials in quantum mechanics. In Subsection 4.2 we show explicitly how the field theory dynamics become “ultralocal” as the singularity is approached, thus making it plausible that the quantum field is described by an independent set of identical quantum mechanical systems, one for each spatial point.

4.1 Quantum Mechanics in a $-\lambda x^p/4$ Potential for $p > 2$

We are interested in a theory of a scalar field which is classically conformal invariant but unstable. Let us first emphasize the generality of this setup, in a holographic context. We consider a classically conformal-invariant scalar field theory on a d -dimensional conformal boundary of the form $\mathbb{R} \times S^{d-1}$ where \mathbb{R} is time. The action is

$$\int d^d x \sqrt{-g_d} \left(-\frac{1}{2} (\partial\phi)^2 - \xi_d R_d \phi^2 + \frac{1}{4} \lambda_p \phi^p \right), \quad (4.1)$$

where R_d is the Ricci scalar, and the coupling λ_p is an arbitrary constant. Conformal invariance requires $p = 2 + 4/(d-2)$ and $\xi_d = (d-2)/(4(d-1))$. For any $d > 2$, p is greater than 2 and provided λ_p is positive, ϕ will run to infinity in a finite time. When focusing on the behavior near the singularity, where the ϕ^p term dominates in the potential, we shall neglect the $R_d \phi^2$ term.

The simple fact that the spatial volume of the conformal boundary is finite is very important for the quantum behavior of the boundary theory. Consider the quantum description of the homogeneous mode $\bar{\phi}$ of the scalar field. Its kinetic term in the action is $V^{d-1} \int dt \frac{1}{2} \dot{\bar{\phi}}^2$ where the volume of space, V^{d-1} , acts as the “mass” of $\bar{\phi}$. In the infinite volume limit, this “mass” becomes infinite, and $\bar{\phi}$ undergoes no quantum spreading: it becomes a classical variable. (This is the essential reason why spontaneous symmetry breaking is possible in quantum field theory but impossible in quantum mechanics). When V^{d-1} is finite, as here, the homogeneous mode $\bar{\phi}$ undergoes quantum spreading. It is convenient to canonically normalize the homogeneous mode, setting $x = (V_{d-1})^{\frac{1}{2}} \bar{\phi}_0$ and $\lambda = (V_{d-1})^{1-p/2} \lambda_p$, which is constant (for now, we are ignoring the running of the coupling constant). We then have a unit mass quantum mechanical particle with coordinate x and potential

$$V(x) = -\frac{1}{4} \lambda x^p. \quad (4.2)$$

The quantum mechanics of such potentials is discussed in Refs. [50] and [51], the latter emphasizing the Euclidean path integral description. Here, we briefly summarize the operator approach as reviewed in [51], to which we refer the reader for more details.¹¹ Later on in this paper we shall present an equivalent approach, more suited to describing the time evolution of Gaussian wavepackets, using the time-dependent semiclassical expansion and complex solutions of the classical equations of motion.

A classical particle rolling down the potential (4.2), with $p > 2$, reaches infinity in finite time. The same is true for a quantum mechanical wavepacket, and this at first sight appears to lead to a loss of probability, *i.e.*, to non-unitary evolution. However, if a self-adjoint Hamiltonian could be defined for this system, unitary quantum mechanical evolution would be guaranteed. As we shall now review, this can be done by carefully specifying an appropriate domain for the Hamiltonian

$$\hat{H} = -\frac{1}{2} \frac{d^2}{dx^2} + V(x). \quad (4.3)$$

Since the WKB approximation becomes increasingly accurate at large x , we can use it to study the generic behavior of energy eigenfunctions there. The two WKB wavefunctions for fixed energy E are proportional to

$$\chi_E^\pm(x) = [2(E + \lambda x^p/4)]^{-1/4} \exp\left(\pm i \int^x \sqrt{2(E + \lambda y^p/4)} dy\right), \quad (4.4)$$

where the lower limit of the integral may be chosen arbitrarily.

The Hamiltonian is self-adjoint if for any wavefunctions ϕ_1, ϕ_2 in its domain, $(\hat{H}\phi_1, \phi_2) = (\phi_1, \hat{H}\phi_2)$. Using integration by parts, one sees that this is equivalent to

$$\left[\frac{d\phi_1^*}{dx} \phi_2 - \phi_1^* \frac{d\phi_2}{dx} \right]_{x=\infty} = 0. \quad (4.5)$$

¹¹For a related recent discussion, see [52].

This can be arranged if for each energy E we select the linear combination of the two WKB wavefunctions which behaves like

$$\psi_E^\alpha(x) \sim x^{-p/4} \cos\left(\frac{\sqrt{2\lambda} x^{p/2+1}}{p+2} + \alpha\right) \quad (4.6)$$

at large x , where α is an arbitrary constant phase. (The angle $0 \leq \alpha \leq \pi$ labels a one-parameter family of inequivalent self-adjoint Hamiltonians.) If E is positive, for example, we set

$$\psi_E^\alpha(x) = [2(E + \lambda x^p/4)]^{-1/4} \cos\left(\int_0^x \sqrt{2(E + \lambda y^p/4)} dy + \varphi_E^\alpha\right) \quad (4.7)$$

with

$$\varphi_E^\alpha = \alpha - \int_0^\infty \left[\sqrt{2(E + \lambda y^p/4)} - \sqrt{\lambda y^p/2}\right] dy, \quad (4.8)$$

which tends to the required form at large x . A similar construction can be given for negative E [51].

As a consequence of the fact that every energy eigenfunction tends to the same, energy-independent form (4.6), equation (4.5) is satisfied if $\phi_1 = \psi_E^\alpha$ and $\phi_2 = \psi_E^\alpha$, with the same value of α . The domain of the “self-adjoint extension” of \hat{H} labelled by α can now be defined as all wavefunctions

$$\phi(x) = \int dE \tilde{\phi}(E) \psi_E^\alpha(x) \quad (4.9)$$

that satisfy $\int dE |\tilde{\phi}(E)|^2 < \infty$, so ϕ is square integrable, and $\int dE E^2 |\tilde{\phi}(E)|^2 < \infty$, so that $\hat{H}\phi$ is also square integrable, *i.e.*, it is also a normalizable wavefunction. Under these conditions, the inner product $(\phi_1, \hat{H}\phi_2)$ makes sense and, as we have just checked, it equals $(\hat{H}\phi_1, \phi_2)$ so that \hat{H} is self-adjoint.

One can interpret the parameter α as follows [51]. If one placed a “brick wall” at large x , it would force the energy eigenfunctions to vanish there. However, since for finite E the de Broglie wavelength becomes independent of energy at large x , displacing the wall by a half-integral number of de Broglie wavelengths would, in this regime, have no effect. Hence only the location of the brick wall modulo an integer number of half-wavelengths matters physically, and this is the information contained in the phase α .

Physically, one can interpret these self-adjoint extensions as follows. A right-moving wavepacket that moves to infinity is always accompanied by a left-moving “reflected” wavepacket that runs up the hill. The time it takes for a right-moving wavepacket to run to infinity and for the left-moving wavepacket to run back up the potential hill can be shown to be the same as a classical particle would take to fall to infinity and climb up the potential again after being reflected at infinity. If the potential is bounded for $x < 0$, the Hamiltonian allows a continuum of scattering states. It also has an infinite number of bound states with quantized (negative) energies,¹² the values of which depend on α . However, for the scattering problem – the bounce off the singularity – which we study, to a very

¹²We note in passing that there is another approach to applying quantum mechanics to potentials unbounded below, based on a PT symmetry [53]. This approach is motivated by analytic continuation from

good approximation the phase α enters only as an overall phase in the final wavefunction and hence has no physical consequence. We shall compute the Schrödinger wavefunctional $\Psi(\phi(\mathbf{x}))$ for the full quantum field, decomposed into its homogeneous and inhomogeneous parts, $\phi(\mathbf{x}) = \bar{\phi} + \delta\phi(\mathbf{x})$. The homogeneous part $\bar{\phi}$ behaves like the coordinate x considered in this section. We take the initial wavefunction for x to be a Gaussian with a spread chosen to minimize the quantum spread in x over the duration of the bounce. The inhomogeneous part $\delta\phi(\mathbf{x})$ is well-described at early times in terms of its Fourier modes, describing a set of harmonic oscillators which we shall take to be in their incoming ground state. We shall then argue that for all but a narrow band of final values of $\bar{\phi}$ centered on the real classical solution, we can treat the inhomogeneous modes $\delta\phi(\mathbf{x})$ to quadratic order while ignoring their backreaction on $\bar{\phi}$. Therefore, we conclude, the final wavefunction may be calculated reliably, using perturbation theory in $\delta\phi$, for a range of values of $\bar{\phi}$ away from the real classical solution but carrying most of the probability. Provided we are in a certain parameter range, to be detailed below, the system undergoes a bounce and returns close to its initial configuration, with little backreaction from particle creation.

4.2 Ultralocality and Self-Adjoint Extensions in Quantum Field Theory

To address the question whether these methods can be extended to quantum field theory, we shall first consider a simplified model that shares the same finite time singularity, namely the quantum field theory of a single scalar field ϕ with a negative quartic potential. In the context of the actual dual quantum field theory, this approximation amounts to concentrating on the scalar that parameterizes the steepest negative direction: the gauge-invariant magnitude of Φ_1 . We shall argue that the method of self-adjoint extensions indeed applies to this quantum field theory. The main argument is that near the singularity, the scalar field evolution becomes ultra-local: spatial gradients become unimportant and the quantum field theory can be thought of as a collection of independent, identical quantum mechanical systems, one for each point in space. As a consequence, the self-adjoint extension method can be implemented point by point. We assume that at every spatial point, the same value of α enters the self-adjoint boundary condition: this is necessary if the theory is to respect the symmetries of the S^3 .

To begin with, we shall study the classical, conformally-invariant field theory on $\mathbb{R} \times S^3$,

$$\mathcal{L} = -\frac{1}{2}(\partial\phi)^2 + \frac{\lambda_4}{4}\phi^4 - \frac{1}{12}R_4\phi^2, \quad (4.10)$$

where R_4 is the Ricci scalar. We are interested in studying generic solutions, *i.e.*, those specified by the appropriate number of with arbitrary functions of space, in the vicinity of the singularity, which we shall assume to be space-like. The field equation is

$$\square\phi = -\lambda_4\phi^3 + \frac{1}{6}R_4\phi. \quad (4.11)$$

the harmonic oscillator and it results in a positive energy spectrum. In contrast, for all self-adjoint extensions described above, there is an infinite set of negative energies. Since we know the bulk theory has negative energy solutions as well (the instanton discussed in Section 2 provides one example), the approach using self-adjoint extensions seems more appropriate.

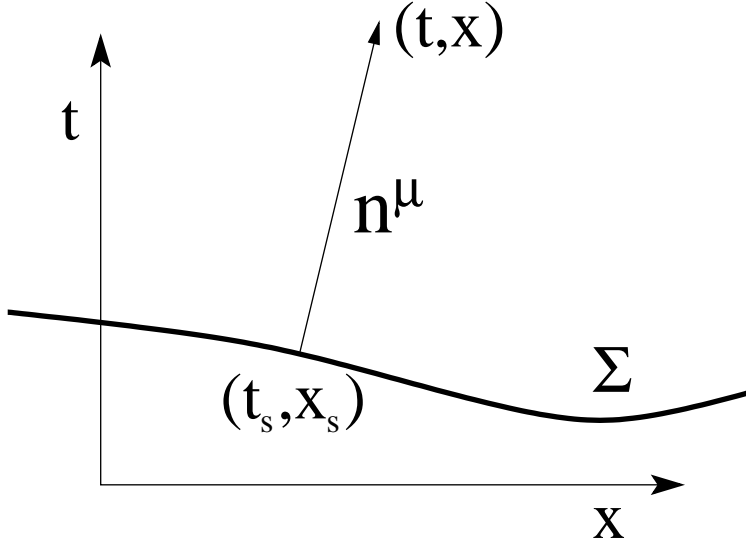


Figure 5: The singular hypersurface Σ , assumed spacelike, upon which ϕ is infinite and χ is zero.

The curvature of the three-sphere plays an important role in determining the initial conditions for the scalar field, but as the field runs down towards the singularity the spatial curvature rapidly becomes irrelevant. Since we are concerned with the behavior of the field near the singularity, in this section we shall ignore the last term in (4.11).

It is also convenient to change variables to $\chi = (2/\lambda_4)^{\frac{1}{2}}\phi^{-1}$ so that the equation of motion assumes the form

$$\chi\partial^2\chi - 2(\partial\chi)^2 = 2, \quad (4.12)$$

and the zero-energy, homogeneous background solution is just $\chi = t_* - t$, with t_* an arbitrary constant.

We would like to construct the generic, spatially inhomogeneous solution to (4.12) as a Taylor series in the proper time away from the singularity, which we assume to be a spacelike surface, Σ . The coordinates of the embedding Minkowski spacetime (recall, we are neglecting the space curvature of the S^3) are t, \mathbf{x} ; the locus of the singular hypersurface Σ is $t = t_s(\mathbf{x}_s)$, $\mathbf{x} = \mathbf{x}_s$. As long as Σ is not too strongly curved, for every spacetime point x^μ there is a unique corresponding point x_s^μ on Σ , connected to x^μ by a geodesic normal to Σ . The unit normal to Σ is

$$n^\mu = (\gamma, \gamma\nabla t_s), \quad \gamma \equiv \frac{1}{\sqrt{1 - (\nabla t_s)^2}}, \quad (4.13)$$

where ∇ indicates the gradient with respect to \mathbf{x}_s . It is then natural to change coordinates from (t, \mathbf{x}) to τ , the proper time from Σ , and \mathbf{x}_s , the corresponding point on Σ , given by $x^\mu - x_s^\mu = n^\mu\tau$, or

$$t = t_s(\mathbf{x}_s) + \gamma\tau, \quad \mathbf{x} = \mathbf{x}_s + \gamma\tau\nabla t_s, \quad (4.14)$$

where $\tau = \sqrt{(t - t_s)^2 - (\mathbf{x} - \mathbf{x}_s)^2}$ is (the absolute value of) the proper time from Σ .

To construct the scalar field equation we need the metric in the new coordinates. From the Minkowski line element in t, \mathbf{x} , and (4.14), we find the line element in (τ, \mathbf{x}_s) coordinates is $-d\tau^2 + h_{ij}dx_s^i dx_s^j$, where

$$\begin{aligned} h_{ij} &= h_{ij}^{(0)} + 2K_{ij}\tau + K_{ik}h_{(0)}^{kl}K_{lj}\tau^2 \\ h_{ij}^{(0)} &\equiv \delta_{ij} - \partial_i t_s \partial_j t_s, \quad K_{ij} \equiv \gamma \partial_i \partial_j t_s. \end{aligned} \quad (4.15)$$

Here, $t_s(\mathbf{x}_s)$ is the locus of the singular hypersurface, whose metric is $h_{ij}^{(0)}$ and inverse metric is $h_{(0)}^{ij}$. All space derivatives ∂_i are taken with respect to \mathbf{x}_s , at fixed τ . The matrix K_{ij} is the extrinsic curvature (or second fundamental form) of the singular hypersurface Σ . (Since the embedding space is flat, the intrinsic curvature of Σ can also be expressed in terms of K_{ij} , by the Gauss relation $R_{jkl}^i(\Sigma) = K_{jk}K_l^i - K_{jl}K_k^i$, and is thus not an independent quantity.)

In these coordinates, the field equation (4.12) reads

$$2\chi_{,\tau}^2 - \chi h^{-\frac{1}{2}}(h^{\frac{1}{2}}\chi_{,\tau})_{,\tau} - 2h^{ij}\partial_i\chi\partial_j\chi + \chi h^{-\frac{1}{2}}(h^{\frac{1}{2}}h^{ij}\chi_{,i})_{,j} = 2, \quad (4.16)$$

where h is the determinant and h^{ij} the inverse of h_{ij} . By substituting (4.15) into (4.16), we obtain an asymptotic expansion for χ ,

$$\begin{aligned} \chi &= \tau + \frac{1}{6}K_1\tau^2 + \frac{1}{18}(K_1^2 - 3K_2)\tau^3 + \frac{1}{4}(K_3 - \frac{13}{18}K_2K_1 + \frac{7}{54}K_1^3 - \frac{1}{6}\nabla^2 K_1)\tau^4 \\ &+ \ln\tau \left[\frac{1}{5} \left(-7K_4 + \frac{29}{3}K_1K_3 + \frac{11}{3}K_2^2 - \frac{67}{9}K_1^2K_2 + \frac{34}{27}K_1^4 - \frac{1}{18}(\partial K_1)^2 \right. \right. \\ &\left. \left. + \frac{2}{9}K_1\nabla^2 K_1 - \frac{1}{6}\nabla^2 K_2 \right) \tau^5 + C_6\tau^6 + \dots \right] + \frac{\lambda_4\rho(x_s)}{10}\tau^5 + D_6\tau^6 + \dots, \end{aligned} \quad (4.17)$$

where $K_1 = h_{(0)}^{ij}K_{ij} = h^{-\frac{1}{2}}\partial_\tau h^{\frac{1}{2}}|_{\tau=0}$, $K_2 = \text{Tr}(K^2)$, and so on, and traces are taken using the metric $h_{(0)}^{ij}$. The higher coefficients $C_n(\mathbf{x}_s)$, $n \geq 6$, are all determined in terms of $t_s(\mathbf{x}_s)$, and the higher coefficients $D_n(\mathbf{x}_s)$, $n \geq 6$, are determined in terms of the second arbitrary function $\rho(\mathbf{x}_s)$. The reason for the entrance of the logarithm, and the second arbitrary function, at order τ^5 is seen by examining the first two terms of (4.16), at order τ^4 . At this order, it is necessary for consistency to introduce a term proportional to $\tau^5 \ln \tau$ into the series expansion, and the coefficient of τ^5 is then left undetermined.

Let us comment on the general form of the full nonlinear solution (4.17). First, if we re-express τ in terms of the global time coordinate,

$$\tau = |t - t_s(\mathbf{x}_s)| + O((\nabla t_s)^2), \quad (4.18)$$

(4.17) can be viewed as an expansion in powers of ∇t_s as well as in $(t - t_s)\nabla_s$. Working only to linear order in ∇t_s , we obtain for $t < t_s$

$$\chi(t, \mathbf{x}) = -t + t_s(\mathbf{x}) + \frac{1}{6}(t_s - t)^2 \nabla^2 t_s - \frac{1}{24}(t_s - t)^4 (\nabla^4 t_s) + \dots + \frac{\lambda_4 \rho(\mathbf{x}_s)}{10} (t_s - t)^5 + \dots, \quad (4.19)$$

which is actually completely regular at $t = t_s$. Within this linearized approximation, the two arbitrary functions of space that appear are easily interpreted. The first, $t_s(\mathbf{x})$, is the *time delay* to or from the singularity, given in linear theory by the limit of $\delta\phi/\dot{\phi}$ as t tends to zero. The second, $\rho_s(\mathbf{x})$, is the linearized *perturbation in the Hamiltonian density*, evaluated at the singularity: setting

$$\delta\mathcal{H} = \dot{\phi}\delta\dot{\phi} + V_{,\phi}\delta\phi = \partial_t \left(\frac{\delta\phi}{\dot{\phi}} \right) \dot{\phi}^2, \quad (4.20)$$

we find that as $t \rightarrow 0$, \mathcal{H} tends to $\rho(\mathbf{x})$. Note that spatial gradients do not appear in \mathcal{H} at linearised order because the background solution $\phi = -(2/\lambda_4)^{\frac{1}{2}}t^{-1}$ is spatially homogeneous.

Second, (4.17) is clearly an expansion in $\tau\nabla_s$, so that gradients become less and less significant in the dynamical evolution as the singularity $\tau = 0$ is approached: the evolution of χ becomes *ultralocal* in this limit. To see this, consider the “velocity-dominated” version of the equation of motion (4.12), *i.e.*, the equation of motion with the gradient terms omitted. The solution of the velocity-dominated equations of motion is

$$\chi^{(0)} = t_s(\mathbf{x}) - t + \frac{\lambda_4\rho(\mathbf{x})}{10} (t_s(\mathbf{x}) - t)^5. \quad (4.21)$$

Therefore, we see that the full solutions (4.17) differ from the velocity-dominated ones only by terms that are unimportant near the singularity $t = t_s$, so that the gradient terms are indeed dynamically unimportant there.

Finally, note that the non-analytic terms in (4.17), involving $\ln\tau$, enter only at quadratic and higher order in the perturbations. If these nonlinear terms are constructed perturbatively by expanding in the linearized perturbation, then no new functions enter: the nonlinear terms are completely dictated by the equations of motion, for $t_s - t$ positive or negative. Hence, a matching condition within the linear theory completely determines the matching of the full nonlinear solution, as long as the latter is well-described by linear perturbation theory.

To summarise, we have exhibited a generic class of solutions which are singular on an arbitrary spacelike hypersurface Σ . The solutions are constructed as an expansion in proper time τ times spatial gradients. The solutions explicitly show that if we follow a solution with spatial structure on some wavenumber k , gradients become unimportant in the evolution when $|k\tau|$ falls below unity. At this point, the evolution becomes ultralocal so that the field values at different spatial points decouple. In constructing the quantum theory, it is then natural to use the same self-adjoint extension (or boundary condition) at every spatial point, to evolve the quantum field across the singularity. A key question is whether the UV regime of the quantum field theory can be consistently treated, or whether the presence of structure on smaller and smaller scales will lead to divergences. The remainder of this paper will largely be devoted to tackling this question. Our answer will be that once the spatially homogeneous mode $\bar{\phi}$ on the S^3 is treated quantum mechanically, then due to quantum spreading, most of the probability is associated with final values of $\bar{\phi}$ significantly

displaced from the real classical solution, and for these values, the theory defines its own UV cutoff in a natural way.

Although most of our calculations will be done in linearized perturbation theory around the homogeneous background, it is conceptually clearer to view the self-adjoint extension as being implemented point by point, with a short-wavelength cutoff. This description has the advantage that it is fully nonlinear. Furthermore, as indicated in the previous section and more fully described below, the semiclassical expansion becomes increasingly accurate near the singularity. Therefore our demonstration of ultralocal behavior in the classical field theory extends to the full quantum description in this limit.

For the purposes of the explicit, leading-order calculations we shall perform in this paper, the ultralocal description will not be needed. The field ϕ is decomposed into a homogeneous component $\bar{\phi}$, treated nonlinearly, and an inhomogeneous component $\delta\phi(\mathbf{x})$ which we treat only at the linearized level. We are interested in starting from a nearly homogeneous state (representing an empty universe) and computing how the inhomogeneous perturbations are generated from quantum fluctuations. This process involves powers of the small coupling λ_4 (or equivalently Planck's constant \hbar), and therefore effects nonlinear in the inhomogeneities are consistently small. The ingoing and outgoing states are most conveniently described using Fourier modes for $\delta\phi$ and, since we work only at the linearized level, this description is valid throughout. The ultralocal behavior is reflected in the fact that the k^2 term in the equation of motion for Fourier modes of wavenumber k becomes unimportant around the singularity, and this will occasionally help with interpreting or guessing the mode solutions. The full nonlinear ultralocality is only expected to be useful at higher order in perturbation theory. We have given them here mainly to illustrate that, in principle, there is no obstacle to describing the full nonlinear physics of the bounce in an ultralocal manner.

5 Quantum Evolution of the Homogeneous Component

In this and the following section we shall calculate the Schrödinger wavefunctional $\Psi(t, \phi(\mathbf{x}))$ for the quantum field $\phi(\mathbf{x})$ in the semiclassical expansion. We are interested in computing Ψ at times t_f corresponding to the classical roll of the field to infinity and back, *i.e.*, for the bounce to be completed and for the system to return close to its initial state. We write the field as the sum of its homogeneous and inhomogeneous parts, $\phi = \bar{\phi} + \delta\phi(\mathbf{x})$. We shall assume that the inhomogeneous component starts out in its quantum ground state, so its fluctuations are parametrically suppressed by \hbar (or, equivalently, the quartic coupling λ_ϕ) and it makes sense to start by considering the quantum behavior of the homogeneous component $\bar{\phi}$.

As emphasized in Subsection 4.1, on a finite space like the S^3 of the boundary theory, $\bar{\phi}$ is quantum mechanical. This simple fact plays an essential role in what follows: the quantum spread in $\bar{\phi}$, combined with the self-adjoint boundary condition at infinite $\bar{\phi}$ forcing the probability density to vanish there, means that the probability density stays away from infinity. In semiclassical language, this will translate into the fact that the relevant classical trajectories are generically complex and generically avoid the singularity at infinity in the complex $\bar{\phi}$ -plane.

In this section, we show how the self-adjoint extension described in Subsection 4.1 can be implemented in the semiclassical expansion. Since the first term in this expansion, the semiclassical approximation, becomes exact near the singularity, the calculation should accurately capture the physics there. We impose the required boundary condition on the wavefunction at infinite $\bar{\phi}$ by the method of images, using the reflection symmetry of the Hamiltonian to satisfy the boundary condition with the sum of two semiclassical wavefunctions. The result of this construction is a wavefunction which bounces from infinity and returns close to its starting point. The quantum spread in the wavefunction is represented by a small imaginary part in each of the relevant complex classical solutions which is, for generic final values of $\bar{\phi}$, nonzero at all times and which dominates at times corresponding to the classical encounter with the singularity.

Having determined the wavefunction $\Psi(\bar{\phi})$ in the approximation where $\delta\phi$ was ignored, the next step is to construct the full wavefunction $\Psi(t_f, \bar{\phi}, \delta\phi(\mathbf{x}))$ at the final times of interest, ignoring the backreaction of $\delta\phi$ on $\bar{\phi}$. We again employ the semiclassical expansion, finding the relevant (spatially inhomogeneous) complex classical solution which incorporates the initial condition that the inhomogeneous fluctuation modes of $\delta\phi$ are in their incoming adiabatic ground state. Working to quadratic order in $\delta\phi$ in the action and ignoring backreaction, the solution for $\delta\phi$ is determined from the relevant linearized field equation. The small imaginary part in the complex solution for the background $\bar{\phi}$, representing its quantum spread, now plays an essential role: it provides a UV cutoff on the production of high k modes. Including this effect, we find that, within a certain parameter regime, for generic final values for $\bar{\phi}$ particle production is parametrically suppressed and backreaction is under control.

The combined inhomogeneous classical solution yields $\Psi(t_f, \bar{\phi}, \delta\phi(\mathbf{x}))$, in a consistent approximation scheme, for values of $\bar{\phi}$ carrying most of the final probability. The approximation breaks down for values of $\bar{\phi}$ very close to the real classical solution corresponding to the initial center and momentum of the Gaussian wavepacket. As the final value for $\bar{\phi}$ is taken near to this classically predicted value, the imaginary part of the relevant complex classical solution disappears. If backreaction is neglected, the quantum particle production of inhomogeneous modes diverges in this limit, indicating that our approximation breaks down. However, the relevant band of final $\bar{\phi}$ yielding strong backreaction is parametrically small within our chosen parameter regime. For all other values of $\bar{\phi}$, our calculation of the joint probability density $|\Psi(t_f, \bar{\phi}, \delta\phi(\mathbf{x}))|^2$ appears to be reliable. Since we are working in a theory where unitarity has been built in, we conclude that the most probable outcome is a bounce, with parametrically small particle production.

We begin this section with a review of the use of complex classical solutions to construct the solution of the time-dependent Schrödinger equation in a semiclassical expansion.

5.1 Complex Classical Solutions and Quantum Mechanics

Our discussion of the evolution of the quantum field ϕ will rest upon the use of complex classical solutions. These are used to obtain the first semiclassical approximation to the Schrödinger wavefunction, which then forms the basis of the semiclassical expansion. The

method is ideally suited to the present problem because the first semiclassical approximation becomes exact as the singularity is approached.

Consider a quantum mechanical particle with Hamiltonian $H(x, p) = \frac{1}{2}p^2 + V(x)$. At the initial time $t = t_i$ we prepare the system in a Gaussian wavepacket centred on $x = x_c$ and with momentum $p = p_c$. Our initial condition may be written as

$$\frac{x}{2L} + i\frac{pL}{\hbar} = \frac{x_c}{2L} + i\frac{p_cL}{\hbar} \equiv \alpha, \quad t = t_i, \quad (5.1)$$

because this equation, when regarded as an eigenvalue equation with $p = -i\hbar d/dx$, yields for the wavefunction

$$\Psi(x, t_i) \sim e^{i\frac{p_c x}{\hbar}} e^{-\frac{(x-x_c)^2}{4L^2}}. \quad (5.2)$$

The corresponding probability density is a Gaussian with variance $\Delta x^2 = L^2$. Equation (5.1) can also be written as

$$\frac{x}{\Delta x} + i\frac{p}{\Delta p} = \frac{x_c}{\Delta x} + i\frac{p_c}{\Delta p}, \quad (5.3)$$

because for a Gaussian, $\Delta x \Delta p = \hbar/2$, saturating the uncertainty relation.

For a given choice of $\Delta x = L$, a set of Gaussian wavepackets with x_c and p_c running over all real values can be thought of as providing a smeared description of classical phase space (x, p) , with the minimal ‘‘smearing area’’ $\Delta x \Delta p$.

The normalized states labeled by x_c and p_c ,

$$\Psi_{x_c, p_c}^L(x) = \frac{1}{(2\pi L^2)^{\frac{1}{4}}} e^{i\frac{p_c x}{\hbar}} e^{-\frac{(x-x_c)^2}{4L^2}}. \quad (5.4)$$

are sometimes called ‘‘coherent squeezed states’’ and the complex number α defined in (5.1) is the coherent state parameter. For given L , these states form an *overcomplete* basis: they are not orthogonal, but any state can be expressed as a linear combination of them. To see this, note that

$$\int \frac{dx_c dp_c}{2\pi\hbar} \Psi_{x_c, p_c}^{L*}(x) \Psi_{x_c, p_c}^L(x') = \delta(x - x'), \quad (5.5)$$

gives the resolution of the identity operator. An arbitrary wavefunction $\Psi(x)$ can be expressed as a linear combination of the Ψ_{x_c, p_c}^L by multiplying each side of (5.5) by $\Psi(x')$ and integrating over x' . Clearly, if we determine the time evolution of the coherent squeezed states, for some L , we will have determined the time evolution of any state.

For a harmonic oscillator with frequency ω , *i.e.*, $V = \frac{1}{2}\omega^2 x^2$, the semiclassical approximation is exact. Furthermore, in this case there is a natural choice for L given by the width of the ground state $L^2 = \hbar/(2\omega)$. The left hand side of (5.1) is then just the annihilation operator $a = \sqrt{\omega/(2\hbar)}(x + ip/\omega)$ obeying $[a, a^\dagger] = 1$, and in fact this was the reason for adopting the normalization of the coherent state parameter α in (5.1). The initial condition corresponding to the oscillator being in its ground state is simply $a = 0$: we shall adopt this initial condition for the inhomogeneous modes of the scalar field on the S^3 which, at times well away from the bounce, are accurately described as harmonic oscillators with adiabatically varying frequency ω . More generally, one can consider initial and final states

which are eigenstates of a with eigenvalue α , just as in (5.1). These eigenstates are given by $|\alpha\rangle \propto e^{\alpha a^\dagger}|0\rangle$. The transition amplitude between such states $\langle\beta, \text{out}|\alpha, \text{in}\rangle$ provides the generating function of the S-matrix between arbitrary n-particle Fock states. [54] Therefore the formalism of complex classical solutions extends naturally to a computation of the full S-matrix, in the semiclassical expansion.

The semiclassical expansion may be derived as a formal expansion in powers of \hbar : substituting

$$\Psi(x, t) = A(x, t)e^{iS(x, t)/\hbar} \quad (5.6)$$

into the time-dependent Schrödinger equation

$$i\hbar\frac{\partial\Psi}{\partial t} = \left(-\frac{\hbar^2}{2}\frac{\partial^2}{\partial x^2} + V(x)\right)\Psi, \quad (5.7)$$

at leading order in \hbar we obtain the Hamilton-Jacobi equation for S , namely

$$\frac{\partial S}{\partial t} = -\left(\frac{1}{2}\left(\frac{\partial S}{\partial x}\right)^2 + V(x)\right) = -H\left(x, \frac{\partial S}{\partial x}\right). \quad (5.8)$$

This equation is solved by the classical action, *i.e.*, $S = S_{Cl}$ being the action evaluated on the appropriate classical path x_{Cl} . Since our initial condition (5.1) is complex, we shall in general be interested in complex solutions of the classical equations of motion. The classical action is

$$S_{Cl}(x, t) = \int_{t_i}^t dt' (p_{Cl}\dot{x}_{Cl} - H(x_{Cl}, p_{Cl}))(t') + B(x_i, p_i) \quad (5.9)$$

for a classical path satisfying the initial condition (5.1) at time t_i and the final condition $x_{Cl} = x$ at the final time t . (We often abbreviate the final coordinate x_f as x and the final time t_f as t : the context should make our meaning clear.) It is necessary to add the boundary term B to ensure that the stationarity of the action $\delta S = 0$ under all variations $\delta x(t)$ respecting the given boundary conditions is equivalent to the classical equations of motion. Our initial condition (5.1) implies $\delta x_i + 2i\delta p_i L^2/\hbar = 0$, and the correct boundary term is found to be

$$B(x_i, p_i) = \frac{p_i^2 L^2}{i\hbar}. \quad (5.10)$$

Now consider the value of the classical action S_{Cl} when the final time t and the final position x are varied, $t \rightarrow t + \delta t$, $x \rightarrow x + \delta x$. The variation in the corresponding classical path is $x_{Cl}(t) \rightarrow x_{Cl}(t) + \delta x_{Cl}(t)$, and the variation of the classical action is

$$\delta S_{Cl} = \delta t(p_{Cl}\dot{x}_{Cl} - H(x_{Cl}, p_{Cl}))(t) + [p_{Cl} \delta x_{Cl}]_{t_i}^t + \delta B \quad (5.11)$$

where we used integration by parts and Hamilton's equations for the classical solution, $\dot{x}_{Cl} = (\partial H/\partial p)_{Cl}$, $\dot{p}_{Cl} = -(\partial H/\partial x)_{Cl}$. The value of the final coordinate at the final time $t + \delta t$ has the first order variation

$$\delta x = \delta x_{Cl}(t + \delta t) = \delta x_{Cl}(t) + \dot{x}_{Cl}\delta t, \quad (5.12)$$

hence

$$\delta S_{Cl} = -H\delta t + p\delta x - p_i\delta x_i + \delta B = -H\delta t + p\delta x, \quad (5.13)$$

because B was chosen precisely to ensure that $\delta B - p\delta x_{Cl}$ vanishes at $t = t_i$ for our chosen initial condition. Thus we have

$$\frac{\partial S_{Cl}}{\partial t} = -H(x, p), \quad \frac{\partial S_{Cl}}{\partial x} = p, \quad (5.14)$$

and the wavefunction (5.6), with $S = S_{Cl}$, satisfies both the initial condition (5.1) and the time-dependent Schrödinger equation (5.8) to leading order in \hbar .

For completeness, let us give the equation for the time evolution of the prefactor $A(x, t)$:

$$\frac{\partial A}{\partial t} + p\frac{\partial A}{\partial x} = -\frac{1}{2}\frac{\partial p}{\partial x}A + \frac{i\hbar}{2}\frac{\partial^2 A}{\partial x^2}. \quad (5.15)$$

With the neglect of the last, higher order term, this equation is straightforwardly solved by integrating A along the classical trajectories of the system. For example, if A is independent of t , then the solution is just $A \propto p^{-\frac{1}{2}}$.

As a simple illustration, consider a free particle, with $H = \frac{1}{2}p^2$. In this case the Lagrangian is quadratic and the second variation of S with respect to x , *i.e.* $(\partial p/\partial x)$, depends only on t . Here, as can be seen from (5.15), it is consistent to set $(\partial A/\partial x)$ zero. The x -dependence of the wavefunction then arises solely from the classical action S_{Cl} . Since the equation of motion is trivial, the classical solution satisfying our chosen boundary conditions is easily found,

$$x(t) = x_f + (t - t_f)\frac{p_c + \frac{i\hbar}{2L^2}(x_f - x_c)}{1 + \frac{i\hbar}{2L^2}(t_f - t_i)}, \quad (5.16)$$

where the subscript f denotes final quantities. The classical action (5.9), with (5.10), is then

$$S_{Cl}(x_f, t_f) = \frac{L^2}{i\hbar} \frac{\left(p_c + \frac{i\hbar}{2L^2}(x_f - x_c)\right)^2}{1 + \frac{i\hbar}{2L^2}(t_f - t_i)}. \quad (5.17)$$

Substituting this expression in (5.15), we find

$$A(t) = \frac{N}{\sqrt{1 + i\frac{\hbar t}{2L^2}}} \quad (5.18)$$

with N a constant determined by normalising the wavefunction, $N = e^{-p_c^2 L^2/\hbar^2}/(2\pi L^2)^{\frac{1}{4}}$. Equation (5.6) then gives the familiar free-particle solution to the time-dependent Schrödinger equation, describing a spreading wavepacket.

There are several points worth noting. First, the relevant classical solution is generally complex, and only real in the special case where x_f lies precisely on the classical trajectory, $x_f = x_c + p_c(t_f - t_i)$. Second, in general the solution does not start at x_c , nor is its momentum p_c . The initial value of x at $t = t_i$ is

$$x_i = x_c + \frac{x_f - x_c - p_c(t_f - t_i)}{1 + \frac{i\hbar}{2L^2}(t_f - t_i)}, \quad (5.19)$$

and value of the conserved momentum is

$$p_i = p = p_c + \frac{i\hbar}{2L^2} \frac{x_f - x_c - p_c(t_f - t_i)}{1 + \frac{i\hbar}{2L^2}(t_f - t_i)}. \quad (5.20)$$

If x_f is chosen to lie ahead of (or behind) the classical solution then the imaginary part of x_i is negative (or positive) and the complex classical trajectory lies in the lower (or upper) half of the complex x -plane. The initial condition (5.1) implies that $p_i - p_c$ is directed at right angles to $x_i - x_c$ in the complex x -plane. Finally, the magnitude of the imaginary part of $x_i - x_c$ is set by the difference between x_f and the value predicted by the classical solution, $x_f - x_c - p_c(t_f - t_i)$, times the dimensionless number $(\hbar/L^2)(t_f - t_i)$ which is the fractional spreading of the wavepacket, $\Delta L/L \sim \Delta p(t_f - t_i)/L$ where $\Delta p \sim \hbar/L$ is the initial spread in momentum implied by the uncertainty relation. If the fractional spreading of the wavepacket is small over the relevant interval of time, then for typical values of x_f the imaginary part of the relevant classical solution will also be small.

We can easily generalize to a free particle confined to the positive half-line by a brick wall located at $x = 0$, forcing the wavefunction to vanish there. We can satisfy this boundary condition with free particle wavefunctions by the method of images. Assume that the particle starts out described, to a good approximation, by a Gaussian wavefunction obeying (5.1), with x_c large and positive and p_c negative. To ensure the wavefunction vanishes on the wall, we subtract the mirror image wavefunction obtained by reflecting the initial conditions, $x_c \rightarrow -x_c$, $p_c \rightarrow -p_c$. Squaring the complete wavefunction, one finds the probability density

$$|\Psi|^2(x, t) = C \left(e^{-\frac{(x-x_c-p_c(t-t_i))^2}{2\sigma^2}} + e^{-\frac{(x+x_c+p_c(t-t_i))^2}{2\sigma^2}} - 2e^{-\frac{x^2+(x_c+p_c(t-t_i))^2}{2\sigma^2}} \cos\left(\frac{2xp_cL^2}{\hbar\sigma^2}\right) \right), \quad (5.21)$$

with $C = 1/\sqrt{2\pi\sigma^2}$, $\sigma^2 = L^2 + \frac{\hbar^2(t-t_i)^2}{4L^2}$ the growing dispersion of the Gaussian and $\hat{p}_c(t) = p_c - x_c\hbar^2(t-t_i)/(4L^4)$. We minimize the spread of the wavefunction over the time $t - t_i$ of interest if we choose $L = \sqrt{\hbar(t-t_i)/2}$.

At early times, the probability density (5.21) is well-approximated by the first term alone, namely a slowly spreading Gaussian centered on the first classical trajectory. When the wavepacket hits the wall, at $t - t_i \sim -x_c/p_c$, interference between the incident and reflected waves leads to strongly oscillatory behavior in both space and time. It is this regime which will be most closely analogous to the bounce from the singularity in our problem. As time runs forward, the second classical solution, obeying the mirror image initial conditions, now determines the dominant piece of the wavefunction. The probability once again assumes a smooth Gaussian form but now moving away from the wall. Similar behavior will be encountered below, when we deal with “reflection from infinity” in our problem.

The semiclassical formalism we are using emphasizes the similarities between the quantum and classical problems, but their differences emerge in two interesting and important ways. First, more than one classical solution can be relevant to determining the wavefunction. In the brick wall problem, two are needed and it is the interference between them

which forces the wavefunction to vanish at the wall. Second, the relevant classical solutions are generically complex, and, in the brick wall problem, generically avoid the location of the wall in the complex x -plane.

5.2 The Self-Adjoint Extension via Complex Classical Solutions

In our problem, the homogeneous mode of the scalar field is described by the action for a quantum mechanical particle,

$$S = \int dt \left(\frac{1}{2} \dot{x}^2 - V(x) \right), \quad (5.22)$$

in which $V(x)$ satisfies two general properties. First, it is unbounded below and falls faster than quadratically at large x so generic real trajectories lead to finite-time singularities. Second, $V'(x)/(-V(x))^{\frac{3}{2}}$ tends to zero at large x so the semiclassical approximation becomes exact there. As discussed in Subsection 4.1, under these two conditions the singularity can be quantum mechanically resolved by restricting the allowed stationary states to those proportional to a fixed real function of x at large x . For example, for $V = -\frac{1}{4}\lambda x^4$ the allowed energy eigenfunctions behave as

$$\psi_E^\alpha(x) \sim x^{-1} \cos \left(\sqrt{\frac{\lambda}{2}} \frac{x^3}{3\hbar} + \alpha \right), \quad x \rightarrow \infty, \quad (5.23)$$

with α an arbitrary constant phase labeling the particular self-adjoint extension.

For the case we are interested in, the use of the energy eigenfunction basis turns out to be an inessential complication. We are interested in the time evolution of a non-stationary state in which the homogeneous component of the field $\bar{\phi}$ is localized around some small value in propagating the state across the quantum “bounce.” In principle, we could compute the quantum evolution by expressing the initial state in terms of energy eigenfunctions, but it is far more convenient to describe the process using squeezed coherent states. As we shall now show, the self-adjoint extension may be implemented directly using complex classical solutions, for a class of potentials including those of interest here.

The first step is to represent the theory (5.22) in the complex x -plane, viewed as a Riemann sphere including the point at infinity. The simplest potentials to deal with are those which are meromorphic in the region containing the singularity and symmetric under reflection through the singularity, $x \rightarrow -x$. The potential $V(x) = -\frac{1}{4}\lambda x^4$ satisfies these requirements and we shall start by considering this case.

Consider an initial Gaussian wavepacket with coordinates (x_c, p_c) and spread $\Delta x = L$. The initial condition (5.1) provides one complex equation for x_i and $p_i = \dot{x}_i$. A second equation is obtained from energy conservation: since $e = \frac{1}{2}\dot{x}^2 - \frac{1}{4}\lambda x^4$ is constant, we have

$$t_f - t_i = \int_{x_i}^{x_f} \frac{dx}{\sqrt{2(e + \frac{1}{4}\lambda x^4)}}. \quad (5.24)$$

For each value of x_f , and at fixed t_f , equations (5.1) and (5.24) provide two complex equations for the unknowns x_i and \dot{x}_i (or equivalently, e), which completely specify the first classical solution $x_1(t)$.

By analogy with the brick wall problem, we construct a second, “image,” classical solution $x_2(t)$ by reflecting the initial condition (5.1) through infinity,

$$\frac{x_{2,i}}{2L} + i\frac{p_{2,i}L}{\hbar} = -\left(\frac{x_c}{2L} + i\frac{p_cL}{\hbar}\right), \quad t = t_i, \quad (5.25)$$

but imposing the same final condition $x_{2,f} = x_{1,f} = x_f$ at time t_f . As for the brick wall, we expect the corresponding semiclassical wavefunction to start out “behind” the singularity, moving towards it, and to emerge from it.

Now we want to show that the full semiclassical wavefunction for the self-adjoint extension is just the sum of two terms

$$\Psi^\alpha(x, t) = A_1(x, t)e^{iS_1/\hbar} + e^{-2i\alpha} A_2(x, t)e^{iS_2/\hbar}, \quad (5.26)$$

each determined by the appropriate classical solution. As in the brick wall problem, the boundary conditions are satisfied by the method of images, due to the interference between the two terms. The main difference here is that whereas we had to take $\alpha = \pi/2$ to ensure the wavefunction vanished at the brick wall, in the present problem we can take any real $0 \leq \alpha < \pi$ and still ensure the Hamiltonian is self-adjoint.

To show that the Hamiltonian is self-adjoint, we simply compute the wavefunction (5.26) in the limit of large x_f . In this limit, the second classical solution becomes the reflected image of the first, $x_2(t) = -x_1(t)$, and this leads to the desired asymptotic behavior. Explicitly, we express the action in canonical form,

$$S = \int p dx - e(t_f - t_i) + \frac{p_i^2 L^2}{i\hbar}. \quad (5.27)$$

Because the two solutions are related by simple reflection in the limit of large x_f , they involve opposite momenta in this limit: in the first solution $p_1 = +\sqrt{2(e_1 + \frac{1}{4}\lambda x^4)}$, whereas $p_2 = -\sqrt{2(e_2 + \frac{1}{4}\lambda x^4)}$. Substituting into (5.27) and integrating by parts to extract the leading dependence for large x_f , we find

$$\begin{aligned} S_1 &\rightarrow \sqrt{\frac{\lambda}{2}} \frac{x_f^3}{3} + \frac{e_0}{3}(t_f - t_i) + \mathcal{O}(x_f^{-1}) \\ S_2 &\rightarrow -\sqrt{\frac{\lambda}{2}} \frac{x_f^3}{3} + \frac{e_0}{3}(t_f - t_i) + \mathcal{O}(x_f^{-1}), \quad x_f \rightarrow \infty \end{aligned} \quad (5.28)$$

where e_0 is the limiting energy of either solution as x_f tends to infinity, and $e_{1,2} = e_0 + \mathcal{O}(x_f^{-1})$, as can be straightforwardly shown from equation (5.24). The semiclassical wavefunction (5.26) thus behaves as

$$\Psi^\alpha(x, t) \sim e^{-i\alpha} e^{i\frac{1}{3}e_0 t/\hbar} x^{-1} \cos\left(\sqrt{\frac{\lambda}{2}} \frac{x^3}{3\hbar} + \alpha\right), \quad x \rightarrow \infty. \quad (5.29)$$

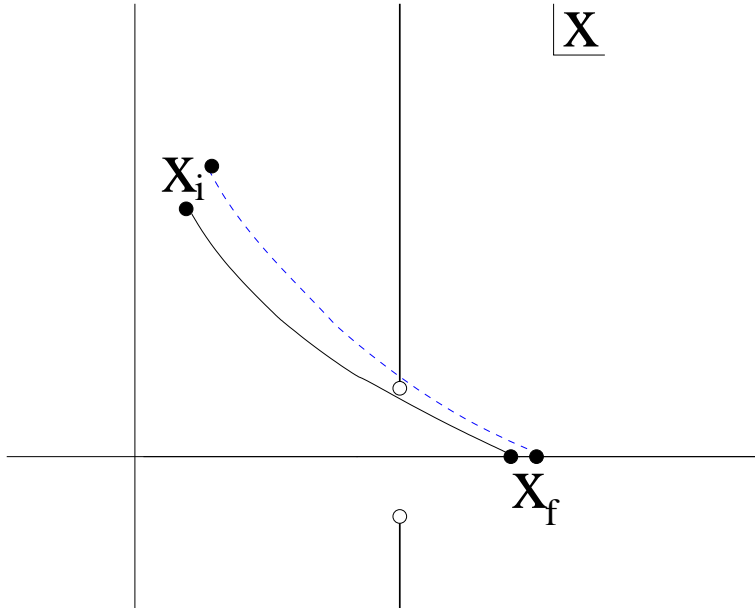


Figure 6: Two complex classical trajectories passing on either side of a branch point in $V(x)$, somewhere in the complex x -plane.

Since this is proportional to (5.23), it is obvious that $\Psi^\alpha \frac{d}{dx} \psi_E^\alpha - \psi_E^\alpha \frac{d}{dx} \Psi^\alpha$ vanishes as $x \rightarrow \infty$, for any energy eigenfunction ψ_E^α . Thus our time-dependent wavefunction $\Psi^\alpha(x, t)$ lies within the domain of the self-adjoint extension.

In this section, we have dealt only with the homogeneous mode. The analysis of Subsection 4.2 shows how this can be extended to include inhomogeneous modes, in the presence of a UV cutoff. By changing coordinates to the (τ, \mathbf{x}_s) coordinates described there, one can show that the asymptotic behavior of the classical action near the singularity locally takes the form of (5.28) and hence that the self-adjoint extension is implemented point by point in the nonlinear theory, in the presence of a UV cutoff. Our calculation of the final wavefunction $\Psi(t_f, \bar{\phi}, \delta\phi(\mathbf{x}))$ will, for values of $\bar{\phi}$ carrying most of the probability, turn out to be insensitive to the UV cutoff. Hence we can describe the most probable final states in a manner independent of the UV cutoff, although we shall not be able to do so for all values of $\bar{\phi}$.

5.3 Dealing with Branch Cuts in $V(x)$ at Complex x

The above discussion is straightforwardly generalised to potentials whose analytic continuations are meromorphic in the region of the complex plane containing the singularity and which are symmetric under reflection through it. Some additional considerations are needed to deal with potentials, like that of interest in this paper, which possess branch points in the relevant region of the complex plane.

Let us start by considering the general problem of constructing the semiclassical wavefunction in a theory where $V(x)$ possesses branch points somewhere off the real axis (Figure

6). Since $V(x)$ is real on the real x -axis, the branch points will occur in complex conjugate pairs. The branch points imply that $V(x)$ is only single valued on a nontrivial cover of the complex x -plane consisting of a set of Riemann sheets glued together across the branch cuts, which indicate the passage from one Riemann sheet to the next. A classical trajectory which runs into a branch cut should be continued onto the next Riemann sheet, upon which the potential $V(x)$ takes a different set of values at the corresponding complex coordinate x . For example, if $V(x) = \ln(x^2 + a^2)$ with a real, then there are two branch points at $x = \pm ia$. If we cross a branch cut emanating from one of them the potential changes by $\pm 2\pi i$ as we pass onto the next Riemann sheet.

We are interested in potentials $V(x)$ which are real on the real x -axis where we want to compute the wavefunction. However, if $V(x)$ has branch cuts then it is possible for a classical trajectory to cross a branch cut and go to the next Riemann sheet, on which the potential will no longer be real on the real x -axis. In some cases the branch cut can be moved out of the way and then we can simply ignore it. However, in general this will not be possible. For a given initial condition, as we vary the final coordinate x_f or the final time t_f , at some critical value the relevant classical solution may encounter the branch point. Computing the wavefunction at values of x_f or t_f just beyond the critical value then involves dealing with solutions which cross the branch cut. If we continue the solutions onto the next Riemann sheet so that they again end on the real x -axis, the resulting semiclassical wavefunction will solve the Schrödinger equation with the wrong potential $V(x)$ - the one appropriate to the next Riemann sheet. Instead, we have to change the *initial* condition of the relevant classical solution so that it begins on the next Riemann sheet and ends on the correct Riemann sheet, where $V(x)$ takes the physical value on the real x axis.

Luckily, there is a simple procedure which allows us to calculate the correct initial condition for classical solutions which cross a branch cut. It relies on the fact that as long as $V(x)$ is sufficiently well-behaved and, in particular, has no δ -function contributions, the Schrödinger wavefunction Ψ and its first space derivative $(\partial/\partial x)\Psi(t, x)$ must be continuous functions of x . Recalling that within the semiclassical approximation, $(\hbar/i)(\partial/\partial x)\Psi(t, x) \sim p(x)\Psi(t, x)$ at leading order, we see that the momentum of the classical solutions being considered must be continuous as the final coordinate x is varied.

For a given initial condition (5.1), with fixed x_c and p_c , consider decreasing x_f along the real x -axis so that at some critical value x_f^* the classical solution hits the branch point. First consider a classical solution ending just before the critical value, at $x_f^* - \epsilon$ say, with ϵ infinitesimal and positive. This solution passes just below the branch point, and ends on the real x axis with some final (generically complex) canonical momentum p_f^* . Now consider a solution ending just beyond the critical point, at $x_f^* + \epsilon$. If the semiclassical wavefunction $\Psi(t, x)$ is to be continuous and have a continuous first derivative at x_f^* , then in the limit of small ϵ the classical solution ending at $x_f^* + \epsilon$ must have the *same* final momentum p_f^* . With its final coordinate and momentum now determined, we can run this supercritical solution back in time from t_f to t_i . It will pass just above the branch point, across the branch cut, and onto the next Riemann sheet. The potential $V(x)$ will be different on this sheet and hence the trajectory followed will differ from that of the original solution. Likewise, the classical action calculated for this second solution will differ from

that of the first. Running the second solution back to t_i , we find the initial values x_i and p_i and hence the initial value of the coherent state parameter in (5.1). This new value is to be used as the initial condition for the classical solutions determining the wavefunction beyond x_f^* , assuming these solutions cross no additional branch cuts. Besides shifting the initial condition for these solutions by a discrete amount, we must also add a (complex) constant to the action S in order to ensure that the wavefunction is continuous across x_f^* . This can be thought of as a “boundary term” associated with passing around the branch point and onto the next Riemann sheet. Finally, although we have described crossing the branch point in terms of varying the final position x_f , we could have just as easily varied the final time t_f . The same procedure we have given then ensures that the wavefunction is continuous when considered as a function of time.

To summarize, when the classical solutions of interest move across a branch point, we have to make a one-off change to both their initial condition (coherent state parameter) and their action. Both changes are determined by the continuity of the wavefunction and its first x derivative on the real x -axis.

5.4 Resolving the Branch Points arising from Renormalization

For the theory at hand, we have a double problem. The renormalized effective potential for the scalar field ϕ , when written in terms of the canonically normalized variable x , is proportional to $-x^4/\ln(Cx)$. We can examine the behavior at infinite x by setting $\chi = x^{-1}$, so the potential takes the form $\chi^{-4}/\ln(\chi/C)$, with C a constant. The logarithm gives rise to a branch point at $\chi = 0$ which vitiates the construction of the self-adjoint extension given in Subsection 5.2.

In order to apply the method of images, the analytically continued potential must be even under $\chi \rightarrow -\chi$. This will be the case if $V(\chi)$ is defined with two branch cuts, running along the positive and negative portions of the real χ -axis respectively. The logarithm may then be taken to be real just above the positive real axis and just below the negative real axis. However, to solve the correct Schrödinger equation we must ensure that the potential $V(x)$ is real at the endpoint of *both* classical solutions - one of which hits the positive real χ -axis from above, and one from below. Unfortunately, we cannot have it both ways - we cannot simultaneously symmetrize the potential under $\chi \rightarrow -\chi$ and have it real on both sides of the positive real axis.

The solution of the problem is to separate the branch cuts from the fourth order pole. In Appendices C and D we show this is naturally accomplished by renormalizing the theory at a large but finite cutoff ρ , constructing the self-adjoint extension from the relevant classical solutions and then taking the cutoff to infinity at the end of the calculation. Cutting off the high momentum modes turns off the running of the coupling λ_ϕ so that, for $|\phi| \gg \rho$, λ_ϕ tends to a constant. Therefore $V(\phi)$ only has a fourth order pole and no branch point at $\phi = \infty$. The branch points associated with the logarithmic running of the coupling with $|\phi|$ have therefore been moved away from $\chi = 0$. In Appendix C we study the running coupling in detail, showing that for finite ρ there are four branch points arranged in a symmetrical pattern roughly $\sqrt{\lambda_\infty}/\rho$ from $\chi = 0$, where λ_∞ is the value of the running coupling at

$\phi = \infty$. Furthermore, the running coupling is finite and roughly equal to λ_∞ at the four branch points.

We can now discuss the construction of the semiclassical wavefunction using two classical trajectories as in Subsection 5.2. The branch cuts in V can be placed in such a way as to respect the symmetry $\chi \rightarrow -\chi$ while leaving V real on the real χ axis. As we shall see in Subsection 5.6, for very short times and small χ_f both classical solutions run close to the real axis in the small χ region. Both miss the branch cuts and the method of images works just as in Subsection 5.2. Now consider increasing the time $t_f - t_i$ or the value of χ_f , so that one of the two solutions encounters a branch point. As explained in the previous subsection, we must correct the initial conditions and the action for all subsequent solutions in order to ensure continuity of the wavefunction and its first x derivative. This procedure may be complicated to implement in practice, but its existence guarantees that, at finite cutoff ρ , we can construct a semiclassical wavefunction satisfying the correct Schrödinger equation and lying within the domain of the self-adjoint extension.

We now want to consider the limit as ρ tends to infinity. We would like to know whether the complex classical solutions we need are sensitive to the details of the UV cutoff ρ . The fact that the effective potential is finite at the branch points and varies smoothly away from them on a given Riemann sheet suggests that the infinite ρ limit may be smoothly taken. Consider two neighbouring classical solutions, as in Figure 6 running back from neighbouring values of χ_f and possessing the same energy and final momentum. They pass respectively just above and below the branch point, with one of them crossing the branch cut. Their trajectories are each given by $\dot{x} = \sqrt{2(e - V(x))}$, so the velocity difference grows smoothly away from the branch point, and the two trajectories gradually diverge. Since the difference between the trajectories builds up slowly, it is plausible that detailed structure of the potential near the branch points does not matter, and that the $\rho \rightarrow \infty$ limit can be taken *before* calculating the two relevant complex solutions.

In the limit of infinite ρ , the effective potential is proportional to $\chi^{-4}/\ln(\chi/C)$. In order to respect the $\chi \rightarrow -\chi$ symmetry we place two branch cuts along the positive and negative real χ -axis respectively. Defining $\ln(z)$ to be real for positive real z and to possess a branch cut along the negative real z -axis, $l_1(\chi) = \frac{1}{2}(\ln(\chi) + \ln(-\chi) + i\pi)$ is even and real just above the positive real χ -axis or just below the negative real χ -axis. Likewise, $l_2(\chi) = l_1(\chi) - i\pi$, which is the extension of l_1 to the next Riemann sheet, is real just below the positive real axis and just above the negative real axis.

Consider the physical situation we are interested in. We start the field in a squeezed coherent state rolling gently downhill, at nearly zero potential energy. We would like to calculate the wavefunction after one bounce, when the field has returned to a state of nearly zero potential energy. The self-adjoint wavefunction comprises two pieces, corresponding to the first and second, “image,” classical solution respectively. At the times of interest to us, the latter part of the wavefunction dominates, depending on the classical solution which started “behind” the singularity and passed around $\chi = 0$ before ending at large, positive χ_f . (Figure 9 below shows such a trajectory.) In this case, we should define the effective potential V using $l_2(\chi)$ to ensure it is real as χ approaches χ_f from below the positive real axis. This second classical solution is defined with a certain coherent state parameter

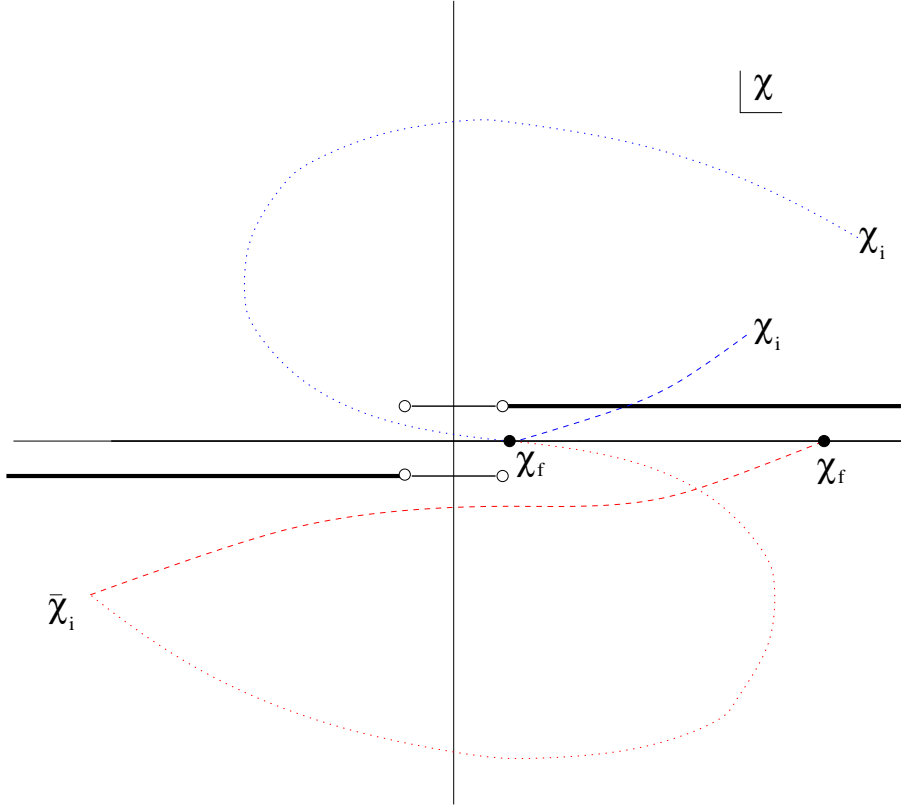


Figure 7: Contour used to show equivalence of complex class solns and SA extension.

defining x_c and p_c appearing in the initial condition (5.1). However, this is not just minus the coherent state parameter of the first classical solution, because the two solutions evolve on different Riemann sheets, where the logarithm takes the values defined by l_1 and l_2 respectively. The coherent state parameter of the first classical solution is the one which is most directly specified by the initial conditions.

In order to relate the two coherent state parameters, we must study the transition from a regime in which both solutions evolve on a single Riemann sheet. This is pictured in Figure 7. Consider the wavefunction at a time $t_f - t_i$ given by roughly twice the classical roll-down time and focus on the behavior as we vary the final value χ_f . As χ_f is lowered, the second classical solution deforms smoothly to the lower curve shown in Figure 7. This solution has to reach small χ_f in roughly twice the normal classical time. It does so by “loitering” in the lower half χ -plane with its real part first crossing zero and “rolling uphill” before turning around and rolling back to small χ . Recalling the location of the branch points in the finite ρ theory, we can draw the branch cuts so that the potential is symmetrical and the first solution is just the reflection of the first, $\chi_1(t) = -\chi_2(t)$, as long as χ_f is sufficiently small. It is clear that this entire family of classical trajectories never encounters a branch point. So we can use the potential with the log defined by $l_2(\chi)$ for all of them.

Now let us study the first classical solution. In the limit of small χ_f and in the finite ρ theory, we can draw the branch cuts as shown in Figure 7 so that the potential is symmetrical

and the first solution it is just the reflection of the first, $\chi_1(t) = -\chi_2(t)$. As χ_f is increased, the first solution crosses the branch point and runs onto the next Riemann sheet. Increasing χ_f further, the first solution has crossed both branch points. Now consider taking the $\rho \rightarrow \infty$ limit but still focusing on the values of χ_f near zero, for which the solution passes just above or below the branch points. The solution passing just below the branch points should, in this limit, evolve for almost the whole of its length on the sheet where the logarithm is l_2 . Whereas the solution passing just above both branch points should evolve for almost the whole of its length on the sheet where the logarithm is given by l_1 . Since the logarithm is very large for small $|\chi|$, the effective potential on the two sheets hardly differs at small $|\chi|$. The difference between the two classical trajectories builds up along the solution as they run to larger values of $|\chi|$.

In Appendices C and D we justify the neglect of all of the details of the finite- ρ potential in the vicinity of the branch points by first showing that all of the features of the potential, including the branch cuts, are finite and suppressed by a positive power of the perturbative coupling constant. Then we show that such small features of the potential, only relevant in the small χ region of the trajectory, have a negligible effect on the trajectory. This justifies our direct use of the infinite- ρ potential in order to compute the classical solutions.

We calculate the coherent state parameter for the first solution as follows, using the infinite ρ limit directly. We first find the solution which, with initial conditions given by reflecting those of the second classical solution and with the l_2 definition of the logarithm, hits $\chi_f = 0$ at the time t_f of interest. We then measure $\dot{\chi}$ and χ at some time very close to t_f on this solution. Then, taking these same values we switch to the l_1 definition of the logarithm and run the solution backwards in time to t_i . The values of $\dot{\chi}$ and χ measured there define the coherent state parameter for the first classical solution, and this is used to define the first piece of the semiclassical wavefunction for all positive χ_f .

In subsequent subsections, we will implement this procedure in some detail. First, we will find the relevant complex solutions analytically, in the approximation where the logarithmic dependence of the potential can be ignored. Then, after explaining how the nonzero momentum modes can be simultaneously described using the semiclassical approximation, we shall move on to a full numerical calculation of the relevant complex solutions.

5.5 Complex Solutions for ϕ with a Fixed Coupling

In this subsection, we want to explicitly construct the complex classical solution describing a bounce off the singularity at $x = \infty$. We shall in the first instance ignore the logarithmic running of the quartic coupling λ_ϕ , treating it as a constant. After a field and coupling redefinition to remove factors of the spatial volume, the action is just

$$S = \int dt \left(\frac{1}{2} \dot{x}^2 + \frac{\lambda}{4} x^4 \right). \quad (5.30)$$

Furthermore, we can remove λ by setting $\chi = \sqrt{2/\lambda} x^{-1}$, so

$$S = \frac{1}{\lambda} \int dt \frac{1}{\chi^4} ((\dot{\chi}^2 + 1)). \quad (5.31)$$

We want to find classical solutions satisfying (5.1), which reads

$$-2iL^2 \frac{\dot{\chi}_i}{\chi_i^2} + \frac{1}{\chi_i} = -2iL^2 \frac{\dot{\chi}_c}{\chi_c^2} + \frac{1}{\chi_c}, \quad t = t_i, \quad (5.32)$$

and $\chi = \chi_f$, real, at $t = t_f$. Energy conservation reads

$$\dot{\chi}^2 = 1 + 2e\chi^4, \quad (5.33)$$

with e a constant. Integrating, we obtain

$$t_f - t_i = \int_{\chi_i}^{\chi_f} \frac{d\chi}{\sqrt{1 + 2e\chi^4}}. \quad (5.34)$$

Note that L is the width of the Gaussian in the variable x : the width in the homogeneous component of the field, $\bar{\phi}$, is $\Delta\bar{\phi} = L/\sqrt{V_3}$. Eliminating $\dot{\chi}_i$ in favour of e using (5.33), equations (5.34) and (5.32) provide two complex equations for two complex unknowns, χ_i and e .

We shall solve the equations in the regime most relevant to the description of the final state after a bounce. For this, we need the second, ‘‘image’’ solution, with initial conditions that χ_c is large and negative and $\dot{\chi}_c \approx 1$ so that we are close to the zero-energy scaling solution. We want to evolve to a final χ_f which is large and positive so that we have crossed the singularity and returned to the configuration where the homogeneous component $\bar{\phi}$ is close to its initial position.

We shall look for complex classical solutions close to the real classical solution $\chi = t$, hence the imaginary part of χ will be small. Setting $\chi_i = r_i + is_i$, we first calculate the real and imaginary parts of (5.32). To linear order in s_i these read

$$\begin{aligned} s_i &\approx -\frac{2L^2}{\hbar}(\dot{r}_i - \dot{r}_c \frac{r_i^2}{r_c^2}), \\ \frac{1}{r_i} - \frac{1}{\chi_c} &\approx -\frac{2L^2}{\hbar} \left(\frac{\dot{s}_i}{r_i^2} - 2\frac{s_i \dot{r}_i}{r_i^3} \right), \end{aligned} \quad (5.35)$$

where $r_c \equiv \chi_c$ (which is real). Since the energy of the solutions we are interested in is small, it is reasonable to expand the square root in (5.34) in $e\chi^4$, assumed small. To leading order in e we obtain

$$t_f - t_i \approx \chi_f - \chi_i - \frac{e}{5}(\chi_f^5 - \chi_i^5). \quad (5.36)$$

Now we make several further approximations, again related to our assumption that the complex solutions of interest are close to the real classical solution. First, we assume s is small throughout, so we need only work to first order in s . Second, we assume that χ_i is close to χ_c , so that $r_i = \chi_c(1 - \delta)$, with $\delta \ll 1$. And finally, we assume that since δ , e and s are all small, we can ignore any term involving products of them.

The initial conditions (5.35) now give

$$s_i \approx -\frac{4L^2}{\hbar}\delta - \frac{L^2}{\hbar}2e_0\chi_c^4,$$

$$\delta \approx \frac{2L^2}{\hbar} \left(\frac{2s_i}{r_c^2} - e_1 r_c^3 \right), \quad (5.37)$$

where $e = e_0 + ie_1$, with e_0 and e_1 real. In the same approximation, (5.36) reads

$$\begin{aligned} t_f - t_i &\approx \chi_f - \chi_c - \frac{e_0}{5}(\chi_f^5 - \chi_c^5) + \chi_c \delta, \\ s_i &\approx -\frac{e_1}{5}(\chi_f^5 - \chi_c^5). \end{aligned} \quad (5.38)$$

Equations (5.37) and (5.38) provide four equations for four unknowns, s, δ, e_0 and e_1 . We consider a final χ_f close to $-\chi_c$, so we are looking at the final wavefunction around the initial value of $\bar{\phi}$, to first order in small quantities. We find

$$\begin{aligned} s_i &= -\frac{5L^2}{\hbar} \frac{\mathcal{J}}{\chi_c} \frac{1}{1 + L^4(\hbar\chi_c)^{-2}}, \\ \delta &= -\frac{L^2}{\hbar\chi_c^2} s_i, \\ e_0 &= -\frac{5}{\chi_f^5 - \chi_c^5} (\mathcal{J} - \chi_c \delta), \\ e_1 &= -\frac{5}{\chi_f^5 - \chi_c^5} s_i, \end{aligned} \quad (5.39)$$

where $\mathcal{J} = t_f - t_i - (\chi_f - \chi_c)$ measures the deviation of the argument of the wavefunction from the classical zero-energy solution.

Of particular interest to us later will be the minimum value of $|\chi|$ attained, since that will act as a UV cutoff for the quantum production of inhomogeneous fluctuations. Evaluating (5.34), with t_i replaced by t , we find s is quintic in r and

$$s_{min} = -\frac{e_1}{5} \chi_f^5 = \frac{1}{2} s_i, \quad (5.40)$$

with s_i given by (5.39). Neglecting the quantum spreading term, we have

$$s_{min} \approx -\frac{5}{2} L^2 \frac{\mathcal{J}}{\chi_c}, \quad (5.41)$$

where, as we recall, L is the width of the initial Gaussian wavepacket in x , χ_c is the initial value of the homogeneous mode of χ and \mathcal{J} is the deviation of χ_f from the final value expected from classical evolution.

Let us now translate this result into the situation of interest. We want to consider an initial Gaussian wavepacket with nearly zero energy, but over the barrier, *i.e.*, centered on $\phi_c \sim \lambda_\phi^{-1/2} R_{AdS}^{-1}$. We parameterize the initial width $\Delta\phi$ of the Gaussian in terms of the width $\Delta\phi_{min}$ which minimizes the spread of the wavepacket over the entire duration of the putative bounce, a time of order R_{AdS} . It makes sense to perform the calculation in terms of the variable χ , defined so that $\chi = |t|$ is the classical zero-energy scaling solution. In the presence of the running logarithm we thus define $\chi = \int_\phi^\infty d\phi (2/\lambda_\phi)^{1/2} \phi^{-2}$. The final

variance in χ is then approximately given by $\Delta\chi_i^2 + R_{AdS}^2(\Delta\dot{\chi}_i)^2$. Here $\Delta\dot{\chi}_i \sim \Delta\dot{\phi}\lambda_\phi^{-1/2}\phi^{-2} = \pi_\phi V_3^{-1}\lambda_\phi^{-1/2}\phi^{-2} \sim (\Delta\phi)^{-1}V_3^{-1}\lambda_\phi^{-1/2}\phi^{-2} \sim \lambda_\phi R/(\Delta\chi_i)$. Thus the final variance is $\Delta\chi_i^2 + \lambda_\phi^2 R_{AdS}^4/(\Delta\chi_i)^2$, minimized by $\Delta\chi_i \sim \lambda_\phi^{1/2}R_{AdS} \ll \chi_i \sim R_{AdS}$. The corresponding value of $\Delta\phi_{min}$ is $R_{AdS}^{-1} \ll \phi_c$.

We shall write the width of our initial wavepacket $\Delta\phi = W\Delta\phi_{min}$, where W is a dimensionless parameter. From (5.41), the value of s_{min} is, for typical values of χ_f where the wavefunction has most of its support, of order $R_{AdS}\Delta\chi_i/\chi_i \sim W\lambda_\phi^{1/2}R_{AdS}$. As we shall see later, this small imaginary part for the classical homogeneous background $\bar{\phi}$ provides a UV cutoff on particle production across the bounce, for a range of final values of $\bar{\phi}_f$ carrying most of the probability.

Before we calculate particle production in this background, however, we want to study the large- $\bar{\phi}$ behavior of the wavefunction at very short times, in order to justify our claim that the quantum spreading cannot be ignored, in principle, for arbitrarily short times and hence the dynamical evolution cannot even be discussed without imposing a unitary boundary condition at $\bar{\phi} = \infty$.

5.6 Behavior of the Wavefunction at Large $\bar{\phi}$ and Small t

One of the unusual features of the system we are considering is that even though the quantum evolution of any state is perfectly well-defined, neither the expectation value of the homogeneous mode $\bar{\phi}$, nor any of its correlators, exist. Hence the usual description of quantum field theory in terms of correlation functions of fields, does not, strictly speaking, make sense. Instead, one has to deal directly with the wavefunction itself. That the correlation functions are in general ill-defined may be seen from (4.6), for example. Even though the energy eigenfunctions are all normalizable since $|\Psi|^2 \sim x^{-2} \cos^2(Ax^3 + \alpha)$ at large x , the expectation of $x = \bar{\phi}V_3^{1/2}$ is a meaningless logarithmically divergent integral $\sim \int dx/x \cos^2(Ax^3 + \alpha)$ in any one of them.

At first sight, this behavior appears puzzling. There is no problem in setting up a Gaussian wavepacket at time $t = 0$. In such a wavepacket, the expectation value of x or any integral power of x is well-defined. Likewise, the time derivative $(d/dt)\langle x \rangle = \langle \dot{x} \rangle = \langle p \rangle$, is also perfectly well-defined. Using the Heisenberg equations of motion, one can express the n 'th time derivative of $\langle x \rangle$ as an expectation value of a polynomial in x and p , whose value is perfectly well-defined at the initial time. Hence, formally, $\langle x \rangle$ is a function whose value and time derivatives to any order are finite at $t = 0$. Nevertheless, $\langle x \rangle$ does not actually exist, for any $t > 0$.

We can understand what happens by calculating the semiclassical wavefunction using complex classical solutions. Consider the case where we are given a Gaussian wavepacket for x whose initial coordinate x_c is small, and initial speed \dot{x}_c is given by the zero-energy scaling solution. We want to study the form of the wavefunction at very large x_f , at small positive final times t_f . (We set $t_i = 0$ in this subsection.)

As in the previous subsection, we change variables to $\chi = (2/\lambda)^{1/2}x^{-1}$, for which the initial conditions are given by (5.32) with $\chi_c \ll 1$ and $\dot{\chi}_c = -1$. Again, conservation of

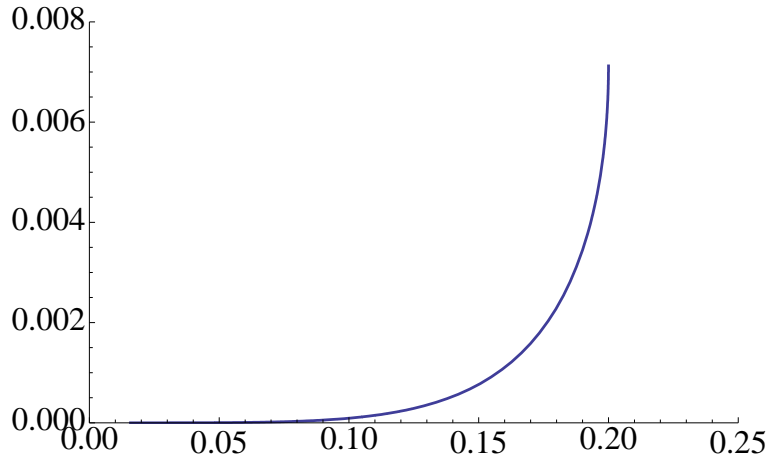


Figure 8: Complex classical solution describing the large- ϕ , small time behaviour of the wavefunction for the homogeneous background. The trajectory of the variable χ is plotted in the complex χ -plane.

energy yields

$$\dot{\chi} = -\sqrt{1 + e\chi^4}, \quad (5.42)$$

with e a constant. The sign is chosen because the solution we are interested in runs from some large initial χ to a very small real final χ_f , after a short time t_f . The form of the solution is illustrated in a specific numerical example in Figure 8.

Recall that the classical solution does not need to start at χ_c . If we take χ_c large, the second term on the right hand side of (5.32) dominates. We now solve for the initial velocity,

$$\dot{\chi}_i = \frac{1}{2iL^2}\chi_i \left(1 - \frac{\chi_i}{\chi_c}\right), \quad (5.43)$$

which is small and nearly negative imaginary if χ_i is nearly real. In order to achieve consistency with (5.42), we must take χ_i close to the branch point in the right hand side of (5.42), $\chi_i \approx \chi_B = (-e)^{-\frac{1}{4}}$. If $e = e_0 + ie_1$ with e_0 large and negative, and e_1 small and positive, then $\chi_B \approx (-e_0)^{-\frac{1}{4}}(1 - ie_1/(4e_0))$ has a small positive imaginary part. Setting $\chi = \chi_B + \delta\chi$, (5.42) reads

$$\dot{\chi} = -2(-\delta\chi)^{\frac{1}{2}}(-e)^{\frac{3}{8}}. \quad (5.44)$$

Thus, if χ starts out just to the right of χ_B , *i.e.*, with $\delta\chi$ small and positive, then from (5.44), $\dot{\chi}_i$ is negative imaginary as required. As χ runs downwards towards the real χ -axis, from (5.44), $\dot{\chi}$ turns towards the origin so that χ heads to small, real values. Solving (5.43) and (5.44) for $\delta\chi$, we find

$$\chi_i = (-e)^{-\frac{1}{4}} \left(1 - \frac{1}{16L^4e}\right), \quad (5.45)$$

just to the right of the branch point.

If the real part of the energy e_0 is large and negative, as we have assumed, then χ_i is small. We are assuming that χ_f is even smaller. But then (5.34) becomes

$$t_f - t_i \approx \int_0^{\chi_i} \frac{d\tilde{\chi}}{\sqrt{1 - (\tilde{\chi}/\chi)^2}} = \chi_i \int_0^1 \frac{dz}{\sqrt{1 - z^4}} = \kappa \chi \quad (5.46)$$

where $\kappa = \sqrt{\pi}(\Gamma(\frac{5}{4})/\Gamma(\frac{3}{4})) = 1.31103\dots$ is the complete elliptic integral of the first kind with parameter i . From this value of χ_i , (5.43) gives $\dot{\chi}_i$. Neglecting terms down by χ_i/χ_c , and using (5.46) we obtain

$$\dot{x} = -\sqrt{2/\lambda} \frac{\dot{\chi}_i}{\chi_i^2} = \frac{i\kappa}{(2\lambda)^{1/2} L^2 t_f^2}, \quad (5.47)$$

at the initial time. Armed with this classical solution, we can compute the classical action, with the boundary term (5.10). The integral is dominated by times t near t_* , the time when the solution, if continued past t_f , would encounter the singularity:

$$S_{Cl} = \int_0^{t_f} dt \frac{1}{\lambda(t_* - t)^4} + \frac{iL^2 \dot{x}_i^2}{i\hbar}. \quad (5.48)$$

The integral is re-expressed in terms of x_f using $t_* = t_f + (2/\lambda)^{1/2} x_f^{-1}$; the boundary term is computed from (5.47). We obtain

$$\frac{iS_{Cl}}{\hbar} \approx i \frac{(\lambda/2)^{1/2} x_f^3}{3\hbar} - \frac{\kappa^2}{2\hbar^2 \lambda L^2 t_f^2}. \quad (5.49)$$

Now we can read off the behavior of the wavefunction at very large x_f for small final times t_f . Including the contribution from the second classical solution, where the initial conditions were reflected through $\chi = 0$, we find for the total wavefunction at large x and small times t_f ,

$$\Psi(x, t_f) \sim x^{-1} \exp\left(-\frac{\kappa^2}{2\hbar^2 \lambda L^2 t_f^2}\right) \cos\left(\sqrt{\frac{\lambda}{2}} \frac{x^3}{3\hbar} + \alpha\right). \quad (5.50)$$

Note that the exponential factor $\sim e^{-ct_f^{-2}}$, with c a constant, is indeed a function whose value and time derivatives of arbitrary order vanish at $t = 0$. Nevertheless, the function is nonzero for any nonzero t . Thus, although correlators of x or p are well defined at $t = 0$, for any positive t the probability acquires a tail at large x proportional to x^{-2} times an oscillatory factor which averages to $\frac{1}{2}$. Thus for any positive time t , the expectation value of x^n with $n \geq 1$ does not exist.

5.7 Complex Solutions for ϕ with a Running Coupling

As we shall see later, a critical factor in our calculations will be the running of the quartic coupling λ : although this is a weak effect, without it, the particle production would vanish

at linearized order. We start from the effective potential obtained in (3.22),

$$S = \int d^4x \left(-\frac{1}{2}(\partial\phi)^2 + \frac{\lambda_\phi}{4}\phi^4 \right), \quad (5.51)$$

and we again ignore the curvature of the S^3 because this is unimportant near the singularity. We are interested in the regime where the logarithm l in the denominator of λ_ϕ is large: in this regime, the logarithm varies slowly with ϕ and we can solve the equations of motion in an expansion in inverse powers of l .

As before, we first change variables to $\chi = (2/\lambda_0)^{\frac{1}{2}}\phi^{-1}$, obtaining the action

$$\mathcal{S} = \frac{1}{\lambda_0} \int \frac{d^4x}{\chi^4} (-(\partial\chi)^2 + l^{-1}). \quad (5.52)$$

In order to minimize the effect of the logarithm, we redefine the field variable, setting

$$d\chi_l = l^{\frac{1}{2}}(\chi) d\chi, \quad (5.53)$$

where $l = \ln \left((2/\lambda_0)^{\frac{1}{2}}/(NM\chi) \right)$. This is solved by

$$\chi_l = l^{\frac{1}{2}}h(l)\chi; \quad h(l) = 1 + \frac{1}{2l} - \frac{1}{4l^2} + \frac{3}{8l^3} \dots \quad (5.54)$$

We obtain the following action for χ_l ,

$$\mathcal{S} = \frac{1}{\lambda_0} \int \frac{d^4x l h^4(l)}{\chi_l^4} (-(\partial\chi_l)^2 + 1), \quad (5.55)$$

in which form it is clear that at small χ , one obtains a large classical action and therefore one can expect the semiclassical approximation to become accurate. The equation of motion for χ_l is

$$-\chi_l \partial^2 \chi_l + 2(\partial\chi_l)^2 + 2 = -2g(l) \left((\partial\chi_l)^2 + 1 \right), \quad (5.56)$$

where $g(l) = h(l) - 1 - \frac{1}{4}l^{-1}h(l) = \frac{1}{4}l^{-1}(1 - \frac{3}{2}l^{-1} + \frac{7}{4}l^{-2} + \dots)$.

From (5.56) one observes that $\chi_l = \pm(t_s - t)$ with constant t_s still solves the equation, just as before. By redefining the field as we have, we have removed the logarithmic corrections from the background solution. We could proceed to write the general solution in the vicinity of a spacelike singularity by simply modifying (4.17) so that each coefficient of τ^n , $n \geq 2$ and $\tau^n \ln \tau$, $n \geq 5$, becomes a series in inverse powers of l . Near the singularity, l diverges so these logarithmic corrections become less and less significant.

Figure 9 shows an example of a complex solution to equation (5.56) describing the homogeneous mode $\chi_l(t)$. This solution corresponds to the “image” solution which starts out behind the singularity at $\chi = 0$ and runs to a positive real final value χ_f . Notice that the behavior of the complex solution is very simple in the vicinity of the origin: χ_l is well-approximated in this region as $\chi_l = t - i\epsilon$ with ϵ a constant. In the next section, we shall discuss the evolution of the inhomogeneous modes in this background.

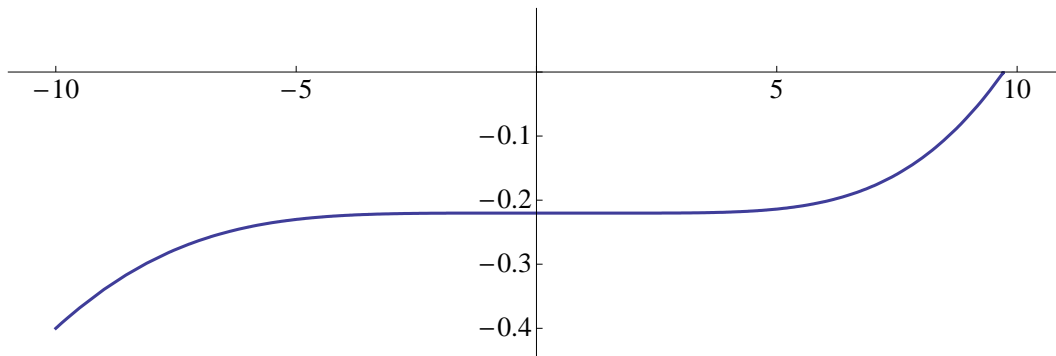


Figure 9: Complex classical background solution in which particle production is computed, including the effect of the running coupling. The parameters used were $NM = 10^{-5}$, $L = 1$, $t_i = -10$, $r_i = 10^{-5}$, $s_i = -0.4$, $t_f = 8.4$.

6 Quantum Evolution of the Inhomogeneous Modes

Having discussed the quantum description of the homogeneous mode of the scalar field, we turn to the quantum evolution of the inhomogeneous modes,

$$\phi(t, \mathbf{x}) = \sum_{\mathbf{k}} \phi_{\mathbf{k}}(t) Y_{\mathbf{k}}(\mathbf{x}), \quad (6.1)$$

where $Y_{\mathbf{k}}(\mathbf{x})$ are the spherical harmonics on S^3 , and \mathbf{k} are the corresponding eigenvalues. We shall be interested in modes whose wavelength is much shorter than the radius of the S^3 , *i.e.*, R_{AdS} , so that we can approximate the spherical harmonics with plane waves $e^{i\mathbf{k}\cdot\mathbf{x}}$. As explained in Appendix B, our calculational procedure is to integrate out the oscillatory modes, *i.e.*, those for which $|kt| > 1$, and to study the long-wavelength modes, *i.e.*, those for which $|kt| < 1$, in the linearized approximation where we neglect their backreaction on the homogeneous mode. As we shall see, particle creation will turn out to be finite and suppressed by powers of the coupling λ_ϕ (see (3.23)), so this approximation is reasonable for small λ_ϕ .

We want to describe the homogeneous mode, and the $\mathbf{k} \neq 0$ modes, in a single semi-classical wavefunction, obtained from complex, spatially inhomogeneous solutions to the classical equation of motion for the field. In the case where the quantum spreading of the wavefunction is negligible for the homogeneous background, this treatment will reproduce the usual description of quantum field theory in time-dependent backgrounds, where one uses the Heisenberg picture to compute Bogoliubov coefficients, and then studies particle creation etc. We shall describe the same phenomena in the more general context of a quantum mechanical background, using the Schrödinger wavefunction, calculated from complex classical solutions. Before proceeding with our specific case, let us then briefly review how a quantum field in a time-dependent background can be described in the Schrödinger picture (see, for example, Ref. [55]).

6.1 Particle Production Using Complex Classical Solutions

The description of linearised perturbations around a time-dependent, spatially homogeneous background can always be framed (after a possible field redefinition to put the kinetic term into canonical form) in terms of a quadratic action

$$\mathcal{S} = \int dt \frac{1}{2} (\dot{q}^2 - \omega^2(t)q^2), \quad (6.2)$$

where q is the coordinate of the particular linearized mode being considered (for example, the real or imaginary part of the $\phi_{\mathbf{k}}$ mode coefficients in (6.1) above) and $\omega^2(t)$ is a time-dependent frequency squared.

We would like to describe the situation where the inhomogeneous modes start out in the incoming adiabatic vacuum. That is, we assume that for the modes of interest, ω^2 is positive, and $\dot{\omega}/\omega^2$ is far smaller than unity, so that the mode behaves like a harmonic oscillator with a slowly-varying frequency. We also assume that every mode starts out in its adiabatic ground state. This is a special case of the formalism described above, for describing the time evolution of Gaussian wavepackets. In the present case, the initial width of the Gaussian is determined in terms of the frequency ω . It is straightforward to determine the classical action, including the boundary term needed to describe the incoming adiabatic vacuum: in canonical Hamiltonian form,

$$\mathcal{S}_{Cl} = \int dt \left(p\dot{q} - \frac{1}{2}(p^2 + \omega^2(t)q^2) \right) + \frac{p_i^2}{2i\omega_i}, \quad (6.3)$$

where p_i and $\omega(t_i)$ are the initial momentum and frequency. In order to calculate the Schrödinger wavefunction for the mode, the correct initial and final conditions are:

$$p = \dot{q} = i\omega(t_i)q, \quad t = t_i; \quad q = q_f, \quad t = t_f, \quad (6.4)$$

with q_f real. The equation of motion is just $\ddot{q} = -\omega^2 q$, and we assume that at t_i the evolution is adiabatic. Hence the two independent solutions are proportional to $e^{+i\int \omega dt}$ and $e^{-i\int \omega dt}$ respectively. Clearly, the initial condition (6.4) selects the former – the incoming positive frequency mode, which we shall denote $R_{in}^{(+)}$, while the final condition specifies its amplitude. The desired solution is then just

$$q(t) = \frac{R_{in}^{(+)}(t)}{R_{in}^{(+)}(t_f)} q_f. \quad (6.5)$$

We then easily compute the classical action (6.3), using integration by parts and the equation of motion to obtain

$$\Psi \sim e^{i\frac{\mathcal{S}_{Cl}}{\hbar}}, \quad \mathcal{S}_{Cl} = \frac{1}{2} \frac{\dot{R}_{in}^{(+)}}{R_{in}^{(+)}} q_f^2. \quad (6.6)$$

This formula agrees with that obtained by solving the time-dependent Schrödinger equation, given for example in Ref. [55].

Having obtained the complete q_f dependence of the Schrödinger wavefunction, we would like to calculate the number of particles in the final state. The calculation is straightforward. First, we construct the creation and annihilation operators in the Schrödinger picture, at the final time t_f :

$$a = \frac{ip_f + \omega_f q_f}{\sqrt{2\omega_f \hbar}} = \frac{1}{\sqrt{2\omega_f \hbar}} \left(\hbar \frac{d}{dq_f} + \omega_f q_f \right), \quad a^\dagger = \frac{-ip_f + \omega_f q_f}{\sqrt{2\omega_f \hbar}} = \frac{1}{\sqrt{2\omega_f \hbar}} \left(-\hbar \frac{d}{dq_f} + \omega_f q_f \right). \quad (6.7)$$

Since $\omega_f \equiv \omega(t_f)$ is real, a^\dagger is the Hermitian conjugate of a , and the number of particles in this mode in the final state is

$$\langle n \rangle = \frac{\int dq_f \Psi^* a^\dagger a \Psi}{\int dq_f \Psi^* \Psi} = \frac{|\dot{R}_{in}^{(+)} - i\omega_f R_{in}^{(+)}|^2}{(-2i\omega_f) \left((R_{in}^{(+)*})^* \dot{R}_{in}^{(+)} - R_{in}^{(+)} (\dot{R}_{in}^{(+)*})^* \right)}. \quad (6.8)$$

This is our final result, giving the expected number of particles in mode k in terms of the behavior of the incoming positive frequency mode at late times. In the next subsections, we shall use this formula to derive the spectrum of produced particles.

In passing, let us note the relation between (6.8) and the usual Bogoliubov coefficients, calculated by evolving the inhomogeneous field modes in a real classical background. If the mode evolution is adiabatic at the final time t_f , we can express the incoming positive frequency mode in terms of the outgoing positive and negative frequency modes,

$$\begin{aligned} R \equiv \dot{R}_{in}^{(+)} &\rightarrow \frac{e^{+i \int^t \omega dt}}{\sqrt{2\omega}}, & t \rightarrow t_i, \\ &\rightarrow \frac{\alpha e^{+i \int^t \omega dt} + \beta e^{-i \int^t \omega dt}}{\sqrt{2\omega}}, & t \rightarrow t_f, \end{aligned} \quad (6.9)$$

with ω nearly constant and real. Substituting (6.9) into (6.8) we obtain

$$\langle n \rangle = \frac{|\beta|^2}{|\alpha|^2 - |\beta|^2}. \quad (6.10)$$

If ω is always real, then the conservation of the Wronskian $R^* \dot{R} - \dot{R}^* R$ yields $|\alpha|^2 - |\beta|^2 = 1$. However, when ω is complex, we have to use the more general result (6.10).

In this subsection we have shown how complex solutions of the classical field equations may be used to compute the Schrödinger wavefunction for the fluctuation modes. In the following subsections we shall solve for the positive frequency mode and explicitly determine $\langle n \rangle$ for various particle species in the dual theory.

Before doing so, let us make the following general point. When the Higgs field Φ_1 , whose magnitude we have parameterised by ϕ , rolls to large values, certain gauge, Higgs and Fermi particles acquire time-dependent masses \mathcal{M} of order $g\phi$, where g is the Yang-Mills gauge coupling. A dimensionless measure of the slowness of increase of \mathcal{M} , *i.e.* the adiabaticity of the change in \mathcal{M} , as the singularity approaches is $\dot{\mathcal{M}}/\mathcal{M}^2$. If this quantity is small, one expects particle production of particles of mass \mathcal{M} to be exponentially suppressed. In our

case, using the scaling solution $\dot{\phi} \sim (\lambda_\phi/2)^{1/2}\phi^2$ we have $\dot{\mathcal{M}}/\mathcal{M}^2 \sim \sqrt{\lambda_\phi}/g$, which tends to zero as the singularity approaches because λ_ϕ is asymptotically free (see (5.51)). The situation is further improved when one takes into account the dependence on N , arising from the gauge group $SU(N)$ of the dual theory. To study the theory at large N , one keeps the 't Hooft coupling $g_t = g^2 N$ fixed, while $\lambda_\phi = 2a^2/N^2 \ln(\phi/NM)$ (see (5.51) and (3.23)). Hence the parameter measuring the departure from adiabaticity in the massive fields is $\dot{\mathcal{M}}/\mathcal{M}^2 \sim 1/(g_t N \ln(\phi/NM))^{1/2}$.

Therefore, when the logarithm and N are large, it should be a good approximation to integrate out the particles with masses of order $g\phi$ and consider only the remaining degrees of freedom with tachyonic masses (the fluctuations $\delta\phi$ in the rolling field itself), with light masses, like Higgs modes acquiring their mass only from the deformation, or zero mass, like the massless gauge bosons.

In the following subsection, we shall derive the equations of motion for the relevant quantum field in each case and show that, in an expansion in inverse powers of the logarithm $l \equiv \ln(\phi/NM)$, to lowest order there is no particle creation in the vicinity of the singularity. Then, in the subsequent three subsections, we shall calculate the particle production in each species at the first nontrivial order in an expansion in inverse powers of l .

6.2 Equations of Motion for Inhomogeneous Fluctuations

In the following subsections, we shall compute the evolution of the inhomogeneous modes and the resulting particle production. We focus on those wavenumbers which depart from adiabatic oscillatory behavior (or, in more colloquial language, which “freeze out”), in the regime of large ϕ where the classical background is well-described by the zero-energy scaling solution.

Let us start by recalling the zero energy real scaling solution,

$$\dot{\phi} = -\sqrt{\frac{\lambda_\phi}{2}}\phi^2, \quad \lambda_\phi = \frac{\lambda_0}{l}, \quad l = \ln(\phi/NM), \quad \lambda_0 = \frac{2a^2}{N^2}. \quad (6.11)$$

Note that for the final times we are considering, roughly the time taken for the field to roll classically to infinity and bounce back, the quantum wavefunction is dominated by the second, “image” complex classical solution in which ϕ emerges from “behind” the singularity. We can integrate (6.11) to obtain

$$\sqrt{\frac{\lambda_0}{2}}|t| = \int_\phi^\infty \frac{d\phi l^{\frac{1}{2}}}{\phi^2} = \frac{l^{\frac{1}{2}}}{\phi} \left(1 + \frac{1}{2l} + \dots\right) \quad (6.12)$$

where the singularity has been placed at $t = 0$ and the series in l^{-1} is obtained by repeated integration by parts. From this we obtain

$$\phi = \sqrt{\frac{2}{\lambda_0}} \frac{l^{\frac{1}{2}}}{|t|} \left(1 + \frac{1}{2l} + \dots\right) \quad (6.13)$$

It is also useful to calculate the time derivative of l ,

$$\dot{l} = -\frac{1}{t} \left(1 + \frac{1}{2l} + \dots\right). \quad (6.14)$$

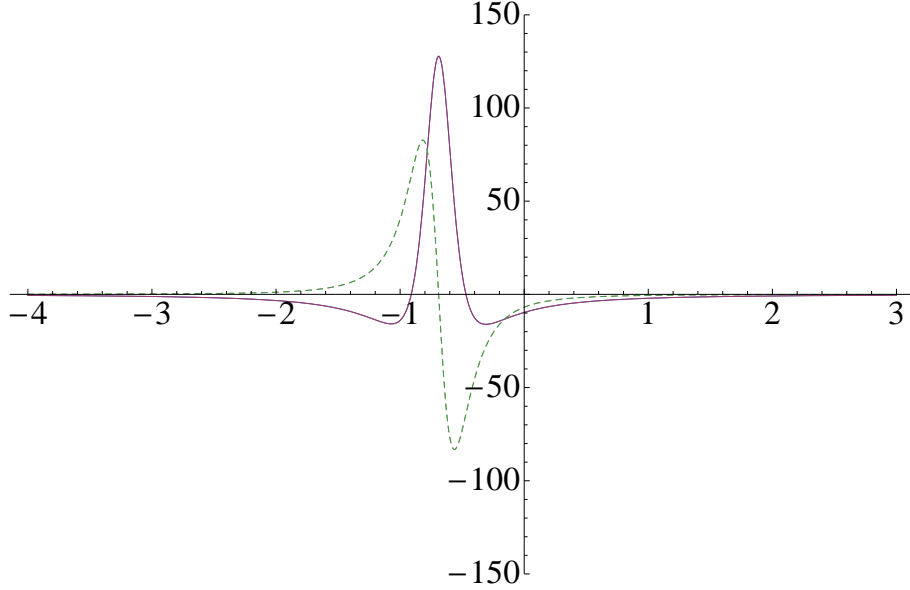


Figure 10: The frequency squared ω^2 (see equation (6.15)) from the full complex numerical solution compared with the approximation $\chi_l = t - i\epsilon$. The two sets of curves show the real part of ω^2 and its approximation (solid curves, red and blue), and the imaginary part of ω^2 and its approximation (dashed curves, green and yellow). The curves corresponding to numerical and approximate solutions are indistinguishable in the figure. Parameters are as in Figure 9.

As we have explained at the end of Subsection 5.7, the complex solution which describes the homogeneous mode in the vicinity of the singularity is obtained by replacing t with $t - i\epsilon$ in the above expressions.

The equation of motion for the inhomogeneous perturbation modes is obtained by computing $V_{,\phi\phi}$ and substituting (6.13). One finds

$$\begin{aligned}
\ddot{\delta\phi} &= \left(-k^2 + \frac{3\lambda_0\phi^2}{l} \left(1 - \frac{7}{12}l^{-1} + \frac{1}{6}l^{-2} \dots \right) \right) \delta\phi \\
&\approx \left(-k^2 + \frac{6}{\chi_l^2} \left(1 + \frac{5}{12}l^{-1} - \frac{2}{3}l^{-2} \dots \right) \right) \delta\phi \\
&\equiv -\omega^2\delta\phi,
\end{aligned} \tag{6.15}$$

where in obtaining the second line we have used the definition (5.54) of χ_l , which is well-approximated by $t - i\epsilon$ in the complex classical background of interest (see Subsection 5.7). A check on the accuracy of this substitution is given in Figure 10, where we plot the numerically calculated complex frequency squared, ω^2 in (6.15), versus the approximation obtained by setting $\chi_l = t - i\epsilon$, with ϵ a constant. Clearly, this is an excellent approximation over a wide range of times, and hence for a wide range of wavenumbers k .

We wish to solve equation (6.15) as a series in l^{-1} . At lowest order, (6.15) becomes

$$\delta\ddot{\phi} = \frac{6}{(t - i\epsilon)^2} \delta\phi - k^2 \delta\phi, \quad (6.16)$$

which is regular for real t . The solutions are $(t - i\epsilon)^{\frac{1}{2}}$ times Bessel functions of order $\nu = 5/2$. The two linearly independent solutions may be taken to be:

$$f^{(1)} = \cos k\tilde{t} \left(\frac{1}{(k\tilde{t})^2} - \frac{1}{3} \right) + \frac{\sin k\tilde{t}}{k\tilde{t}}, \quad f^{(2)} = \sin k\tilde{t} \left(\frac{1}{3} - \frac{1}{(k\tilde{t})^2} \right) + \frac{\cos k\tilde{t}}{k\tilde{t}}. \quad (6.17)$$

where $\tilde{t} = t - i\epsilon$. The incoming positive frequency mode, *i.e.*, the solution tending to e^{ikt} at large negative times, is just $-3(f^{(1)} - if^{(2)})e^{-k\epsilon}$. Evolving this to large positive times, we find there is no negative frequency component and, from (6.8), the net particle production is zero. To discuss the next order in l^{-1} we shall have to solve (6.15) to this order and we shall do so in the following subsection.

Let us now work out the equation of motion for the light Higgs particles, *i.e.*, those acquiring masses solely from the deformation. The latter contributes a time-dependent positive mass squared $\frac{1}{5}\lambda_\phi \text{Tr}(\Phi_1^2) = \frac{1}{5}\lambda_\phi \phi^2$ to each of the Higgs fields Φ_i , $i = 2, \dots, 6$. In the scaling solution for ϕ , the linearized equations of motion for the light Higgs fields are

$$\ddot{\Phi}_i = -\frac{2}{5(t - i\epsilon)^2} (1 + l^{-1} + \dots) \Phi_i - k^2 \Phi_i, \quad i = 2, \dots, 6. \quad (6.18)$$

To lowest order in l^{-1} , the solutions are $(t - i\epsilon)^{\frac{1}{2}}$ times Bessel functions of imaginary order $\nu = i\sqrt{3/20}$. As for the tachyonic modes, an incoming positive frequency mode evolves to an outgoing positive frequency mode and there is no particle production. We solve (6.18) to next order in l^{-1} in Subsection 6.3.

Finally, let us consider the gauge bosons that do not acquire a mass from Φ_1 . Even with the deformation, there is no coupling between these light gauge fields and Φ_1 in the classical Lagrangian. The rolling field generates no gauge current, and therefore does not directly source the gauge fields. However, a coupling does arise at one loop order. As can be seen from the results of Ref. [56] for example, integrating out the massive Higgs, Fermi and gauge bosons results in an effective Lagrangian for the remaining massless gauge bosons of the form $-\frac{1}{4}F^2 \left(1 + \alpha \sum_{i=S,F,V} c_i \text{Tr}(M_i^2/\mu^2) \right)$, where $\alpha = g^2/(16\pi^2)$, μ is a renormalization scale and the trace is taken over scalars (with $c_S = \frac{1}{6}$), fermions (with $c_F = \frac{4}{3}$ per Dirac fermion) and gauge bosons (with $c_V = -\frac{11}{3}$). The mass matrices for the heavy particles depend on the orientation of the Higgs field Φ_1 in $SU(N)$ space. In general position, the simplest case to consider, the gauge group breaks to $U(1)^{N-1}$ and all but $N - 1$ gauge, Higgs or fermi particles acquire masses of order $g\phi$. In the undeformed theory, there are six scalars, two Dirac fermions and one vector so the correction vanishes by supersymmetry. The deformation alters the scalar mass matrix, $M_S^2 \sim g^2\phi^2 \rightarrow g^2\phi^2 + \lambda_\phi\phi^2$, up to numerical factors, leaving the other terms unchanged. The effective massless gauge boson Lagrangian is then $-\frac{1}{4}F^2(1 + Cl^{-1})$, with C a constant. The second term can also be derived from the finite Feynman diagram shown in Figure 11.

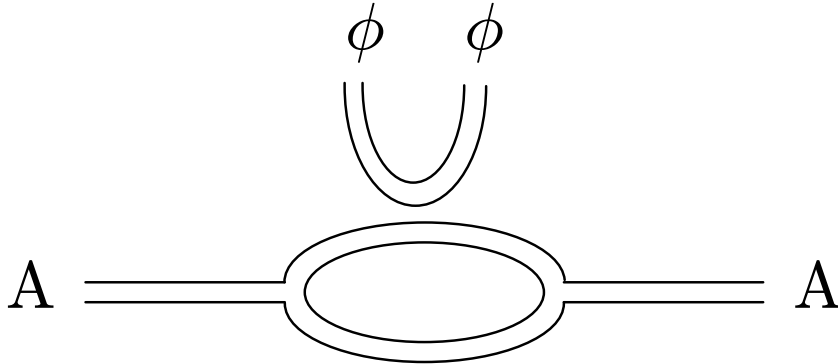


Figure 11: Feynman diagram for the one-loop correction to the kinetic term of the massless gauge bosons.

The equation of motion for the transverse massless gauge bosons acquires a damping correction term as follows, to leading nontrivial order,

$$\ddot{A}_\perp - Cl^{-2} \frac{1}{(t - i\epsilon)} \dot{A}_\perp + k^2 A_\perp = 0. \quad (6.19)$$

Ignoring the l^{-2} term, the solutions are trivial and a positive frequency incoming mode evolves to a positive frequency outgoing mode. We solve (6.19) to order l^{-2} in Subsection 6.5.

In summary, in this subsection we have derived the equations of motion for the quadratic fluctuations which cannot be integrated out and which suffer significant particle production. In each case, to zeroth order in l^{-1} , the incoming positive frequency mode is proportional to $(t - i\epsilon)^{\frac{1}{2}} H_\nu^{(2)}(k(t - i\epsilon))$ and it evolves to an outgoing positive frequency mode, so there is no particle production across the singularity. Similar behavior was encountered in Ref. [57], which studied quantum fields on compactified Milne spacetime. In that case, ϵ was introduced to define a particular choice of continuation across the singularity. Here, we are in a better situation: ϵ is a physical parameter determined by the final state of the homogeneous “background” and for $\epsilon \neq 0$ the time evolution of the linearized perturbations is completely unambiguous. Later in this paper we shall argue that, within a certain parameter regime, except for a small band of final states very close to the real classical solution, with ϵ nearly zero, the backreaction due to particle creation is perturbatively small.

In the next three subsections, we compute the particle production to leading nontrivial order in the asymptotically free coupling λ_ϕ .

6.3 Production of $\delta\phi$ Excitations with a Running Coupling

In this subsection, we shall compute the evolution of the inhomogeneous modes when the logarithmic running is included in an expansion in l^{-1} . It is convenient to ignore ϵ at first:

having obtained the solution of (6.15) we can then simply replace t with $t - i\epsilon$ and continue unambiguously from negative to positive times.

The effect of the logarithm on the linearized perturbations at long wavelengths $|kt| \ll 1$ and at leading order in l^{-1} is easily seen. A constant time delay $t_s(\mathbf{x})$ in the classical background leads to a perturbation of ϕ of the form

$$\delta\phi^{(1)} \sim \frac{\delta\chi}{\chi^2} \sim l^{\frac{1}{2}} h^2 \frac{\delta\chi_l}{\chi_l^2} \sim l^{\frac{1}{2}} t_s(\mathbf{x}) t^{-2} \quad (6.20)$$

to leading order in l^{-1} as $t \rightarrow 0$. Whereas a local perturbation of the Hamiltonian density, $\delta\mathcal{H}(\mathbf{x}, 0) \sim \rho(\mathbf{x})$, leads from (4.20) to a linearized perturbation

$$\delta\phi^{(2)} \sim \rho(\mathbf{x}) \dot{\phi} \int^t \dot{\phi}^{-2} \sim l^{-\frac{1}{2}} \rho(\mathbf{x}) t^3, \quad (6.21)$$

again to leading order in l^{-1} as $t \rightarrow 0$. Here, we used $\dot{\phi} \propto -\dot{\chi}/\chi^2 = -l^{\frac{1}{2}} h^2 \dot{\chi}_l/\chi_l^2 \sim l^{\frac{1}{2}} t^{-2}$ at leading order in l^{-1} . As we shall see, we need to include these logarithmic corrections in order to compute the production of particles and stress-energy perturbations as we follow the system across the bounce. At zeroth order in l^{-1} , the particle production vanishes - the in vacuum maps to the out vacuum at this order. But at first order in l^{-1} , there is particle production as well as creation of a nearly scale-free spectrum of linearized stress-energy perturbations.

The physical evolution of modes on different wavelengths may be pictured as follows. When modes of a given wavenumber k are inside the effective horizon, *i.e.*, $|kt| \gg 1$, they are oscillatory and one must study their evolution using quantum field theory. However, once they have passed into the regime where $|kt| \ll 1$, spatial gradients become unimportant and the evolution is ultralocal. At this point, one can switch to a local, quantum mechanical description in which the field at every spatial point evolves independently, and in which, after carefully specifying the self-adjoint extension, the quantum wavefunction may be matched across the singularity.

From (6.20) and (6.21), and taking into account the corrections in inverse powers of l , we expect to obtain one solution to (6.15) representing a time delay perturbation, of the form

$$\delta\phi^{(1)} = l^{\frac{1}{2}} f^{(1)}(kt) + l^{-\frac{1}{2}} g^{(1)}(kt) + \dots, \quad (6.22)$$

where $f^{(1)} \propto t^{-2}$ as $|kt| \rightarrow 0$ and subsequent terms in the series are suppressed by further powers of l^{-1} . We also expect a second solution, representing a local perturbation to the Hamiltonian density, of the form

$$\delta\phi^{(2)} = l^{-\frac{1}{2}} f^{(2)}(kt) + l^{-\frac{3}{2}} g^{(2)}(kt) + \dots, \quad (6.23)$$

with $f^{(2)} \propto t^3$ at small $|kt|$. Substituting these ansätze into (6.15), $f^{(1),(2)}$ obey (6.16), as in the previous subsection, which is again solved by (6.17).

We can correct both these mode function solutions to next order in l^{-1} by substituting (6.22) and (6.23) into (6.15) and equating the coefficients of the first subleading power in

l^{-1} . We find

$$\begin{aligned} \ddot{g}^{(1)} - \frac{6}{t^2}\dot{g}^{(1)} + k^2 g^{(1)} &= 2\frac{f^{(1)}}{t^2} + \frac{\dot{f}^{(1)}}{t}, \\ \ddot{g}^{(2)} - \frac{6}{t^2}\dot{g}^{(2)} + k^2 g^{(2)} &= 3\frac{f^{(2)}}{t^2} - \frac{\dot{f}^{(2)}}{t}, \end{aligned} \quad (6.24)$$

whose particular solutions are

$$\begin{aligned} g^{(1)} &= \frac{1}{2}\text{Si}(2kt)f^{(2)}(kt) + \frac{1}{2}\text{Cin}(2kt)f^{(1)}(kt) + \frac{4\cos kt}{3(kt)^2} + \frac{1\sin kt}{3kt}, \\ g^{(2)} &= \frac{1}{2}\text{Si}(2kt)f^{(1)}(kt) - \frac{1}{2}\text{Cin}(2kt)f^{(2)}(kt) + \frac{1\cos kt}{3kt} - \frac{4\sin kt}{3(kt)^2}, \end{aligned} \quad (6.25)$$

where it is conventional to define the integrals

$$\text{Si}(y) \equiv \int_0^y dx \frac{\sin x}{x}, \quad \text{Cin}(y) \equiv \int_0^y dx \frac{(1 - \cos x)}{x}. \quad (6.26)$$

In fact, the solutions (6.25) are only determined up to an arbitrary multiple of $f^{(1)}$ and $f^{(2)}$, respectively (note that only one of them is consistent with the parity of either solution), but such an extra contribution shall not be important to us since it does not contribute to the particle number $\langle n \rangle$ at the leading order in l^{-1} to which we calculate.

Equations (6.22) and (6.23), with t replaced by $t - i\epsilon$ throughout, solve (6.15) in our complex classical background. Since the background avoids the singularity at $\chi = 0$, there is no ambiguity in the evolution of the perturbation modes. We now want to take the linear combination of $\delta\phi^{(1)}$ and $\delta\phi^{(2)}$ that behaves as the incoming positive frequency mode, and evolve it to a time well after the quantum ‘‘bounce,’’ when it is undergoing oscillations with an adiabatically changing frequency once more, and it makes sense to calculate the particle number.

We work to leading order in an expansion in inverse powers of the logarithm, which we assume is large. The classical background solution which dominates is the ‘‘image’’ solution starting behind the singularity: as explained in Subsection 5.4, we must define the logarithm to be real below the positive real χ axis (where $\chi = 1/\phi$), *i.e.*, as $\frac{1}{2}(\ln(\chi) + \ln(-\chi) - i\pi)$. Recall that at leading order in the large logarithm, *i.e.* ignoring $\ln(\phi/NM)$ where it occurs inside the logarithm, we have $\chi \propto t - i\epsilon = \tilde{t}$ in the classical background.

We start by extracting the time-dependence in the logarithm, as follows:

$$\ln(\phi/NM) \equiv l \rightarrow \ln\left(\frac{k}{M}\right) - \frac{1}{2}(\ln(-k\tilde{t}) + \ln(k\tilde{t}) - i\pi) \equiv l_0 - \frac{1}{2}(\ln(-k\tilde{t}) + \ln(k\tilde{t}) - i\pi), \quad (6.27)$$

where we ignored $\ln(\phi/NM)$ inside the logarithm. Our asymptotic ‘‘in’’ and ‘‘out’’ regions will be defined where $|kt|$ is large, so that the mode evolution is oscillatory, but $|Mt|$ is small so that l is still large. We now identify the positive frequency mode in an expansion in l_0^{-1} .

At zeroth order in l_0^{-1} , the incoming positive frequency mode is just $-3l_0^{-\frac{1}{2}}\delta\phi^{(1)} + 3il_0^{\frac{1}{2}}\delta\phi^{(2)}$ and this evolves across $t = 0$ to the positive frequency outgoing mode. At next order, we must include the corrections $g^{(1)}$ and $g^{(2)}$ derived in (6.25). When taking the large $|kt|$ limit, we use

$$\text{Si}(2kt) \rightarrow \frac{\pi}{2} - \int_{2kt}^{\infty} \frac{dx \sin x}{x}, \quad \text{Cin}(2kt) \rightarrow \ln(kt) + \gamma + \int_{2kt}^{\infty} \frac{dx \cos x}{x}, \quad (6.28)$$

where the integrals are easily expanded as a series in $1/(kt)$ by repeated integrations by parts. Notice that in the complex t -plane, $\text{Si}(2kt)$ is an odd function of t whereas $\text{Cin}(2kt)$ is an even function.

For large negative times $-(k/M) \ll tk \ll -1$, we find

$$\begin{aligned} \delta\phi^{(1)} &\rightarrow l_0^{\frac{1}{2}} \left(1 - \frac{1}{2} \frac{\ln(-kt)}{l_0} + i \frac{\pi}{2l_0} \right) \left(-\frac{1}{3} \cos(kt) \right) \\ &\quad + l_0^{-\frac{1}{2}} \left(-\frac{1}{6} \cos kt (\ln(-2kt) + \gamma) - \frac{\pi}{12} \sin kt \right) \\ &= l_0^{\frac{1}{2}} \left(-\frac{1}{3} \cos kt - \frac{\pi}{12l_0} \sin kt \right) - \frac{1}{6} l_0^{-\frac{1}{2}} \cos kt (i\pi + \gamma + \ln 2). \end{aligned} \quad (6.29)$$

Notice that the time-dependent logarithm from the first term has canceled with the logarithm in the correction $g^{(1)}$ to the second term. A similar cancellation occurs in $\delta\phi^{(2)}$:

$$\delta\phi^{(2)} \rightarrow l_0^{-\frac{1}{2}} \left(\frac{1}{3} \sin kt + \frac{\pi}{12l_0} \cos kt \right) - \frac{1}{6} l_0^{-\frac{3}{2}} \sin kt (i\pi + \gamma + \ln 2). \quad (6.30)$$

Similarly, at large kt we obtain

$$\delta\phi^{(1)} = l_0^{\frac{1}{2}} \left(-\frac{1}{3} \cos kt + \frac{\pi}{12l_0} \sin kt \right) - \frac{1}{6} l_0^{-\frac{1}{2}} \cos kt (\gamma + \ln 2), \quad (6.31)$$

and

$$\delta\phi^{(2)} \rightarrow l_0^{-\frac{1}{2}} \left(\frac{1}{3} \sin kt - \frac{\pi}{12l_0} \cos kt \right) - \frac{1}{6} l_0^{-\frac{3}{2}} \sin kt (\gamma + \ln 2). \quad (6.32)$$

We now replace t by $t - i\epsilon$ and read off the incoming positive frequency mode

$$\begin{aligned} &R_{in}^{(+)} \\ &= e^{-k\epsilon} \left(-3l_0^{-\frac{1}{2}}\delta\phi^{(1)} + 3il_0^{\frac{1}{2}}\delta\phi^{(2)} \right) - e^{-k\epsilon} l_0^{-1} \left(\frac{3i\pi}{4} + \frac{\gamma + \ln 2}{2} \right) \left(-3l_0^{-\frac{1}{2}}\delta\phi^{(1)} - 3il_0^{\frac{1}{2}}\delta\phi^{(2)} \right) \\ &\rightarrow e^{ikt} \quad \quad \quad - (k/M) \ll kt \ll -1 \\ &\rightarrow e^{ikt} - \frac{i\pi}{l_0} e^{-2k\epsilon} e^{-ikt} \quad \quad \quad 1 \ll kt \ll k/M. \end{aligned} \quad (6.33)$$

The last term describes the particle production, from (6.8) we have

$$\langle n \rangle = \frac{\pi^2}{l_0^2} e^{-4k\epsilon}, \quad (6.34)$$

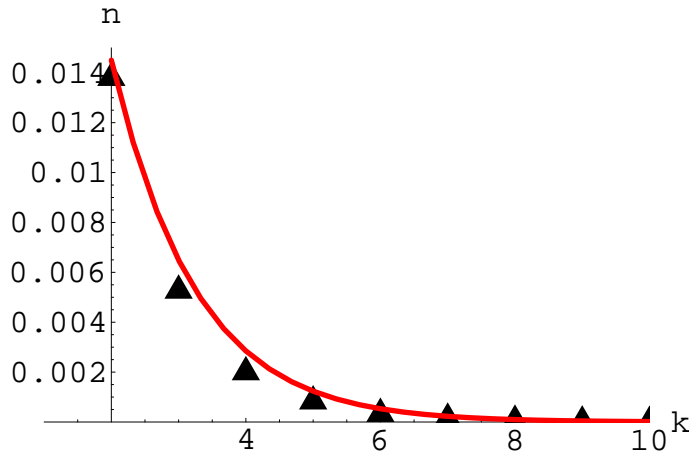


Figure 12: Numerical calculation of particle production ($\langle n \rangle$ versus k) in the complex background of Figure 9, compared with the analytical calculation given in (6.34).

explicitly revealing the exponential UV cutoff at large k due to the complex classical solution for the background missing the singularity at $\chi = 0$ by the finite quantity ϵ .

As a check of the validity of our approximations, we have computed $\langle n \rangle$ numerically, using the full complex solution for the background, shown in Figure 9, and a numerical solution of the mode equations at each k with the field fluctuation in the incoming positive frequency mode. Figure 12 compares the analytical result (6.34), shown as the solid curve, with the numerical result of the full computation.

We can now write down the energy density in $\delta\phi$ particles produced:

$$\rho_{c,\delta\phi} = \int \frac{d^3\mathbf{k}}{(2\pi)^3} k \frac{\pi^2}{\ln^2(k/M)} e^{-4k\epsilon}, \quad (6.35)$$

where, as we have emphasized, the integral is only to be taken over those values of k so large that the transition from oscillatory to ultralocal evolution occurs while the homogeneous mode was accurately following the zero-energy scaling solution.

6.4 Production of Light Higgs Particles

To compute the quantum production of light Higgs particles, namely the excitations of Φ_i , $i = 2, \dots, 6$, which commute with Φ_1 and whose mass is proportional to λ_ϕ , we must solve (6.18) to first order in l^{-1} . We proceed similarly to the previous subsection. Setting $\tilde{t} = t - i\epsilon$, we set

$$\Phi_i = l^\beta (f(\tilde{t}) + g(\tilde{t})l^{-1} + \dots), \quad (6.36)$$

and solve (6.18) order by order in l^{-1} . The two linearly independent solutions for f at small \tilde{t} are easily identified: $f_\pm \sim \tilde{t}^{\frac{1}{2} \pm ia}$, with $a = \sqrt{3/20}$. At next order in l^{-1} , (6.18) yields $\beta_\pm = \mp 2i/\sqrt{15}$. These solutions are extended to large times as follows. Solving (6.18) to

lowest order in l^{-1} , we find $f_{\pm} \sim \tilde{t}^{\frac{1}{2}} J_{\pm ia}(k\tilde{t})$. At next order, we obtain

$$\ddot{g}_{\pm} + \frac{2}{5\tilde{t}^2} g_{\pm} + k^2 g_{\pm} = \frac{2\beta_{\pm}}{\tilde{t}} \dot{f}_{\pm} - \frac{\beta_{\pm} + \frac{2}{5}}{\tilde{t}^2} f_{\pm}. \quad (6.37)$$

The right hand side is easily evaluated using standard Bessel function relations to be $-2\beta_{\pm} k\tilde{t}^{-1/2} J_{1\pm ia}(k\tilde{t})$. We now solve (6.37) using a Green's function, obtaining

$$g_{\pm}(\tilde{t}) = \pm \frac{\pi\beta_{\pm}ki}{\sinh a\pi} \tilde{t}^{\frac{1}{2}} \left(J_{\pm ia}(k\tilde{t}) \int_0^{\tilde{t}} dt' J_{1\pm ia}(kt') J_{\mp ia}(kt') - J_{\mp ia}(k\tilde{t}) \int_0^{\tilde{t}} dt' J_{1\pm ia}(kt') J_{\pm ia}(kt') \right), \quad (6.38)$$

where we used the Wronskian $t^{1/2} \left(\dot{J}_{ia}(kt) J_{-ia}(kt) - \dot{J}_{-ia}(kt) J_{ia}(kt) \right) = (2i \sinh a\pi)/\pi$. The first term in (6.38) is proportional to $f_{\pm}(\tilde{t})$. Using the large-argument asymptotic form for Bessel functions,

$$J_{\nu}(kt) \sim \sqrt{\frac{2}{\pi kt}} \cos\left(kt - \nu\frac{\pi}{2} - \frac{\pi}{4}\right), \quad kt \gg 1, \quad (6.39)$$

we see the first (second) integrand in (6.38) tends to $\mp i(\sinh a\pi)/(\pi kt')$ plus oscillatory terms which integrate to a constant. The first integral in (6.38) thus diverges logarithmically, giving a contribution to g_{\pm} of the form $\beta_{\pm} \ln(k\tilde{t}) \tilde{t}^{1/2} J_{\pm ia}(k\tilde{t})$. This is just what is required to cancel the time dependence of the overall coefficient l^{β} in (6.36) to first order in $\ln(k\tilde{t})/l_0$, where $l_0 \equiv \ln(k/M)$ and we are interested in the regime $1 \ll |k\tilde{t}| \ll k/M$ as in the previous subsection. Recalling that $l \approx l_0 - \ln(-k\tilde{t}) + i\pi$ for $-k/M \ll kt \ll -1$ and $l \approx l_0 - \ln(k\tilde{t})$ for $1 \ll kt \ll k/M$, we can check that the same cancellation occurs for large negative t using $J_{-ia}(kt) = e^{\pi a} J_{-ia}(-kt)$ and $J_{1+ia}(kt) = -e^{-\pi a} J_{1+ia}(-kt)$, which hold when t is analytically continued to negative values by passing below the origin. The coefficient of $J_{\pm ia}(k\tilde{t})$ in the first term of (6.38) is hence an even function of \tilde{t} , tending to $\beta_{\pm} \ln(|kt|)$ for large $|kt|$.

The second term in (6.38) involves an integral which converges at large $|t'|$. Here, we can make use of the formula $\int_0^{\infty} dx J_{1+\xi}(kx) J_{\xi}(kx) = 1/(2k)$, [58] to obtain for our two linearly independent modes, to first order in l_0^{-1} and at large $|t|$ (still $\ll M^{-1}$),

$$\begin{aligned} \Phi_{i,\pm} &\rightarrow ie^{\mp\pi a} l_0^{\beta_{\pm}} (-\tilde{t})^{1/2} \left(J_{\pm ia}(-k\tilde{t}) \left(1 + \frac{i\pi\beta_{\pm}}{l_0}\right) \mp \frac{i\pi\beta_{\pm}}{l_0 \sinh a\pi} J_{\mp ia}(-k\tilde{t}) \right), \quad kt \ll -1 \\ &\rightarrow l_0^{\beta_{\pm}} \tilde{t}^{1/2} \left(J_{\pm ia}(k\tilde{t}) \mp \frac{i\pi\beta_{\pm}}{l_0 \sinh a\pi} J_{\mp ia}(k\tilde{t}) \right), \quad kt \gg 1. \end{aligned} \quad (6.40)$$

Using (6.39) we now construct the incoming positive frequency mode as a linear combination of $\Phi_{i,\pm}$, and then use (6.40) to evolve it to large positive kt . Explicitly, at large negative kt , we have

$$R_+ \sim e^{ikt} \sim e^{-\epsilon k} e^{-i\pi/4} \frac{1}{2} \sqrt{\frac{\pi(-k\tilde{t})}{2}} \left(J_{ia}(-k\tilde{t}) \left(\frac{1}{c} - \frac{1}{s}\right) + J_{-ia}(-k\tilde{t}) \left(\frac{1}{c} + \frac{1}{s}\right) \right), \quad kt \ll -1, \quad (6.41)$$

where $c \equiv \cosh(\pi a/2)$ and $s = \sinh(\pi a/2)$. Evolving to large positive kt using (6.40) and working to first order in l_0^{-1} , we find

$$R_+ \sim e^{i\pi/4} \left(e^{ikt} \left(1 + 2i \frac{\beta_+ \pi}{l_0} \right) + i e^{-ikt} e^{-2\epsilon k} \frac{\pi \beta_+}{l_0} \coth \pi a \right). \quad (6.42)$$

The last term yields our final result for the mode-mixing coefficient. Using $\beta_+ = -2i/\sqrt{15}$, $a = \sqrt{3/20}$, we infer the energy density in light Higgs particles

$$\rho_{c,\Phi} = \int \frac{d^3 \mathbf{k}}{(2\pi)^3} k \frac{4\pi^2 \coth^2(\pi \sqrt{3/20})}{15 \ln^2(k/M)} e^{-4k\epsilon}, \quad (6.43)$$

which is parametrically of the same order as the result (6.35) for $\delta\phi$ particles. However, we have still to multiply by the total number of light Higgs particles. The simplest case to consider is where the $SU(N)$ symmetry is broken by Φ_1 to $U(1)^{N-1}$. In this case, there are of order N surviving light Higgs bosons whose mass will be due solely to the deformation term. Hence the result (6.43) is multiplied by N . (In more general cases, there could be of order N^2 such light Higgs modes.)

6.5 Production of Massless Gauge Bosons

To calculate the production of remaining light gauge bosons, we need to solve equation (6.19) to the first nontrivial order in l^{-1} . The effect of the l^{-2} correction is more modest in this case and a suitable ansatz for the transverse mode functions is

$$A_\perp = A_0 \sin kt (1 - Cl^{-1}) + A_1 \cos kt + gl^{-2} + \dots \quad (6.44)$$

Substituting into (6.19) we obtain

$$\ddot{g} + k^2 g = A_0 C (kt^{-1} \cos kt - t^{-2} \sin kt) + A_1 C kt^{-1} \sin kt, \quad (6.45)$$

whose solution is

$$g = \frac{1}{2} C A_0 [\sin kt (\text{Cin}(2kt) - 1) + \cos kt \text{Sin}(2kt)] \\ + \frac{1}{2} C A_1 [\sin kt \text{Sin}(2kt) - \cos kt \text{Cin}(2kt)]. \quad (6.46)$$

Using the large time limits of the Cin and Sin functions, as given in Subsection 6.3, we may obtain the behavior of an incoming positive frequency mode $A_\perp^{(+),in} \sim e^{ikt}$, $k/M \ll kt \ll -1$, including the effect arising from the continuation of l , to obtain

$$A_\perp^{(+),in} \rightarrow e^{ikt} + \frac{i\pi C}{2l_0^2} e^{-ikt}. \quad (6.47)$$

From this we read off the mode mixing coefficient, and hence the energy density in created light gauge bosons:

$$\rho_{c,A} = \int \frac{d^3 \mathbf{k}}{(2\pi)^3} k \frac{\pi^2 C^2}{4 \ln^4(k/M)} e^{-4k\epsilon}, \quad (6.48)$$

which is suppressed relative to the other cases by the square of the logarithm.

As for the light Higgs particles, we can discuss the dependence on N . If the $SU(N)$ symmetry breaks to $U(1)^{N-1}$, then there are of order N massless bosons remaining, so the result (6.48) is multiplied by N . However, the diagram which gives rise to the coupling C involves only one closed line (hence one power of N) and is proportional to $\lambda_\phi \sim N^{-2}l^{-1}$. Hence C scales as N^{-1} . (For symmetry breaking to a larger group, there can be of order N^2 massless gauge bosons remaining.) The quantum production of massless gauge bosons is always subdominant to light Higgs production, by two powers of $1/\ln(k/M)$ (and, for breaking to $U(1)^{N-1}$, by one power of $1/N$).

6.6 Backreaction

We now want to estimate the backreaction effect of particle production on the homogeneous mode of the field ϕ . We do so using energy conservation: the total energy is always zero so any energy which goes into particles will lower the energy available in the homogeneous mode and therefore cause it to sink lower down the negative potential.

One possible criterion for the backreaction to be small is that the energy density ρ_c in created particles should be small compared to (minus) the potential energy density reached at times $|t| \sim \epsilon$. In the previous subsections, we have shown that most of the energy density goes into light Higgs particles. Keeping in mind that the number of light Higgs species is of order N and that for most of the final wavefunction $\epsilon \sim W^2 R_{AdS}/(N|\ln(MR_{AdS})|^{1/2})$, with a minimal spread wavepacket corresponding to $W = 1$, we find from (6.43) that

$$\rho_c \sim \frac{N}{\epsilon^4 |\ln(MR_{AdS})|^2} \sim \frac{N^5}{W^8 R_{AdS}^4}. \quad (6.49)$$

Comparing this with (minus) the potential energy at $|t| \sim \epsilon$,

$$\frac{1}{4}\lambda_\phi\phi^4 \sim \frac{N^2|\ln(M\epsilon)|}{\epsilon^4} \sim \frac{N^2|\ln(MR_{AdS})|}{\epsilon^4}, \quad (6.50)$$

we see that the energy density in created particles is smaller by powers of $1/N$ and $1/|\ln(MR_{AdS})|$, suggesting that backreaction is small. (We are assuming $MR_{AdS} \ll 1$, so that the quartic coupling near the starting value of ϕ , $f \sim 1/|\ln(MR_{AdS})|$, is small and perturbation theory reliable.)

A more conservative criterion for the backreaction to be small is that the homogeneous mode should keep enough energy to roll back up the hill to nearly its starting value. The potential for ϕ is

$$V = \frac{\phi^2}{6R_{AdS}^2} - \frac{\lambda_0\phi^4}{4\ln(\phi/NM)}. \quad (6.51)$$

Setting $V = 0$ to obtain the starting value of ϕ , we find

$$\phi_{start} = \sqrt{\frac{2}{3\lambda_0}} \frac{1}{R_{AdS} \ln(\phi_{start}/NM)^{1/2}} \approx \sqrt{\frac{2}{3\lambda_0}} \frac{1}{R_{AdS} |\ln(MR_{AdS})|^{1/2}}. \quad (6.52)$$

The minimal value of ϕ reached after the bounce is obtained by setting $V(\phi_{min}) = -\rho_c$. Demanding that $\phi_{min} - \phi_{start} \ll \phi_{start}$ in order to have small backreaction, one finds the condition $\rho_c \ll N^2 |\ln(MR_{AdS})|/R_{AdS}^4$; using (6.49), this becomes

$$|\ln(MR_{AdS})| \gg \frac{N^3}{W^8}. \quad (6.53)$$

So, for example, if we choose $W \sim N^{3/8}$, backreaction is small as long as $|\ln(MR_{AdS})| \gg 1$, for final values of ϕ carrying most of the probability. This value of W corresponds to a spread in the time delay $\epsilon \sim N^{-1/4} |\ln(MR_{AdS})|^{-1/4} R_{AdS}$, parametrically small compared to the duration $\sim 2R_{AdS}$ of the bounce. Hence our wavepacket is well-described by a classical bouncing solution, with small backreaction. The fraction of the probability associated with final ϕ values for which ϵ is so small that backreaction is large (and hence our calculation breaks down) is $\sim |\ln(MR_{AdS})|^{-1/4}$. Hence we conclude that when the logarithm is large, the most probable outcome is a bounce.

In Appendix B, we mention that the beta function for the coupling f of our double trace deformation is of order f^2 and does not receive higher loop corrections in the large N limit. However, in the large N limit we considered in the appendix, the 't Hooft coupling g_t as well as f were kept fixed. In the present situation, if we choose a minimal width wavepacket, for which we have to choose $f \ll 1/N^3$ in order to have small backreaction, we have to worry about subleading terms in the large N expansion. For instance, if the beta function contained terms linear in f , they might interfere with the logarithmic running of f that led to its asymptotic freedom. In Appendix B, we show that the one-loop effective potential does not receive contributions proportional to $f g_t$. It is conceivable that higher-loop diagrams do give contributions to the beta function for f , for instance of order $f g_t^2/N^2$. If $f \ll 1/N^3$ and if g_t were kept fixed for large N , such contributions would dominate the f^2 contribution considered in this paper. Therefore, for a minimal width wavepacket we would have to choose g_t smaller than the appropriate power of $1/N$, in which case our analysis would go through. This would deepen the gap between the regime in which our computations are reliable and the large 't Hooft coupling regime in which the bulk theory can be reliably described in supergravity. Either way, it will be interesting to explore in future work to what extent our results can be extended to large g_t . In any case, it appears that such problems can be avoided by choosing a sufficiently broad initial wavepacket, as described in the previous paragraph.

7 Stress-Energy Correlators

In addition to computing the quantum creation of particles, we would like to calculate the two-point correlation function of the stress-energy tensor for the scalar field fluctuations as a function of time. There is no gravity (and hence no backreaction) in our system, but stress-energy tensor correlators of the boundary CFT determine the metric perturbations in the bulk, *i.e.*, the cosmological spacetime, and are as such related to cosmological perturbations. In fact, the relation between the stress-energy tensor and the bulk metric is completely analogous to the relation between the operator \mathcal{O} and the bulk scalar field ϕ in Section 3.

We shall consider the conformally improved stress tensor [59], consisting of the canonical stress tensor plus an identically conserved quantity which has been added to make the stress tensor traceless in the limit when the theory is conformally invariant. In our case, this limit is where the logarithm is large so the running of λ may be neglected. In four spacetime dimensions, the conformally improved stress tensor is

$$T_{\mu\nu} = \left(\partial_\mu \phi \partial_\nu \phi - g_{\mu\nu} \left(\frac{1}{2} (\partial\phi)^2 - \frac{1}{4} \lambda \right) \right) - \frac{1}{6} (\nabla_\mu \partial_\nu - g_{\mu\nu} \partial^2) \phi^2. \quad (7.54)$$

We shall calculate the correlators of $T_{\mu\nu}$ to linear order in the field fluctuation $\delta\phi$ about the background solution. We shall treat the latter as a classical background, although strictly speaking, as we detailed in Subsection 5.6, the expectation value of the homogeneous background mode $\bar{\phi}$ does not exist. Nevertheless, at times well after the bounce, in the parameter regime where backreaction is small, we expect the description of $\bar{\phi}$ in terms of a localized wavepacket rolling back up the hill is accurate, so we can replace $\bar{\phi}$ with the appropriate classical solution and take expectation values of the inhomogeneous fluctuation modes $\delta\phi(\mathbf{x})$ using the Schrödinger wavefunction, calculated above. As we shall discuss below, these linearized correlators are in principle sufficient to determine the correlators of the linearized metric perturbations in the bulk.

Denoting the linearized perturbation of the stress tensor as $\delta T_{\mu\nu}$, the linearized components at given wavenumber \mathbf{k} are:

$$\begin{aligned} \delta T_{00} &= \dot{\phi}^2 \frac{d}{dt} \left(\frac{\delta\phi}{\dot{\phi}} \right) + \frac{1}{3} \phi k^2 \delta\phi \\ \delta T_{0i} &= ik_i \left(\frac{2}{3} \dot{\phi} \delta\phi - \frac{1}{3} \phi \dot{\delta\phi} \right) \\ \delta T_{ij} &= \delta_{ij} \left(\frac{1}{3} \dot{\phi} \dot{\delta\phi} + \frac{2}{3} \ddot{\phi} \delta\phi - \frac{1}{3} \phi \ddot{\delta\phi} - \frac{1}{3} \phi k^2 \delta\phi \right) + \frac{1}{3} \phi k_i k_j \delta\phi. \end{aligned} \quad (7.55)$$

We want to compute the fluctuations in the stress tensor in the incoming adiabatic vacuum state for the fluctuations, denoted $|0, \text{in}\rangle$, relative to the vacuum defined by the outgoing adiabatic vacuum state $|0, \text{out}\rangle$. Equivalently, we compute the correlators of $T_{\mu\nu}$ normal ordered with respect to $|0, \text{out}\rangle$. To compute the correlators, we first express the scalar field, and the linearized stress tensor, in terms of the adiabatic positive and negative frequency modes, and creation and annihilation operators, appropriate to $|0, \text{out}\rangle$. We then normal order the expression and calculate the expectation value in $|0, \text{in}\rangle$. This requires expressing the “out” creation and destruction operators in terms of “in” creation and destruction operators:

$$a_{\text{out}} = \alpha a_{\text{in}} + \beta^* a_{\text{in}}^\dagger, \quad a_{\text{out}}^\dagger = \alpha^* a_{\text{in}}^\dagger + \beta a_{\text{in}}. \quad (7.56)$$

Consider some quantity linear in the quantum field fluctuation and its time derivatives: it may be expressed as

$$f(t, \mathbf{x}) = \sum_{\mathbf{k}} \frac{1}{\sqrt{2kV}} \left(a_{\mathbf{k}, \text{out}} \chi_{\text{out}}^{(+)} e^{i\mathbf{k}\cdot\mathbf{x}} + a_{\mathbf{k}, \text{out}}^\dagger \chi_{\text{out}}^{(-)} e^{-i\mathbf{k}\cdot\mathbf{x}} \right), \quad (7.57)$$

where $\chi_{\text{out}}^{(+,-)}$ are the positive and negative frequency parts with respect to the out vacuum. We normalize the creation and destruction operators so $[a_{\mathbf{k}}, a_{\mathbf{k}'}^\dagger] = \delta_{\mathbf{k},\mathbf{k}'}$ etc. We define the vacuum-subtracted expectation of some operator \mathcal{O} as

$$\langle \mathcal{O} \rangle \equiv \langle 0, \text{in} | \mathcal{O} | 0, \text{in} \rangle - \langle 0, \text{out} | \mathcal{O} | 0, \text{out} \rangle. \quad (7.58)$$

Substituting (7.56) into (7.57) and (7.58), using the commutation relations for $a_{\mathbf{k}}$ and $a_{\mathbf{k}}^\dagger$ and their action on the “in” and “out” vacua, and replacing $\sum_{\mathbf{k}}$ with $V \int d^3\mathbf{k}/(2\pi)^3$, we obtain the two-point correlator

$$\langle f(t, \mathbf{x}) f(t, \mathbf{0}) \rangle = \int \frac{d^3\mathbf{k}}{(2\pi)^3} \frac{1}{2k} e^{i\mathbf{k}\cdot\mathbf{x}} \left(2|\beta|^2 |\chi_{\text{out}}^{(+)}|^2 + \alpha^* \beta (\chi_{\text{out}}^{(-)})^2 + \alpha \beta^* (\chi_{\text{out}}^{(+)})^2 \right), \quad (7.59)$$

where we used $|\alpha|^2 - |\beta|^2 = 1$. In the regime of interest, where β is small, we can replace α with -1 .

Since we only want the leading order result, we can use the positive frequency mode functions to zeroth order, namely

$$\delta\phi^{(+)} = e^{-ikt} \left(1 - \frac{3i}{kt} - \frac{3}{(kt)^2} \right), \quad (7.60)$$

which leads to the following positive frequency contributions to $\delta T_{\mu\nu}$:

$$\begin{aligned} \sqrt{\frac{\lambda_\phi}{2}} \delta T_{00}^{(+)} &= \frac{k^2}{3t} e^{-ikt} \\ \sqrt{\frac{\lambda_\phi}{2}} \delta T_{0i}^{(+)} &= ik_i \frac{1+ikt}{3t^2} e^{-ikt} \\ \sqrt{\frac{\lambda_\phi}{2}} \delta T_{ij}^{(+)} &= \delta_{ij} \frac{1+ikt}{3t^3} + k_i k_j \frac{1}{3t} \left(1 - \frac{3i}{kt} - \frac{3}{(kt)^2} \right) e^{-ikt}. \end{aligned} \quad (7.61)$$

Notice that the spatial trace $\delta T_{ii}^{(+)} = \delta T_{00}^{(+)}$ as it has to be from the tracelessness of the stress tensor. Hence it is only the traceless part $\tilde{\delta T}_{ij}^{(+)} \equiv \delta T_{ij}^{(+)} - \frac{1}{3} \delta_{ij} \delta T_{kk}^{(+)}$ which needs to be considered:

$$\sqrt{\frac{\lambda_\phi}{2}} \tilde{\delta T}_{ij}^{(+)} = \left(k_i k_j - \frac{1}{3} k^2 \delta_{ij} \right) \frac{1}{3t} \left(1 - \frac{3i}{kt} - \frac{3}{(kt)^2} \right) e^{-ikt}. \quad (7.62)$$

Equations (7.61) and (7.59) determine the two point correlation function (at equal times) of the stress-tensor in the boundary theory. Here we shall present only a partial discussion of the equal time correlators, postponing a fuller discussion to future work in which we attempt to use the boundary correlations to determine the fluctuations in the bulk.

The first term in (7.59) provides the simplest contribution. In order to compute it, our strategy is to replace factors of k^2 under the integral by minus the spatial Laplacian outside the integral. We then perform the angular integrals in (7.59) to obtain a

factor of $4\pi(\text{sink}r)/kr$. The two powers of k in the denominator then cancel the k^2 factor in the measure, leaving us with $r^{-1} \int_0^\infty dk \text{sink}r$. When performing the integral over $|\beta|^2$, we replace k with r^{-1} , the value of k dominating the integral. For example, $\int_0^\infty dk(\text{sink}r)/(\ln(k/M))^2 \approx r^{-1}/(\ln(1/Mr))^2$. These manipulations are sufficient to compute the first term in (7.59). The second and third terms involve additional oscillatory factors of $e^{\pm 2ikt}$ under the integral, which generates additional structure on the causal scale $r = 2t$, but which suppresses them for $r \ll t$.

In this way, we obtain the equal time correlators of various scalar quantities constructed from the stress-tensor, for example we exhibit the detailed form for $r \ll t$,

$$\begin{aligned} \langle \delta T_{00}(r, t) \delta T_{00}(0, t) \rangle &= \frac{\ln(1/Mt)}{\lambda_0 \pi^2 (\ln Mr)^2} \frac{2}{3r^6 t^2} \\ \langle \partial_i \delta T_{0i}(r, t) \partial_i \delta T_{0i}(0, t) \rangle &= \frac{\ln(1/Mt)}{\lambda_0 \pi^2 (\ln Mr)^2} \left(\frac{20}{r^8 t^2} - \frac{2}{3r^6 t^4} \right) \\ \langle \partial_i \partial_j \tilde{\delta T}_{ij}(r, t) \partial_k \partial_l \tilde{\delta T}_{kl}(0, t) \rangle &= \frac{\ln(1/Mt)}{\lambda_0 \pi^2 (\ln Mr)^2} \left(\frac{4480}{9r^{10} t^2} + \frac{80}{3r^8 t^4} + \frac{8}{3r^6 t^4} \right) \end{aligned} \quad (7.63)$$

The key point is that *all of these correlators are nearly scale-invariant* in form, that is they are all of the form $t^{-n}g(r/t)$, where the overall power of t is determined on dimensional grounds. The only deviation from perfect scale-invariance is due to the logarithmic running of the coupling with scale. As discussed in the introduction, this behavior is the result of the classical scale-invariance, and the modest quantum breaking of scale-invariance, in the boundary conformal field theory.

Although the background energy density is zero, we can define a dimensionless perturbation by comparing the fluctuation $\delta T_{00} = \delta\rho$ with the background quantity $\rho + P = \phi^2$. We find for example

$$\left\langle \frac{\delta\rho(r, t)}{P + \rho} \frac{\delta\rho(0, t)}{P + \rho} \right\rangle \sim \frac{1}{N^2 \ln^2(1/Mr) \ln(1/Mt)} \frac{t^6}{r^6}, \quad (7.64)$$

a slightly red spectrum, with the reddening arising from the running coupling as before. Furthermore, we note that the overall amplitude of the fractional energy density perturbation is proportional to $1/l^3$, where $1/l$ is the appropriate value of the running coupling, which has been our small parameter all along. To summarize, the fluctuations in ϕ give rise to stress-energy perturbations that are naturally small, being suppressed by powers of $1/N$ and $1/l$, approximately scale-invariant, with a slightly red tilt due to asymptotic freedom, scalar, adiabatic and nearly Gaussian in character, to leading order in $1/l$ and $1/N$.

The quantities of physical interest, however, are correlators of metric fluctuations in the bulk cosmology, which couple to the stress-energy tensor of the boundary theory. We would like to compute the bulk perturbations on a spacelike surface at late times, roughly halfway between the past and future singularities in our model, as shown schematically in Figure 13. In general, while knowing the state of the boundary theory is in principle equivalent to knowing the state in the bulk theory, it is in practice not straightforward to extract local information about the bulk theory from the boundary theory (see [60] for a

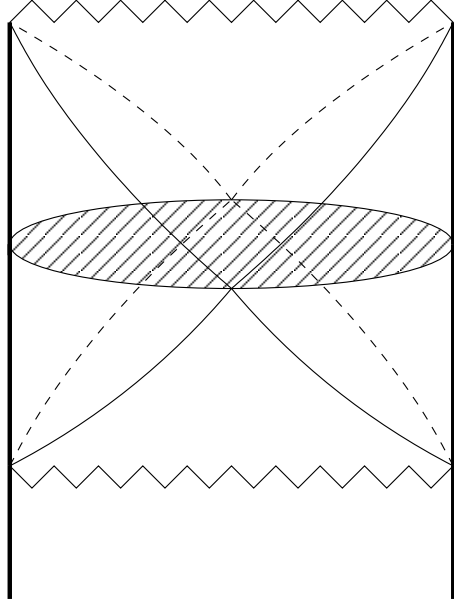


Figure 13: The stress-energy correlators on the boundary may predict the spectrum of classical cosmological fluctuations on a spacelike surface in the bulk at late times.

recent discussion). Our specific problem might be simpler due to the fact that the metric fluctuations behave classically in the relevant regime. Furthermore, it is sufficient to treat them in a linearized approximation.

One idea for how one might be able to compute the spectrum of bulk metric perturbations is as follows. The state of the boundary theory is encoded in the boundary correlators, some of which we have computed in this paper. Since the relevant modes are frozen in, it may be possible to view the boundary correlators as those of a classical ensemble of fluctuating fields. Each member of the ensemble could then be viewed as an expectation value of a boundary operator, which would determine a corresponding bulk solution (see for instance [42]). For instance, knowing the expectation value of the stress-energy tensor on the boundary determines a solution for the bulk metric. So we would end up with a classical ensemble of bulk metric perturbations, which we could use to compute bulk correlators.

Furthermore, since we are interested in wavenumbers $k \gg R_{AdS}^{-1}$, which is the only scale that enters in the correspondence, and since scale-invariance is holographic in the sense that the fluctuations on a planar subspace of a space with scale-invariant fluctuations are scale-invariant, it seems plausible that the bulk metric perturbations will turn out to be scale-invariant too.

8 Conclusions

We have studied the AdS/CFT dual description of $\mathcal{N} = 8$ gauged supergravity in five dimensions where smooth asymptotically AdS initial data can evolve to a big crunch singu-

larity in the future. At the singularity the classical supergravity description breaks down, but we have argued that the dual field theory evolution provides a consistent quantum description of the singularity. Specifically the boundary theory predicts a transition from the big crunch to a big bang as the most probable outcome of cosmological evolution.

If our results extend to more realistic cosmologies this would place cosmological models involving a big crunch/big bang transition on much firmer footing. It is tempting indeed to view AdS as a maximally symmetric box describing a smooth, isotropic patch of the universe which, in the case at hand, collapses to form a spacelike singularity. This applies for example to the cyclic universe models where the universe collapses after a phase of dark energy domination rendering it locally Minkowski on scales corresponding to a Hubble volume today. Since in the near singularity regime the cosmological constant appears to play no significant role, one would then use AdS/CFT, with boundary conditions that are a minimal deformation of the maximally symmetric setup, to model a patch of the universe like this through the singularity. The methods we have developed here may therefore allow the AdS/CFT correspondence to be used as a “laboratory” in which one can construct and study a large variety of cosmological scenarios.

An important limitation of our work is that we have good control over the field theory calculations only at small 't Hooft coupling, for which the bulk is in a stringy regime. There are indications, however, that our results may extend to strong coupling. In particular, the quantum effective potential for the unstable scalar in the boundary theory is negative and unbounded also at large 't Hooft coupling. Therefore the fact that AdS/CFT maps the problem of bulk cosmological singularities into a field theory instability of this type is a universal feature of this class of models.

We should also note there is a narrow band of the final wavefunction in the boundary theory, centered around the value predicted by the real classical bouncing solution, that cannot be calculated in perturbation theory. For final values within this band, which represents a parametrically small fraction of the total probability, we do not know yet whether the dual theory predicts a bounce.

Finally it would be interesting to find a mathematical framework, describing unstable field theories like the one we have been discussing, where the arbitrary phase associated with the choice of self-adjoint extension is incorporated in a more elegant manner. A priori the phase leads to an arbitrary function when one generalizes the self-adjoint extension to quantum mechanics in higher dimensions and to field theory. The self-adjoint extension, however, should really be viewed as part of the definition of the theory – remember that without a boundary condition at large field values, one simply cannot discuss the quantum evolution of a wave packet – so it is natural for it to have the same symmetries as the Lagrangian. This, together with the ultralocality of the evolution, reduces the arbitrariness again to the single free parameter present in one-dimensional quantum mechanics.

A remarkable consequence of the instability and approximate scale-invariance of the boundary theory is that an approximately scale-invariant spectrum of stress-energy perturbations is generated on the boundary, whose amplitude is suppressed by the asymptotically free coupling that governs the instability. If it can be shown that this corresponds to nearly scale-invariant bulk metric perturbations, this would provide a rather compelling explana-

tion for the origin of the observed density variations in the universe, since the approximate scale-invariance of the perturbations arises directly from the underlying approximate conformal invariance of the dual field theory.

Acknowledgments

We would like to thank N. Arkani-Hamed, O. Evnin, D. Gross, G. Horowitz, S. Kachru, S. Kovacs, J. Maldacena, R. Myers, E. Silverstein, K. Skenderis, D. Tong, H. Verlinde and especially N. Dorey for useful discussions. B.C. and T.H. thank the Centre for Theoretical Cosmology in Cambridge for its hospitality at various stages of this project. T.H. and N.T. are grateful for the hospitality of the Mitchell family at their Cook's Branch Conservancy and to Chris Pope for hospitality at the Mitchell Institute at Texas A&M University. T.H. thanks the KITP in Santa Barbara for support. The work of B.C. was supported in part by the Belgian Federal Science Policy Office through the Interuniversity Attraction Poles IAP V/27 and IAP VI/11, by the European Commission FP6 RTN programme MRTN-CT-2004-005104 and by FWO-Vlaanderen through project G.0428.06. N.T. acknowledges the support of STFC(UK) and of the Centre for Theoretical Cosmology in Cambridge.

A More on the Bulk Theory

In this appendix, we first show that the bulk theory discussed in Section 2, with action

$$S = \int \sqrt{-g} \left[\frac{1}{2}R - \frac{1}{2}(\nabla\phi)^2 + \frac{1}{4R_{AdS}^2} (15e^{2\gamma\phi} + 10e^{-4\gamma\phi} - e^{-10\gamma\phi}) \right], \quad (\text{A.1})$$

admits an $O(5)$ -invariant Euclidean instanton solution of the form

$$ds^2 = R_{AdS}^2 \left(\frac{d\rho^2}{b^2(\rho)} + \rho^2 d\Omega_4 \right) \quad (\text{A.2})$$

with $\phi = \phi(\rho)$ and for scalar boundary condition $\alpha_f = f\beta$.

The field equations determine b in terms of ϕ . Asymptotically one finds

$$b^2 = \rho^2 + 1 + \frac{2\alpha^2(\ln\rho)^2}{3\rho^2} + \frac{\alpha(4\beta - \alpha)\ln\rho}{3\rho^2} + \frac{8\beta^2 - 4\alpha\beta + \alpha^2}{12\rho^2}, \quad (\text{A.3})$$

and the scalar field ϕ itself obeys

$$b^2\phi'' + \left(\frac{4b^2}{\rho} + bb' \right) \phi' - R_{AdS}^2 V_{,\phi} = 0, \quad (\text{A.4})$$

where prime denotes ∂_ρ .

Regularity at the origin requires $\phi'(0) = \phi'_0 = 0$. Thus the instanton solutions can be labeled by ϕ_0 , the value of ϕ at the origin. For each ϕ_0 , one can integrate (A.4) and get an instanton. Asymptotically one finds $\phi(\rho) = \alpha \ln \rho / \rho^2 + \beta / \rho^2$, where α and β are now

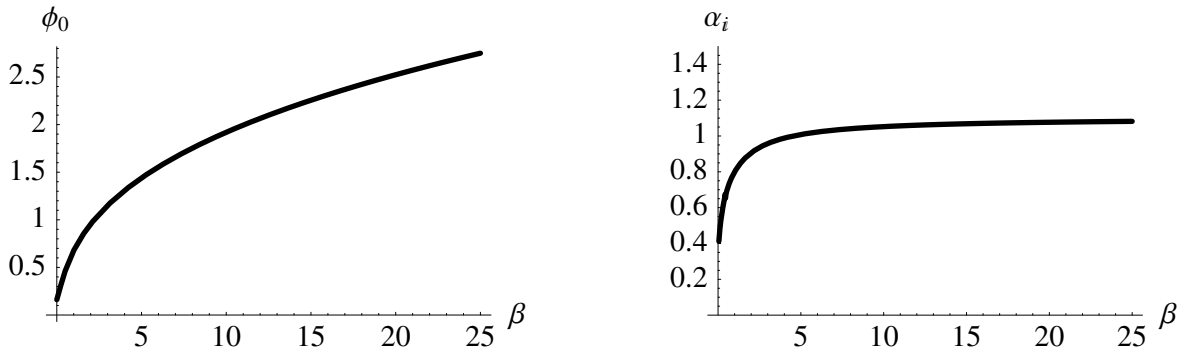


Figure 14: The value of ϕ at the origin as a function of β (left), and the function $\alpha_i(\beta)$ (right) obtained by integrating the field equations outward starting with different values for ϕ_0 .

constants. Hence for each ϕ_0 one obtains a point in the (α, β) plane. Repeating for all ϕ_0 yields a curve $\alpha_i(\beta)$ where the subscript indicates this is associated with instantons. This curve is plotted in Figure 14 (right panel). The left panel of Figure 14 shows ϕ_0 as a function of β .

The slice through the instanton obtained by restricting to the equator of the S^4 defines time symmetric initial data for a Lorentzian solution. The Euclidean radial distance ρ simply becomes the radial distance r on the initial data slice. So given a choice of boundary condition $\alpha(\beta)$, one can obtain suitable initial data by first selecting the instanton corresponding to a point where the curve $\alpha_i(\beta)$ intersects $\alpha(\beta)$, and then taking a slice through this instanton.

One immediately sees that all α_f boundary conditions, for $f > 0$, admit precisely one instanton solution. When $f \rightarrow 0$ one has $\phi_0 \rightarrow \infty$. The dual field theory is supersymmetric in this limit, so one expects there to be no regular instanton solutions that describe the decay of the AdS state in the bulk theory. For small positive f one sees that $\beta \sim 1/f$. This scaling is nicely reproduced by the solutions of the simplified model field theory discussed in the text. From the asymptotic form (A.3) of b it follows that the conserved mass (cf. (2.12)) of the resulting initial data is $M = -\pi^2 R_{AdS}^2 \alpha^2 / 4$, so $M \approx -2R_{AdS}^2$ for small f . The instantons therefore specify initial data with *negative mass* in this theory. It is only for AdS-invariant boundary conditions discussed below that instantons of this type define initial data of exactly zero mass, in line with their interpretation as the solution AdS_5 decays into.¹³

Lorentzian Evolution

Analytic continuation of the instanton geometry yields a Lorentzian solution that describes the evolution of instanton initial data under AdS-invariant boundary conditions

¹³One can also show that these instantons have finite action, which is large for small f and small for large f .

[17, 38]. These differ slightly from α_f boundary conditions and are most conveniently expressed as [34, 35]

$$\alpha\left(1 - \frac{f}{2}\ln\alpha\right) = f\beta, \quad (\text{A.5})$$

where f is again an arbitrary constant. One sees in particular that rescaling r leaves f unchanged. One also sees that the α_f boundary conditions considered in the text are approximately AdS-invariant when f is small, which is the parameter regime we will concentrate on. This restricts us to positive f since $f < 0$ boundary conditions admit instanton solutions only for $|f| > \mathcal{O}(1)$.

After analytic continuation the origin of the Euclidean instanton becomes the lightcone of the Lorentzian solution. Inside the lightcone, the $SO(4, 1)$ symmetry ensures that the solution evolves like an open FRW universe,

$$ds^2 = -dt^2 + a^2(t)d\sigma_4, \quad (\text{A.6})$$

where $d\sigma_4$ is the metric on the four-dimensional unit hyperboloid. Under evolution ϕ rolls down the negative potential. This causes the scale factor $a(t)$ to vanish in finite time, producing a big crunch singularity. Outside the lightcone, the solution is given by (A.2) with $d\Omega_4$ replaced by four-dimensional de Sitter space. The scalar field ϕ remains bounded in this region. On the light cone we have $\phi = \phi_0$ and $\partial_t\phi = 0$ (since $\phi_{,\rho} = 0$ at the origin in the instanton).

One can verify that this analytic continuation indeed satisfies the boundary conditions (A.5) by doing a coordinate transformation in the asymptotic region outside the light cone. The relation between the usual static coordinates (2.7) for AdS_5 and the $SO(4, 1)$ invariant coordinates,

$$ds^2 = R_{AdS}^2 \left(\frac{d\rho^2}{1 + \rho^2} + \rho^2(-d\tau^2 + \cosh^2\tau d\Omega_3) \right), \quad (\text{A.7})$$

is

$$\rho^2 = r^2 \cos^2 t - \sin^2 t. \quad (\text{A.8})$$

Hence the asymptotic behavior of ϕ in global coordinates is given by

$$\phi(r) = \frac{\tilde{\alpha} \ln r}{r^2} + \frac{\tilde{\beta}}{2r^2}, \quad (\text{A.9})$$

where $\tilde{\alpha} = \alpha_i / \cos^2 t$ and $\tilde{\beta}$ is given by (A.5) with α replaced by $\tilde{\alpha}$. Hence $\tilde{\alpha}$ is now time dependent and blows up as $t \rightarrow \pi/2$, when the singularity hits the boundary.

Although for α_f boundary conditions one can in general not obtain the solution by analytic continuation of the instanton, we have argued in Section 2 that when f is small and positive, the effect of the change in the boundary conditions on the evolution is negligible except in the corners of the conformal diagram where the singularity hits the boundary at infinity. In particular, since the evolution of the initial data has trapped surfaces, a singularity will still form in the central region. However, a priori it is now possible that the singularity is enclosed inside a large black hole and does not extend out to infinity. We now investigate this possibility.

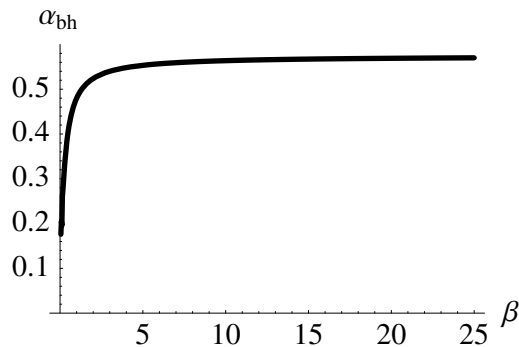


Figure 15: The function $\alpha_{bh}(\beta)$ obtained by integrating the field equations outward starting with different values for ϕ_e at the horizon $R_e = 0.1$ of spherical hairy black holes.

Black Holes with Scalar Hair

We now numerically integrate the field equations derived for static spherical solutions to verify if the theory (A.1) for α_f boundary conditions admits a class of static, spherical black holes with scalar hair outside the horizon. In light of the discussion above, we would like to know whether there are negative mass black holes with scalar hair.¹⁴ Writing the metric as

$$ds_5^2 = R_{AdS}^2 \left(-h(r)e^{-2\delta(r)} dt^2 + h^{-1}(r) dr^2 + r^2 d\Omega_3^2 \right), \quad (\text{A.10})$$

the Einstein equations read

$$h\phi_{,rr} + \left(\frac{3h}{r} + \frac{r}{3}\phi_{,r}^2 h + h_{,r} \right) \phi_{,r} = R_{AdS}^2 V_{,\phi}, \quad (\text{A.11})$$

$$2(1-h) - rh_{,r} - \frac{r^2}{3}\phi_{,r}^2 h = \frac{2}{3}r^2 R_{AdS}^2 V(\phi), \quad (\text{A.12})$$

$$\delta_{,r} = -\frac{r}{3}\phi_{,r}^2. \quad (\text{A.13})$$

We integrate the field equations outward from the horizon. Regularity at the event horizon $r = R_e$ requires

$$\phi_{,r}(R_e) = \frac{R_e R_{AdS}^2 V_{,\phi_e}}{2 - 2R_e^2 R_{AdS}^2 V(\phi_e)/3}. \quad (\text{A.14})$$

The scalar field asymptotically behaves as (2.8), so we obtain a point in the (α, β) plane for each combination (R_e, ϕ_e) . Repeating for all ϕ_e gives a curve $\alpha_{R_e}(\beta)$. We show this curve in Fig 15 for $R_e = .1$. Given a choice of boundary conditions $\alpha_f(\beta)$, the allowed black hole solutions are simply given by the points where the black hole curves intersect the boundary condition curve: $\alpha_{bh}(R_e, \beta) = \alpha_f(\beta)$. One sees that for all values of $f > 0$

¹⁴Negative mass hairy black holes were found in closely related theories in four dimensions [18].

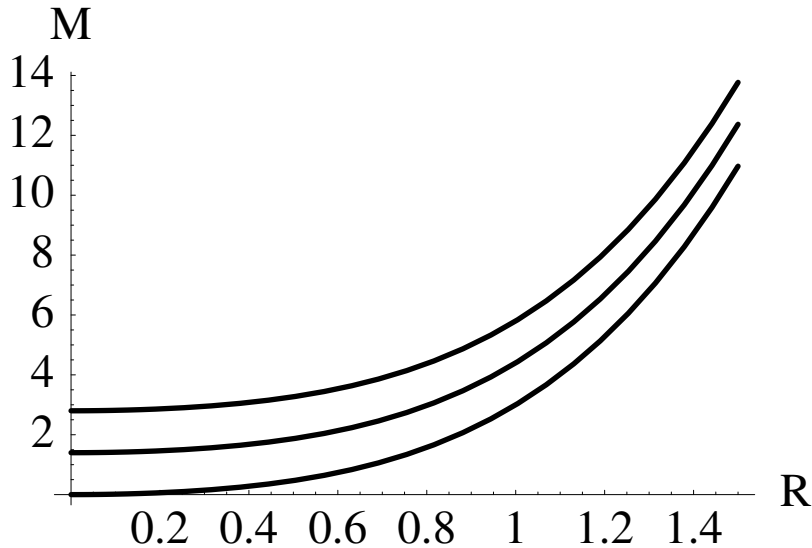


Figure 16: The mass M of static spherical hairy black holes (in units of R_{AdS}^2) as a function of horizon size R (in units of R_{AdS}), for two different choices of α_f boundary conditions and for Schwarzschild-AdS. From top to bottom, the curves correspond to $f = 0.05$, $f = 0.1$ and Schwarzschild-AdS. One sees that all hairy black holes have positive mass.

there is precisely one hairy black hole solution of size $R_e = 0.1$, and the same is true for different radii R_e . For α_f boundary conditions the mass of the hairy black holes is given by

$$M_h = Q[\partial_t] = 2\pi^2 R_{AdS}^2 \left(\frac{3}{2} M_0 + \beta^2 \left(1 - \frac{1}{2} f \right) \right), \quad (\text{A.15})$$

where M_0 is the coefficient of the $O(1/r^6)$ term in the asymptotic expansion of the g_{rr} component of the metric.

This is shown in Figure 16, as a function of horizon size R_e , for two different choices of α_f boundary conditions ($f = 0.05$ (top), and $f = 0.1$ (middle)) and for Schwarzschild-AdS. One sees that the scalar hair increases the mass; the hairy black holes are more massive than a Schwarzschild-AdS black holes of the same size. In particular, one sees that $M_h > 0$ for all R_e . For large R_e one has $E_h \sim R_{AdS}^2 R_e^4$, with $M_h/M_s > 1$ for all R_e and $M_h/M_s \rightarrow 1$ for large R_e . Furthermore, the mass (for given R_e) increases for decreasing f .

The dual interpretation of the increase in mass relative to vacuum black holes is that whereas Schwarzschild-AdS black holes correspond to thermal states in the usual vacuum of the dual field theory, hairy black holes are described by typical excitations around the *local maximum* of the effective potential of the dual theory in the presence of the negative double-trace deformation [18] (see Fig 2 (left)). An important consequence is that the singularity that develops from initial data defined by the instanton cannot be hidden behind an event horizon, since there is no candidate black hole with the required mass. Instead the singularity probably extends all the way to the boundary, cutting of all space.

By contrast there do exist negative mass black holes for bulk boundary conditions that correspond to a deformation of the dual field theory that yields an effective potential with a global negative minimum, such as shown in Figure 2 (right). These negative mass hairy black holes have a natural interpretation in the dual theory as typical excitations above the global vacuum state [18].

For example, in the case at hand, for boundary conditions $\alpha_{f,\epsilon} = f\beta - \epsilon\beta^3$ with ϵ sufficiently small, the boundary condition curve $\alpha_{f,\epsilon}$ will generally have two intersection points with the black hole curves $\alpha_{bh}(R_e)$ of Figure 15. The first set of intersection points specifies a branch of hairy black holes with rather small β and hence with not much hair. Their mass is positive and they correspond to excitations around the local maximum of the effective potential in the dual theory, as before. On the other hand the solutions with the larger β , which are associated with the second intersection point, have much smaller mass and provided ϵ is sufficiently small a subset of these have negative mass. For example, for $f = 1$ and $\epsilon = .05$ the theory admits an $M \approx -3R_{AdS}^2$ black hole of horizon size $R_e = 0.1$ and with $\phi_e = 1.517$.

The existence of an additional branch of hairy black holes - some with negative mass - for $\alpha_{f,\epsilon}$ boundary conditions also means that in this case there does exist a hairy black hole with the same mass as the instanton, $M \approx -\epsilon R_{AdS}^2$. This is therefore the natural end state of evolution of the initial data defined by the instanton, under the modified $\alpha_{f,\epsilon}$ boundary conditions. In general, regularization of the dual theory that makes the effective potential bounded from below encloses the singularity in the bulk inside a horizon. Furthermore if one considers a series of dual theories where for decreasing values of ϵ one finds the horizon size of the black hole of the same mass as the instanton increases. In the limit $\epsilon \rightarrow 0$ the black hole becomes infinitely large and we recover the cosmological solutions we studied here.

B Renormalization of the Boundary Theory

In this appendix, we discuss $\mathcal{N} = 4$ super-Yang-Mills theory with gauge group $SU(N)$,

$$S_0 = \int d^4x \text{Tr} \left\{ -\frac{1}{4} F_{\mu\nu} F^{\mu\nu} - \frac{1}{2} D_\mu \Phi^i D^\mu \Phi^i + \frac{1}{4} g^2 [\Phi^i, \Phi^j] [\Phi_i, \Phi_j] + \text{fermions} \right\}, \quad (\text{B.1})$$

deformed by the double trace potential

$$W = -\frac{f}{2} \int d^4x \mathcal{O}^2, \quad (\text{B.2})$$

see (3.3). In our conventions,

$$F_{\mu\nu} = \partial_\mu A_\nu - \partial_\nu A_\mu + ig[A_\mu, A_\nu], \quad D_\mu \Phi^i = \partial_\mu \Phi^i + ig[A_\mu, \Phi^i]. \quad (\text{B.3})$$

The operator \mathcal{O} was defined in (3.1):

$$\mathcal{O} = \frac{a}{N} \text{Tr} \left[\Phi_1^2 - \frac{1}{5} \sum_{i=2}^6 \Phi_i^2 \right]. \quad (\text{B.4})$$

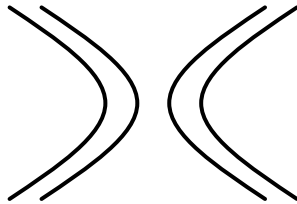


Figure 17: The $(\text{Tr}\Phi^2)^2$ vertex in double line notation.

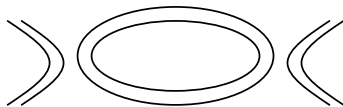


Figure 18: The one-loop diagram that renormalizes the coupling f at large N .

As explained in [21] and reviewed in Section 3, the computation of amplitudes at order f^2 involves matrix elements of

$$\frac{f^2}{8} \int d^4x d^4y \mathcal{O}^2(x) \mathcal{O}^2(y). \quad (\text{B.5})$$

From conformal invariance, $\langle \mathcal{O}(x) \mathcal{O}(y) \rangle = v/|x - y|^4$ on flat \mathbb{R}^4 . This leads to a short distance divergence that renormalizes f and survives in the large N limit (where the 't Hooft coupling $g_t \equiv g^2 N$ as well as f are kept fixed):

$$\frac{f^2}{2} \int d^4x d^4y \mathcal{O}(x) \mathcal{O}(y) \langle \mathcal{O}(x) \mathcal{O}(y) \rangle \sim \pi^2 f^2 \ln \Lambda \int d^4x \mathcal{O}^2(x), \quad (\text{B.6})$$

with Λ an ultraviolet cutoff. This leads to a one-loop beta function for f , which does not receive higher loop corrections in the large N limit [21].

Diagrammatically, we represent the $(\text{Tr}\Phi^2)^2$ vertex in double line notation as in Figure 17. The diagram in Figure 18 then leads to the renormalization discussed above. To see that it survives the large N limit, note that both vertices come with a factor f/N^2 , while the two index loops each contribute a factor of N , so that the one-loop diagram in Figure 18 is of the same order in N as the vertex Figure 17 (if f is kept fixed in the large N limit). This also makes it clear that diagrams such as Figure 19 do not survive the large N limit: there are no index loops that can provide factors of N . By the same token, the higher-loop diagrams that survive the large N limit are those like the one in Figure 20, which are factorizable.

To verify the above one-loop result and to show the absence of higher-loop corrections to the beta function for f , we wish to compute the diagrams that survive the large N

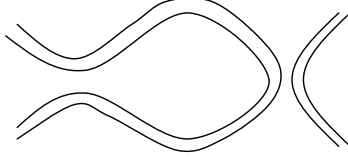


Figure 19: A diagram that does not survive the large N limit.

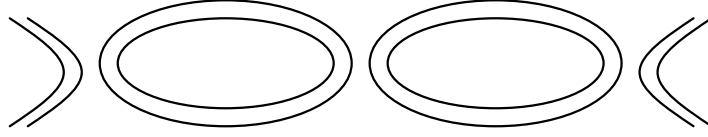


Figure 20: Higher order diagrams that survives the large N limit are factorizable.

limit. Before doing so, let us briefly review the one-loop renormalization of the theory of a single (massive or massless) scalar field with a $-\lambda\phi^4/4$ potential. We use renormalized perturbation theory (see, for instance, [61]):

$$\mathcal{L} = -\frac{1}{2}(\partial_\mu\phi)^2 - \frac{1}{2}m^2\phi^2 + \frac{\lambda}{4}\phi^4 - \frac{1}{2}\delta_Z(\partial_\mu\phi)^2 - \frac{1}{2}\delta_m\phi^2 + \frac{\delta_\lambda}{4}\phi^4, \quad (\text{B.7})$$

where all the fields and parameters are renormalized ones. To one-loop order, the two to two scattering amplitude gets contributions from the diagrams in Figure 21. The result is

$$i\mathcal{M}(p_1p_2 \rightarrow p_3p_4) = 6i\lambda + (6i\lambda)^2 [iV(s) + iV(t) + iV(u)] + 6i\delta_\lambda^{(1)}, \quad (\text{B.8})$$

where

$$iV(p^2) = \frac{1}{2} \int \frac{d^4k}{(2\pi)^4} \frac{-i}{k^2 + m^2} \frac{-i}{(k+p)^2 + m^2} \quad (\text{B.9})$$

and $\delta_\lambda^{(1)}$ is the order λ contribution to δ_λ . We impose the renormalization condition

$$i\mathcal{M}(p_1p_2 \rightarrow p_3p_4) = 6i\lambda \quad \text{at} \quad (p_1 + p_2)^2 = (p_1 + p_3)^2 = (p_1 + p_4)^2 = \mu^2. \quad (\text{B.10})$$

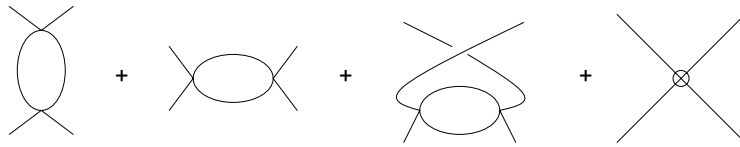


Figure 21: One-loop diagrams and a counterterm for a single scalar field.

This implies

$$\delta_\lambda^{(1)} = 18\lambda^2 V(\mu^2) = -\frac{9\lambda^2}{16\pi^2} \left(\frac{2}{\epsilon} - \ln \mu^2 + \text{finite} \right), \quad (\text{B.11})$$

where in the last equality we used dimensional regularization. To identify the beta function, consider the Callan-Symanzik equation

$$\left[\mu \frac{\partial}{\partial \mu} + \beta(\lambda) \frac{\partial}{\partial \lambda} + n\gamma(\lambda) \right] G^{(n)}(\{x_i\}; \mu, \lambda) = 0, \quad (\text{B.12})$$

where μ is the renormalization scale and $G^{(n)}(x_1, \dots, x_n)$ is the connected n -point function computed in renormalized perturbation theory. For the 4-point function,

$$G^{(4)}(p_1, p_2, p_3, p_4) = i\mathcal{M}(p_1 p_2 \rightarrow p_3 p_4) \prod_{j=1}^4 \frac{-i}{p_j^2}, \quad (\text{B.13})$$

we find

$$\mu \frac{\partial}{\partial \mu} G^{(4)} = \frac{27i\lambda^2}{4\pi^2} \prod_{j=1}^4 \frac{-i}{p_j^2}. \quad (\text{B.14})$$

Therefore the Callan-Symanzik equation is satisfied to order λ^2 if

$$\beta(\lambda) = -\frac{9\lambda^2}{8\pi^2} + O(\lambda^3), \quad (\text{B.15})$$

which is the familiar expression for the one-loop beta function.

In the analogous computation for the renormalization of the double trace deformation, only the ‘‘s-channel’’ part of the above computation survives in the large N limit, as we have argued before. We write

$$\delta_\lambda^{(1)} = \delta_\lambda^{(1)}(s) + \delta_\lambda^{(1)}(t) + \delta_\lambda^{(1)}(u) \quad (\text{B.16})$$

with

$$\delta_\lambda^{(1)}(s) = 6\lambda^2 V(\mu^2) = -\frac{3\lambda^2}{16\pi^2} \left(\frac{2}{\epsilon} - \ln \mu^2 + \text{finite} \right). \quad (\text{B.17})$$

Also at two-loop order, only ‘‘s-channel’’ diagrams will be important to leading order in $1/N$, as we have seen before; the relevant diagrams are in Figure 22, where the insertion of a cross denotes the one-loop counterterm $\delta_\lambda^{(1)}(s)$. We find (suppressing external propagators)

$$G^{(4)} = 6i\lambda + (6i\lambda)^2 [iV(p^2) - iV(\mu^2)] - (6i\lambda)^3 [V(p^2) - V(\mu^2)]^2 + \dots, \quad (\text{B.18})$$

where $p = p_1 + p_2$. The various $V(\mu^2)$ come from one-loop counterterms; a two-loop counterterm has merely cancelled a momentum-independent divergence $(6i\lambda)^3 [V(\mu^2)]^2$. Computing

$$\mu \frac{\partial}{\partial \mu} G^{(4)} = \frac{9i\lambda^2}{4\pi^2} - \frac{27i\lambda^3}{\pi^2} [V(p^2) - V(\mu^2)] + \dots \quad (\text{B.19})$$

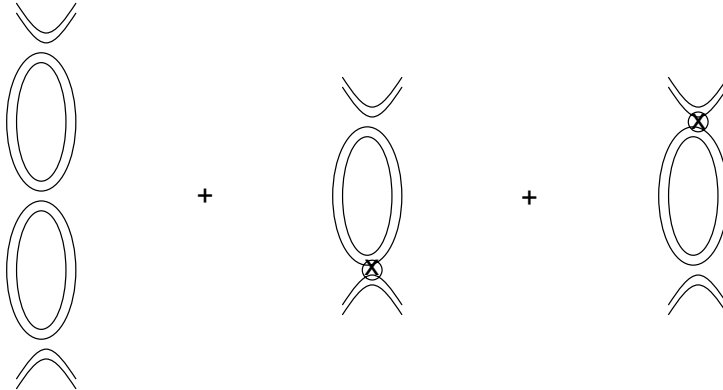


Figure 22: Two-loop diagrams in the large N limit.

and

$$\frac{\partial}{\partial \lambda} G^{(4)} = 6i - 72i\lambda [V(p^2) - V(\mu^2)] + \dots, \quad (\text{B.20})$$

it is easy to see that the Callan-Symanzik equation is satisfied for

$$\beta(\lambda) = -\frac{3\lambda^2}{8\pi^2}. \quad (\text{B.21})$$

It is easy to check that this remains the case at higher order in λ . Thus we have verified that the beta function is one-loop exact.

We will be interested in an approximation of the quantum effective action that is valid for a large range of field values, in particular for large field values. An appropriate framework is that of [46], where the standard Feynman diagram expansion is resummed and the theory is organized in a derivative expansion,

$$\Gamma = \int d^4x [-V(\phi) - \frac{1}{2} \partial_\mu \phi \partial^\mu \phi Z(\phi) + \dots], \quad (\text{B.22})$$

and an expansion in the number of loops. First, we focus on the effective potential, *i.e.*, (minus) the term without derivatives, in the one-loop approximation.

Starting from the classical potential

$$V_{\text{class}} = -\frac{\lambda}{4} \phi^4, \quad (\text{B.23})$$

one computes [46]

$$V_{1\text{-loop}} = \frac{1}{2} \int \frac{d^4k}{(2\pi)^4} \ln \left(1 - \frac{3\lambda\phi^2}{k^2} \right), \quad (\text{B.24})$$

where the integral is over Euclidean four-momenta. This can be rewritten in terms of $x = k^2$:

$$V_{1\text{-loop}} = \frac{1}{32\pi^2} \int_0^\infty dx x \ln \left(1 - \frac{3\lambda\phi^2}{x} \right). \quad (\text{B.25})$$

Since the integral diverges, we introduce a UV cutoff $x \leq \Lambda^2$. For $\lambda > 0$, we also need an IR cutoff $x \geq \mu_{IR}^2$ if we want a real effective potential (see [62]). Thus we compute, dropping terms that vanish as $\Lambda \rightarrow \infty$:

$$\int_{\mu_{IR}^2}^{\Lambda^2} dx x \ln \left(1 - \frac{3\lambda\phi^2}{x} \right) = -\frac{3\lambda\Lambda^2\phi^2}{2} - \frac{9\lambda^2\phi^4}{4} - \frac{\mu_{IR}^4}{2} \ln \left(1 - \frac{3\lambda\phi^2}{\mu_{IR}^2} \right) - \frac{3\lambda\phi^2}{2}(\Lambda^2 - \mu_{IR}^2) - \frac{9\lambda^2\phi^4}{2} \ln \left(\frac{\Lambda^2}{\mu_{IR}^2 - 3\lambda\phi^2} \right). \quad (\text{B.26})$$

For $\lambda < 0$, *i.e.*, a positive quartic potential, we can take $\mu_{IR} = 0$ and recover the standard result [46]

$$V_{1\text{-loop}} = \frac{1}{32\pi^2} \left\{ -3\lambda\Lambda^2\phi^2 - \frac{9\lambda^2\phi^4}{4} + \frac{9\lambda^2\phi^4}{2} \ln \left(\frac{-3\lambda\phi^2}{\Lambda^2} \right) \right\}. \quad (\text{B.27})$$

For $\lambda > 0$, the case of interest in the present paper, choosing $\mu_{IR} = 0$ would give a complex effective potential, signaling the fact that localized wavefunctions are unstable to spreading while keeping the expectation value of ϕ fixed [62]. Therefore we choose instead to integrate out only the “unfrozen” (or “non-tachyonic”) modes; thus we choose

$$\mu_{IR}^2 = 3\lambda\phi^2 + \epsilon^2 \quad (\text{B.28})$$

and let $\epsilon \rightarrow 0$ at the end of the computation. This results in

$$V_{1\text{-loop}} = \frac{1}{32\pi^2} \left\{ -3\lambda\Lambda^2\phi^2 + \frac{9\lambda^2\phi^4}{4} + \frac{9\lambda^2\phi^4}{2} \ln \left(\frac{3\lambda\phi^2}{\Lambda^2} \right) \right\}. \quad (\text{B.29})$$

Now we add counterterms, imposing that the renormalized mass should vanish and defining the renormalized coupling λ_μ by the renormalization condition

$$V(\mu) = -\frac{\lambda_\mu}{4} \mu^4. \quad (\text{B.30})$$

This corresponds to choosing for the sliding scale μ the value of a spacetime-independent external scalar field ϕ rather than, say, the momentum of an external line. This has the virtue that no large logarithms will interfere with perturbation theory, which will thus be reliable as long as the renormalized coupling λ_μ is small. The result is

$$V(\phi) = -\frac{\lambda_\mu}{4} \phi^4 + \frac{9\lambda_\mu^2 \phi^4 \ln(\phi^2/\mu^2)}{64\pi^2}. \quad (\text{B.31})$$

The renormalization group equation can be obtained by demanding that $V(\phi)$ be independent of μ :

$$\mu \frac{d\lambda_\mu}{d\mu} = -\frac{9\lambda_\mu^2}{8\pi^2}. \quad (\text{B.32})$$

Here, we have ignored a contribution from $d/d\mu$ hitting the λ_μ^2 in the second term of (B.31), which is justified as long as $|\lambda_\mu \ln(\phi/\mu)| \ll 1$. Equation (B.32) is solved by

$$\lambda_\mu = \frac{16\pi^2}{9 \ln(\mu^2/M^2)}, \quad (\text{B.33})$$

with M an arbitrary scale (this implements dimensional transmutation). Choosing $\mu = \phi$, *i.e.*, the renormalization scale is set by the value of the field ϕ , the Coleman-Weinberg potential can then be written as

$$V(\phi) = -\frac{4\pi^2\phi^4}{9\ln(\phi^2/M^2)}. \quad (\text{B.34})$$

Now suppose that for some value ϕ_0 , the coupling is small,

$$0 < \lambda_{\phi_0} \ll 1, \quad (\text{B.35})$$

then $M < |\phi_0|$ and (B.34) is trustworthy (*i.e.*, higher order corrections can be ignored) for any ϕ such that $|\phi| > |\phi_0|$. As a result, we can conclude that in this case

$$V(\phi) \rightarrow -\infty \quad \text{for } |\phi| \rightarrow \infty. \quad (\text{B.36})$$

(This also holds for the massive theory, as long as $m \ll |\phi_0|$.) This analysis was for a single scalar field; as can be seen from the above discussion, it extends to the large N adjoint theory with only very minor changes.

As we have seen, the one-loop diagram Figure 18 involving two double trace vertices gives an order f^2 contribution to the beta function for the coupling f , leading to the effective potential (3.6). One can ask whether one-loop diagrams with one double trace vertex and one commutator squared vertex (see (B.1)) could give contributions of order fg^2 to the beta function for f and thus to the effective potential, which would be important at small f . The answer is that the fg^2 contributions to the effective potential cancel. To see this, let us compute the one-loop effective potential for ϕ , where $\Phi^1(x) = \phi(x)U$ with $\text{Tr}U^2 = 1$, in our deformed $\mathcal{N} = 4$ SYM theory, see (3.3) with (B.1) and (B.2). We choose a constant background $\Phi^1 = \phi U$ and compute the masses $M(\phi)$ of the various modes in this background; this involves fixing a gauge and introducing ghosts, see for instance [56]. Up to terms that can be absorbed in counterterms, every bosonic mode contributes

$$\frac{1}{32\pi^2} \frac{1}{2} M^4 \ln\left(\frac{M^2}{\Lambda^2}\right) \quad (\text{B.37})$$

to the effective potential, where Λ is a UV cutoff, while every fermionic mode contributes with a minus sign. In the undeformed $\mathcal{N} = 4$ SYM theory, these contributions cancel exactly between bosons and fermions. Our double trace deformation changes the scalar masses but not the masses of gauge bosons and fermions, leading to a non-trivial effective potential. It is easy to see that the scalars Φ_{ab}^i have

$$(M_{ab}^i)^2 = g^2\phi^2(U_{aa} - U_{bb})^2 + \frac{2fa^2\phi^2}{5N^2}, \quad (\text{B.38})$$

while after gauge fixing as in Ref. [56], p. 122, the scalars Φ_{ab}^1 have

$$(M_{ab}^1)^2 = g^2\phi^2(U_{aa} - U_{bb})^2 - \frac{2fa^2\phi^2}{N^2}(1 + 2\delta_{ab}U_{aa}^2). \quad (\text{B.39})$$

The contributions of order g^4 are those of the undeformed SYM theory and cancel by supersymmetry against those of gauge fields and fermions. Contributions of order fg^2 would have to come from off-diagonal scalars ($a \neq b$), but it is easy to see that they cancel between Φ^1 and Φ^i ($i = 2, \dots, 6$), at least up to terms that can be absorbed in the counterterms. So we have verified that the one-loop contribution to the effective potential is at least of order f^2 .

Since we will be interested in non-static solutions, knowledge of the potential alone is insufficient for our purposes: we also need to know the form of the derivative terms in the quantum effective action. Terms arising from non-divergent Feynman diagrams are suppressed by powers of the effective coupling λ_ϕ , which is small in the regime where we trust our one-loop effective potential. It will turn out that such terms will be small for the configurations of interest. Logarithmically divergent Feynman diagrams induce, upon renormalization, terms involving $\ln(\phi/\mu)$, with μ the renormalization scale. Such terms disappear when we choose $\mu = \phi$, as we have done for the effective potential. From power counting, the only possible divergences involving momenta arise in graphs with two external legs, which lead to wave function renormalization (as it turns out, such divergences do not occur at one-loop order in this theory, but do occur at higher loop order). We choose the renormalization condition $Z(\mu) = 1$ in (B.22), which for our choice $\mu = \phi$ implies that the field ϕ has a canonical kinetic term. Strictly speaking, the last conclusion holds for the theory of a single scalar field; in the adjoint model, the standard kinetic term $-\text{Tr}\partial_\mu\Phi\partial^\mu\Phi$ may be accompanied by terms with a different index structure, e.g. $-(\text{Tr}\Phi\partial_\mu\Phi)(\text{Tr}\Phi\partial^\mu\Phi)/\text{Tr}\Phi^2$, which will, however, be suppressed by powers of the effective coupling (these terms do not arise from ultraviolet divergent Feynman diagrams, but from resumming diagrams with more than two external legs).

The running coupling λ_ϕ given by (B.33) has a branch point at $\phi = \infty$, the place where we want to impose boundary conditions that make the Hamiltonian self-adjoint. To avoid this complication, it is convenient to first study the system with a finite UV cutoff ρ on the momenta, in which case the potential will be meromorphic near $\phi = \infty$. The idea is that after imposing appropriate boundary conditions and computing particle creation, the UV cutoff can be removed and it can be checked that the results have a well-defined limit. So let us compute the one-loop effective potential, with all non-tachyonic (“unfrozen”) modes integrated out, with a (smooth) UV cutoff ρ :

$$\begin{aligned} V_{1-loop}^\rho &= \frac{1}{32\pi^2} \int_{3\lambda\phi^2}^\infty dx x \ln\left(1 - \frac{3\lambda\phi^2}{x}\right) \frac{\rho^8}{(\rho^4 + x^2)^2} \\ &= \frac{3\lambda\phi^2\rho^4}{128\pi^2(9\lambda^2\phi^4 + \rho^4)} \left\{ -\pi\rho^2 + 6\lambda\phi^2 \ln(3\lambda\phi^2) + i\rho^2 \ln\left(1 - \frac{3i\lambda\phi^2}{\rho^2}\right) \right. \\ &\quad \left. - i\rho^2 \ln\left(1 + \frac{3i\lambda\phi^2}{\rho^2}\right) - 3\lambda\phi^2 \ln(\rho^4 + 9\lambda^2\phi^4) \right\}. \end{aligned} \tag{B.40}$$

Adding the tree-level potential and counterterms, we find

$$V = -\frac{\lambda}{4}\phi^4 + V_{1-loop} + A + B\phi^2 + C\phi^4, \tag{B.41}$$

where the last three terms are the counterterms. The coefficients A, B, C are fixed by the renormalization conditions

$$V(0) = 0, \quad V''(0) = 0, \quad V(\mu) = -\frac{\lambda_\mu}{4}\mu^4, \quad (\text{B.42})$$

where the dependence of the renormalized coupling λ_μ on the renormalization scale μ is indicated explicitly. Solving (B.42), we find

$$\begin{aligned} A &= 0, \\ B &= \frac{3\lambda_\mu\rho^2}{128\pi}, \\ C &= \frac{3\lambda_\mu\rho^2}{128\pi^2\mu^2(\rho^4 + 9\lambda_\mu^2\mu^4)} \left\{ -9\pi\lambda_\mu^2\mu^4 - 6\rho^2\lambda_\mu^2\mu^2 \ln(3\lambda_\mu\mu^2) - i\rho^4 \ln\left(1 - \frac{3i\lambda_\mu\mu^2}{\rho^2}\right) \right. \\ &\quad \left. + i\rho^4 \ln\left(1 + \frac{3i\lambda_\mu\mu^2}{\rho^2}\right) + 3\rho^2\lambda_\mu\mu^2 \ln(\rho^4 + 9\lambda_\mu^2\mu^4) \right\}. \end{aligned} \quad (\text{B.43})$$

Substituting (B.40) and (B.43) in (B.41), we obtain for the renormalized one-loop effective potential with renormalization scale μ and UV cutoff ρ

$$\begin{aligned} V &= -\frac{\lambda_\mu}{4}\phi^4 + \frac{3\lambda_\mu\phi^2\rho^2}{128\pi^2\mu^2(\rho^4 + 9\lambda_\mu^2\phi^4)} \times \\ &\times \left\{ \pi\mu^2(\rho^4 + 9\lambda_\mu^2\phi^4) - 9\pi\lambda_\mu^2\mu^4\phi^2 - 6\rho^2\lambda_\mu\mu^2\phi^2 \ln(3\lambda_\mu\mu^2) - i\rho^4\phi^2 \ln\left(1 - \frac{3i\lambda_\mu\mu^2}{\rho^2}\right) \right. \\ &\quad \left. + i\rho^4\phi^2 \ln\left(1 + \frac{3i\lambda_\mu\mu^2}{\rho^2}\right) + 3\rho^2\phi^2\lambda_\mu\mu^2 \ln(\rho^4 + 9\lambda_\mu^2\mu^4) - \pi\mu^2\rho^4 \right. \\ &\quad \left. + 6\rho^2\lambda_\mu\mu^2\phi^2 \ln(3\lambda_\mu\phi^2) + i\rho^4\mu^2 \ln\left(1 - \frac{3i\lambda_\mu\phi^2}{\rho^2}\right) - i\rho^4\mu^2 \ln\left(1 + \frac{3i\lambda_\mu\phi^2}{\rho^2}\right) \right. \\ &\quad \left. - 3\rho^2\mu^2\lambda_\mu\phi^2 \ln(\rho^4 + 9\lambda_\mu^2\phi^4) \right\}. \end{aligned} \quad (\text{B.44})$$

To complete the computation of the one-loop effective potential, we need λ_μ as a function of μ , and we will eventually set $\mu = \phi$. For this reason, we impose that V should be μ -independent at $\phi = \mu$:

$$0 = \mu \frac{\partial}{\partial \mu} V|_{\phi=\mu}. \quad (\text{B.45})$$

This leads to the following equation for the running coupling at the scale $\mu = \phi$:

$$\begin{aligned} \phi \frac{d\lambda_\phi}{d\phi} &= \frac{3\rho^2\lambda_\phi}{16\pi^2\phi^2(\rho^4 + 9\lambda_\phi^2\phi^4)^2} \times \\ &\times \left\{ -12\rho^6\lambda_\phi\phi^2 + \pi\rho^8 + 18\pi\rho^4\lambda_\phi^2\phi^4 + 81\pi\lambda_\phi^4\phi^8 - 54\rho^2\lambda_\phi^3\phi^6 \ln\left(1 + \frac{\rho^4}{9\lambda_\phi^2\phi^4}\right) \right. \\ &\quad \left. - i(\rho^8 + 27\rho^4\lambda_\phi^2\phi^4) \ln\left(1 - \frac{i\rho^2}{3\lambda_\phi\phi^2}\right) + i(\rho^8 + 27\rho^4\lambda_\phi^2\phi^4) \ln\left(1 + \frac{i\rho^2}{3\lambda_\phi\phi^2}\right) \right\}. \end{aligned} \quad (\text{B.46})$$

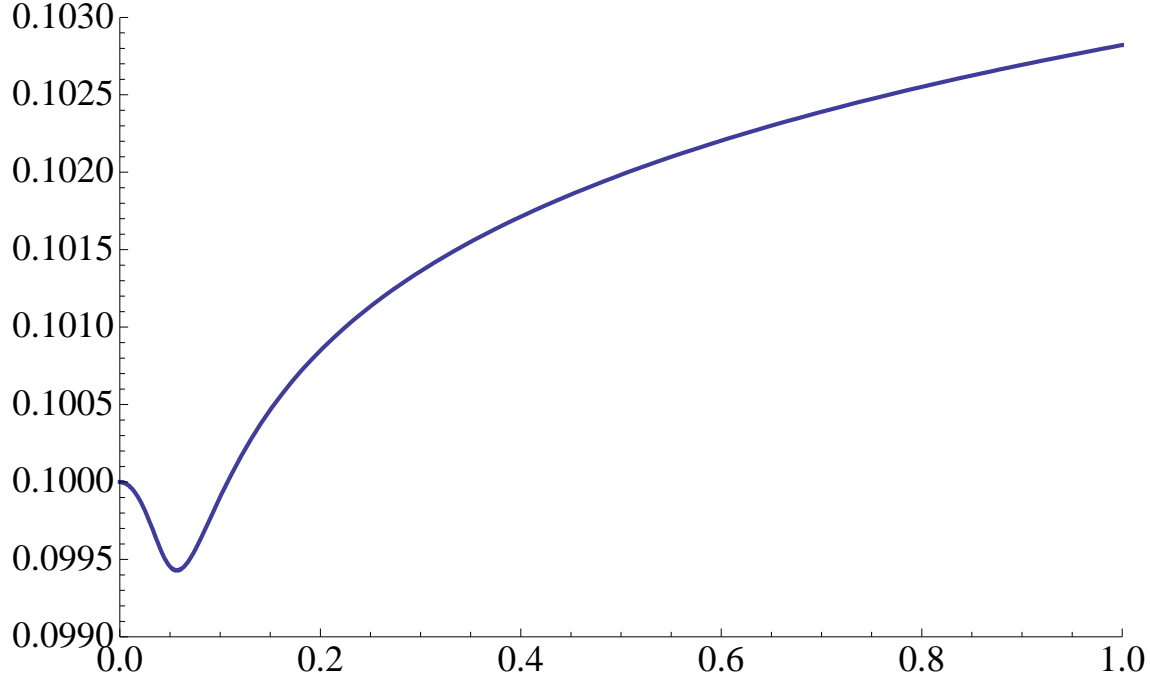


Figure 23: The running coupling λ_ϕ at finite UV cutoff ρ , versus $z = 1/\phi$, showing how it tends to the finite limit λ_∞ .

C The Renormalized Effective Potential $V(\phi)$ in the Complex ϕ -plane

The calculations performed in this paper rely on the use of complex solutions of the classical field equations for the effective theory. In the previous appendix, we computed the effective potential for real ϕ by integrating out the non-tachyonic modes and renormalizing the theory at a scale defined by the value of the scalar field ϕ . The effective potential is simply given by $-\frac{1}{4}\lambda_\phi\phi^4$, where λ_ϕ solves (B.46) with some given initial condition. One can also use (B.46) to analytically continue $V(\phi)$ to complex ϕ . If we take the $\rho = \infty$ limit before continuing, then $V(\phi)$ has a branch point at $\phi = \infty$, which interferes with our construction of the self-adjoint extension via the method of images. Therefore we should rather continue at finite UV cutoff ρ , find the relevant classical solution and only then take the limit $\rho \rightarrow \infty$.

In order to study the form of the effective potential at large ϕ , it is convenient to set $\phi = 1/z$. Equation (B.46) becomes

$$\begin{aligned}
 -z \frac{d\lambda_\phi}{dz} &= \frac{3\rho^2 \lambda_\phi z^2}{16\pi^2 \phi^2 (\rho^4 z^4 + 9\lambda_\phi^2)^2} \times \\
 &\times \left\{ -12\rho^6 \lambda_\phi z^6 + \pi\rho^8 z^8 + 18\pi\rho^4 \lambda_\phi^2 z^4 + 81\pi\lambda_\phi^4 - 54\rho^2 \lambda_\phi^3 z^2 \ln \left(1 + \frac{\rho^4 z^4}{9\lambda_\phi^2} \right) \right. \\
 &\quad \left. - i(\rho^8 z^8 + 27\rho^4 \lambda_\phi^2 z^4) \ln \left(1 - \frac{i\rho^2 z^2}{3\lambda_\phi} \right) + i(\rho^8 z^8 + 27\rho^4 \lambda_\phi^2 z^4) \ln \left(1 + \frac{i\rho^2 z^2}{3\lambda_\phi} \right) \right\}.
 \end{aligned} \tag{C.1}$$

The right hand side is regular at $z = 0$, so given the coupling there, λ_∞ , it is straightforward to numerically integrate the equation to find λ_ϕ at real ϕ (Figure 23). Likewise, one can integrate in any particular direction in z to find the potential at complex ϕ . Since (B.46) is a first order differential equation, the solution λ_ϕ can only fail to be analytic at points where the right hand side is singular. Ignoring the singularity at small ϕ , where λ_ϕ becomes large and perturbation theory fails, the running coupling is singular only at solutions of $\rho^4 + 9\lambda_\phi^2\phi^4 = 0$. Approximating λ_ϕ by its value at $\phi = \infty$, which is a good approximation when λ_∞ is small, one sees that these points are roughly located at $\phi = \rho/\sqrt{3\lambda_\infty}$ times a fourth root of unity. Clearly, as ρ tends to infinity, these four branch points converge to the origin, forming a single branch point at $\phi = \infty$.

The four singularities are all related, by two symmetries. First, the effective potential is real on the real z -axis, so by the Schwarz reflection principle its singularities occur at complex conjugate pairs. Second, as a result of the symmetry under $\phi \rightarrow -\phi$ in the original (bare) theory, (C.1) is invariant under $z \rightarrow -z$. Thus we need only study a single branch point, for example the one at $z = e^{i\pi/4}\sqrt{3\lambda_\phi}/\rho \equiv e^{i\pi/4}3s_\phi/\rho$, where we have defined $3s_\phi^2 \equiv \lambda_\phi$.

Expanding the right hand side of (C.1) around $z = e^{i\pi/4}3s_\phi/\rho$, for example, we find

$$-z \frac{ds_\phi}{dz} \sim \frac{27s_\phi^5 \ln(2e^{-1}(s_\phi - e^{-i\pi/4}\rho z/3))}{128\pi^2(s_\phi - e^{-i\pi/4}\rho z/3)^2} + \mathcal{O}((s_\phi - e^{-i\pi/4}\rho z/3)^{-1}). \quad (\text{C.2})$$

At first sight, there appears to be a second order pole on the right hand side. But the situation is subtle because s_ϕ is itself a function of z . In the vicinity of the branch point, the solution is $s_\phi \approx s_{\phi,c} + \delta s(z)$, where $z_c = 3s_{\phi,c}e^{i\pi/4}/\rho$ is the location of the branch point and $s_{\phi,c}$ is the value of s_ϕ there. Setting $|z| = e^x$, Equation (C.2) becomes

$$\frac{d\delta s}{dx} \approx -\frac{27s_c^5 \ln(2\delta s/e)}{128\pi^2\delta s^2}, \quad (\text{C.3})$$

which is solved for x approaching x_c from below by

$$\delta s / (\ln(e/(2\delta s)))^{\frac{1}{3}} \approx e^{-i\pi/3}(x_c - x)^{\frac{1}{3}} \left(\frac{81s_c^5}{128\pi^2} \right)^{\frac{1}{3}}. \quad (\text{C.4})$$

Figure 24 shows the full numerical solution for s_ϕ , with the branch point being found by shooting, compared with this formula. We conclude that s_ϕ is finite at the branch points and varies in their vicinity roughly as $\delta s \sim (z_c - z)^{\frac{1}{3}}$, with logarithmic corrections. The corresponding deviation of λ_ϕ from its value λ_∞ at infinite ϕ implied by (C.4) is of order $\lambda_\phi^{\frac{4}{3}}$. Thus the fractional deviation in the coupling decreases as the running coupling to the one third power as ρ is raised. Therefore in the large ρ limit, the effective potential in the neighbourhood of each branch point becomes more and more accurately approximated by the effective coupling calculated at infinite ρ .

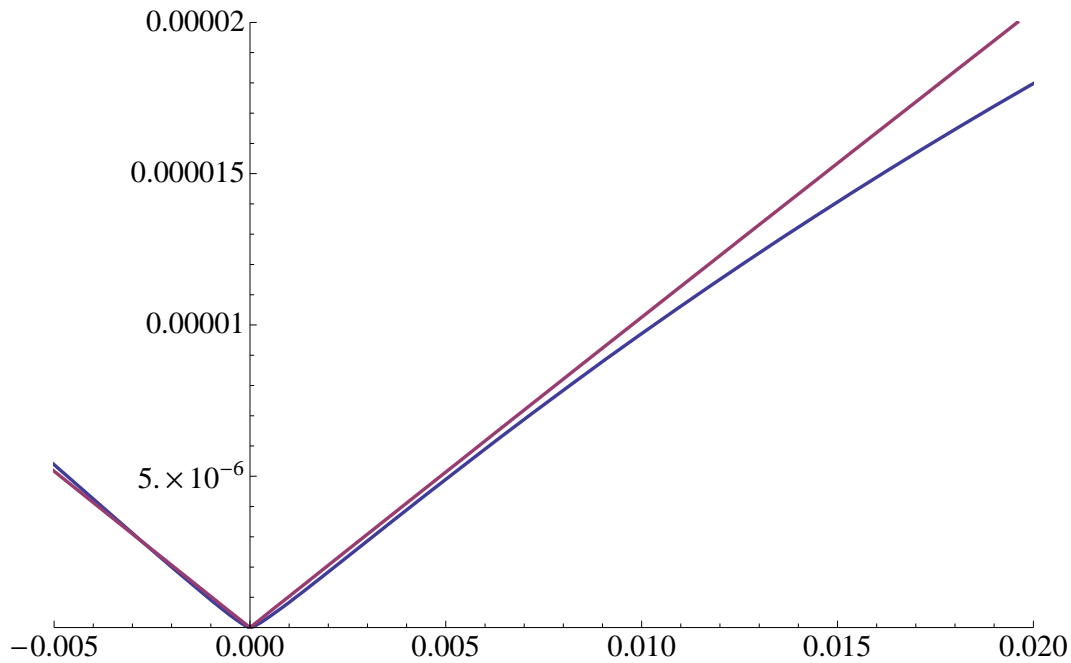


Figure 24: Behavior of the running coupling near a branch point in the complex z -plane. The third power of the left hand side of (C.4) is plotted against $x_c - x$. The upper curve shows a linear fit.

D Complex Classical Solutions in the Infinite Cutoff Limit

In the previous appendix, we studied the behavior of the effective potential in the complex ϕ -plane for finite cutoff ρ . Besides the fourth order pole at $\phi = \infty$, the only singularities are four mild, perturbatively suppressed branch points located at $|z|_B \sim \lambda_{\infty}^{\frac{1}{2}}/\rho$.

In Subsection 5.3, we explained how the coherent state parameter specifying the initial condition must be changed when a family of classical solutions crosses a branch point. We wish to follow the same procedure here, first at finite cutoff ρ and then taking the infinite ρ limit. As explained in Subsection 5.4, we start from classical solutions to the finite- ρ equations of motion which pass around the branch points without encountering any branch cuts so that the method of images may be used to construct the self-adjoint extension. These solutions have very large x_f , of order the cutoff in appropriate units, and times $(t_f - t_i)$ which are roughly twice the classical rolling-down time. We now consider decreasing $(t_f - t_i)$ so that the trajectory of the first classical solution, the upper solution in Figure 7, is deformed towards the positive real χ -axis. As it does so, it encounters the two upper branch points and moves onto a new Riemann sheet. The associated shift in the coherent state parameter is calculated, as explained in Subsection 5.3, by comparing classical solutions passing to either side of the branch point.

The question we want to address in this appendix is to what extent the shift in the coherent state parameter can be calculated directly in the infinite- ρ limit. Because the branch points are very mild, it is plausible that the classical solutions of interest are insensitive

to the details of the finite-cutoff effective potential in their vicinity. Rather, the difference between neighbouring classical solutions which begin on different Riemann sheets accrues along the entire classical trajectory. But this latter effect can be computed by *first* taking ρ to infinity and then comparing the two classical solutions, one on the first Riemann sheet (on which the potential is real just above the positive real axis) and one on the second Riemann sheet (on which the potential is real just below the positive real axis).

In this appendix we shall calculate the difference between two classical trajectories moving in slightly different potentials but with the same initial coherent state parameter (5.1), the same final coordinate χ_f , and the same total time $t_f - t_i$. If we can show that the difference between these two trajectories is small, then we are justified in taking the infinite ρ limit *before* computing the shift in the coherent state parameter associated with moving onto the physical Riemann sheet.

We shall work in the coordinate x used in Subsection 5.2 and the following subsections. We define the difference in potentials $\delta V(x) = V_\infty(x) - V_\rho(x)$ where V_ρ is the effective potential at UV cutoff ρ . We want to see whether the final classical solution is sensitive to the details of the potential at large values of x where the potential has significant dependence on ρ . In order to examine this sensitivity, we will solve the linearized equations for the perturbation to the classical solution induced by a change $\delta V(x)$ in the potential, for x near x_f .

A small perturbation of the trajectory $x(t) \rightarrow x(t) + \delta x(t)$ which does not change the coherent state parameter, the final coordinate x_f and the total time $t_f - t_i$ must obey the constraints

$$\delta x_i + 2iL^2 \frac{\delta e - V'(x)\delta x_i}{\hbar \dot{x}_i} = 0, \quad (\text{D.5})$$

which relates δx_i to δe , and

$$\delta t = \delta \int_i^f \frac{dx}{\dot{x}} = -\frac{\delta x_i}{\dot{x}_i} - \int_i^f dx \frac{\delta e - V'(x)\delta x - \delta V(x)}{\dot{x}^3} = 0, \quad (\text{D.6})$$

where $\dot{x} = \sqrt{2(e - V(x))}$.

The perturbation $\delta x(t)$ to the trajectory is found from the energy equation, $\delta e = \dot{x}\delta \dot{x} + V'(x)\delta x + \delta V(x) = 0$. Imposing the final condition that $\delta x_f = 0$, this integrates to

$$\delta x(t) = -\dot{x} \int_t^{t_f} dt \frac{\delta e - \delta V(x)}{\dot{x}^2} = -\dot{x} \int_x^{x_f} dx \frac{\delta e - \delta V(x)}{\dot{x}^3}. \quad (\text{D.7})$$

Putting (D.5) and (D.7) together, we can calculate the perturbation in the initial position for the trajectory,

$$\delta x_i = \frac{\dot{x}_i}{2} \int_{x_i}^{x_f} dx \frac{V'(x)}{\dot{x}^2} \int_x^{x_f} dx \frac{\delta e - \delta V(x)}{\dot{x}^3}. \quad (\text{D.8})$$

Exchanging orders in the integral, one finds

$$\delta x_i = \frac{\dot{x}_i}{2} \int_{x_i}^{x_f} dx \frac{(\delta e - \delta V(x)) \ln((e - V(x))/(e - V(x_i)))}{(2(e - V(x)))^{\frac{3}{2}}}. \quad (\text{D.9})$$

We are interested in the effect of a small change in the potential $\delta V(x)$, in the region $x \sim x_f$ affected by the cutoff, where the potential dominates over e . At large x the integral over $\delta V(x)$ looks like $\int dx x^{-2} \ln^{\frac{3}{2}}(x) (\delta V/V)$. But we have already argued, in the previous appendix, that for x in the vicinity of the branch points, $\delta V/V$ is perturbatively small. It follows that the integral determining the shift in the initial condition δx_i is convergent at large x . In the limit as ρ goes to infinity, the fractional difference between the finite- and infinite-cutoff potentials, $\delta V/V$ is localized at higher and higher values of x and its effect becomes negligible. Therefore the effect of moving to the next Riemann sheet may be computed using the infinite-cutoff effective potential.

References

- [1] J. B. Hartle and S. W. Hawking, Phys. Rev. D **28**, 2960 (1983).
- [2] M. Gasperini and G. Veneziano, Astropart. Phys. **1** (1993) 317 [arXiv:hep-th/9211021].
- [3] J. Khoury, B. A. Ovrut, P. J. Steinhardt and N. Turok, Phys. Rev. D **64** (2001) 123522 [arXiv:hep-th/0103239].
- [4] J. Khoury, B. A. Ovrut, N. Seiberg, P. J. Steinhardt and N. Turok, Phys. Rev. D **65**, 086007 (2002) [arXiv:hep-th/0108187].
- [5] A. H. Guth, Phys. Rev. D **23**, 347 (1981); A. D. Linde, Phys. Lett. B **108**, 389 (1982); A. Albrecht and P. J. Steinhardt, Phys. Rev. Lett. **48**, 1220 (1982).
- [6] P. J. Steinhardt and N. Turok, Phys. Rev. D **65** (2002) 126003 [arXiv:hep-th/0111098]; J. K. Erickson, S. Gratton, P. J. Steinhardt and N. Turok, Phys. Rev. D **75**, 123507 (2007) [arXiv:hep-th/0607164].
- [7] J. L. Lehners, P. McFadden, N. Turok and P. J. Steinhardt, Phys. Rev. D **76**, 103501 (2007) [arXiv:hep-th/0702153]; E. I. Buchbinder, J. Khoury and B. A. Ovrut, arXiv:hep-th/0702154; arXiv:0706.3903 [hep-th]; arXiv:0710.5172 [hep-th]; P. Creminelli and L. Senatore, arXiv:hep-th/0702165; K. Koyama and D. Wands, JCAP **0704**, 008 (2007) [arXiv:hep-th/0703040]; A. J. Tolley and D. H. Wesley, JCAP **0705**, 006 (2007) [arXiv:hep-th/0703101]; K. Koyama, S. Mizuno and D. Wands, Class. Quant. Grav. **24**, 3919 (2007) [arXiv:0704.1152 [hep-th]]; K. Koyama, S. Mizuno, F. Vernizzi and D. Wands, arXiv:0708.4321 [hep-th]; J. L. Lehners and P. J. Steinhardt, arXiv:0712.3779 [hep-th].
- [8] P. J. Steinhardt and N. Turok, Science **312**, 1180 (2006) [arXiv:astro-ph/0605173].
- [9] L. Cornalba and M. S. Costa, Phys. Rev. D **66** (2002) 066001 [arXiv:hep-th/0203031]; N. A. Nekrasov, Surveys High Energ. Phys. **17**, 115 (2002) [arXiv:hep-th/0203112]; H. Liu, G. W. Moore and N. Seiberg, JHEP **0206** (2002) 045 [arXiv:hep-th/0204168]; JHEP **0210** (2002) 031 [arXiv:hep-th/0206182]; A. Lawrence, JHEP **0211**, 019 (2002)

- [arXiv:hep-th/0205288]; G. T. Horowitz and J. Polchinski, Phys. Rev. D **66**, 103512 (2002) [arXiv:hep-th/0206228]; M. Berkooz, B. Craps, D. Kutasov and G. Rajesh, JHEP **0303**, 031 (2003) [arXiv:hep-th/0212215].
- [10] M. Berkooz, B. Pioline and M. Rozali, JCAP **0408**, 004 (2004) [arXiv:hep-th/0405126]; N. Turok, M. Perry and P. J. Steinhardt, Phys. Rev. D **70** (2004) 106004 [Erratum-ibid. D **71** (2005) 029901] [arXiv:hep-th/0408083]; J. McGreevy and E. Silverstein, JHEP **0508**, 090 (2005) [arXiv:hep-th/0506130].
- [11] N. Turok, M. Perry and P. J. Steinhardt, Phys. Rev. D **70**, 106004 (2004) [Erratum-ibid. D **71**, 029901 (2005)] [arXiv:hep-th/0408083]; D. S. Berman and M. J. Perry, Phys. Lett. B **635**, 131 (2006) [arXiv:hep-th/0601141].
- [12] G. Niz and N. Turok, Phys. Rev. D **75**, 126004 (2007) [arXiv:0704.1727 [hep-th]].
- [13] J. L. Karczmarek and A. Strominger, JHEP **0404**, 055 (2004) [arXiv:hep-th/0309138]; S. R. Das and J. L. Karczmarek, Phys. Rev. D **71** (2005) 086006 [arXiv:hep-th/0412093].
- [14] T. Banks, W. Fischler, S. H. Shenker and L. Susskind, Phys. Rev. D **55** (1997) 5112 [arXiv:hep-th/9610043].
- [15] B. Craps, S. Sethi and E. P. Verlinde, JHEP **0510** (2005) 005 [arXiv:hep-th/0506180]; S. R. Das and J. Michelson, Phys. Rev. D **73** (2006) 126006 [arXiv:hep-th/0602099]; B. Craps, A. Rajaraman and S. Sethi, Phys. Rev. D **73** (2006) 106005 [arXiv:hep-th/0601062]; E. J. Martinec, D. Robbins and S. Sethi, JHEP **0608** (2006) 025 [arXiv:hep-th/0603104].
- [16] J. M. Maldacena, Adv. Theor. Math. Phys. **2**, 231 (1998) [Int. J. Theor. Phys. **38**, 1113 (1999)] [arXiv:hep-th/9711200].
- [17] T. Hertog and G. T. Horowitz, JHEP **0407** (2004) 073 [arXiv:hep-th/0406134].
- [18] T. Hertog and G. T. Horowitz, JHEP **0504** (2005) 005 [arXiv:hep-th/0503071].
- [19] P. Kraus, H. Ooguri and S. Shenker, Phys. Rev. D **67**, 124022 (2003) [arXiv:hep-th/0212277]; L. Fidkowski, V. Hubeny, M. Kleban and S. Shenker, JHEP **0402**, 014 (2004) [arXiv:hep-th/0306170]; G. Festuccia and H. Liu, JHEP **0604** (2006) 044 [arXiv:hep-th/0506202]; A. Hamilton, D. Kabat, G. Lifschytz and D. A. Lowe, Phys. Rev. D **75** (2007) 106001 [Erratum-ibid. D **75** (2007) 129902] [arXiv:hep-th/0612053].
- [20] M. Cvetič, S. Nojiri and S. D. Odintsov, Phys. Rev. D **69** (2004) 023513 [arXiv:hep-th/0306031]. C. S. Chu and P. M. Ho, JHEP **0604** (2006) 013 [arXiv:hep-th/0602054]; arXiv:0710.2640 [hep-th]; S. R. Das, J. Michelson, K. Narayan and S. P. Trivedi, Phys. Rev. D **74** (2006) 026002 [arXiv:hep-th/0602107]; F. L. Lin and W. Y. Wen, JHEP **0605** (2006) 013 [arXiv:hep-th/0602124]; Phys. Rev. D **75** (2007) 026002 [arXiv:hep-th/0610053].

- [21] E. Witten, arXiv:hep-th/0112258.
- [22] J. Khoury, B. A. Ovrut, P. J. Steinhardt and N. Turok, Phys. Rev. D **66**, 046005 (2002) [arXiv:hep-th/0109050].
- [23] N. Turok, B. Craps and T. Hertog, arXiv:0711.1824 [hep-th]
- [24] N. Turok, in *Particles, Strings and Cosmology*, proceedings of PASCOS 2007, Eds. A. Rajantie, P. Dauncey, C. Contaldi and H. Stoica, AIP Conference Proceedings **957**, American Institute of Physics, 2007.
- [25] M. Gunaydin, L. J. Romans and N. P. Warner, Phys. Lett. B **154** (1985) 268.
- [26] M. Gunaydin, L. J. Romans and N. P. Warner, Nucl. Phys. B **272** (1986) 598.
- [27] M. Pernici, K. Pilch and P. van Nieuwenhuizen, Nucl. Phys. B **259**, 460 (1985).
- [28] D. Z. Freedman, S. S. Gubser, K. Pilch and N. P. Warner, JHEP **0007**, 038 (2000) [arXiv:hep-th/9906194].
- [29] P. Breitenlohner and D. Z. Freedman, Annals Phys. **144** (1982) 249.
- [30] G. W. Gibbons, C. M. Hull and N. P. Warner,
- [31] P. K. Townsend, Phys. Lett. B **148** (1984) 55.
- [32] M. Henneaux, C. Martinez, R. Troncoso and J. Zanelli, Annals Phys. **322**, 824 (2007) [arXiv:hep-th/0603185].
- [33] T. Hertog and G. T. Horowitz, Phys. Rev. Lett. **94**, 221301 (2005) [arXiv:hep-th/0412169].
- [34] T. Hertog and K. Maeda, JHEP **0407**, 051 (2004) [arXiv:hep-th/0404261].
- [35] M. Henneaux, C. Martinez, R. Troncoso and J. Zanelli, Phys. Rev. D **70**, 044034 (2004) [arXiv:hep-th/0404236].
- [36] T. Hertog and S. Hollands, Class. Quant. Grav. **22**, 5323 (2005) [arXiv:hep-th/0508181]; A. J. Amsel and D. Marolf, Phys. Rev. D **74**, 064006 (2006) [Erratum-ibid. D **75**, 029901 (2007)] [arXiv:hep-th/0605101]; A. J. Amsel, T. Hertog, S. Hollands and D. Marolf, Phys. Rev. D **75**, 084008 (2007) [arXiv:hep-th/0701038].
- [37] S. de Haro, I. Papadimitriou, A. Petkou, Phys. Rev. Lett **98**, 231601 (2007) [arXiv:hep-th/0611315].
- [38] S. R. Coleman and F. De Luccia, Phys. Rev. D **21** (1980) 3305.
- [39] M. Cvetič, H. Lu, C. N. Pope, A. Sadrzadeh, T. A. Tran, Nucl. Phys. **B586** (2000) 275 [arXiv:hep-th/0003103].

- [40] A. A. Tseytlin and C. Vafa, Nucl. Phys. B **372**, 443 (1992) [arXiv:hep-th/9109048].
- [41] M. Bianchi, D. Z. Freedman and K. Skenderis, JHEP **0108** (2001) 041 [arXiv:hep-th/0105276]; Nucl. Phys. B **631** (2002) 159 [arXiv:hep-th/0112119].
- [42] V. Balasubramanian, P. Kraus and A. E. Lawrence, Phys. Rev. D **59** (1999) 046003 [arXiv:hep-th/9805171].
- [43] M. Berkooz, A. Sever and A. Shomer, JHEP **0205**, 034 (2002) [arXiv:hep-th/0112264].
- [44] S. Elitzur, A. Giveon, M. Porrati and E. Rabinovici, JHEP **0602** (2006) 006 [arXiv:hep-th/0511061].
- [45] T. Banks and W. Fischler, arXiv:hep-th/0606260.
- [46] S. R. Coleman and E. Weinberg, Phys. Rev. D **7** (1973) 1888.
- [47] M. Banados, A. Schwimmer and S. Theisen, JHEP **0609**, 058 (2006) [arXiv:hep-th/0604165].
- [48] J. Polchinski, L. Susskind and N. Toumbas, Phys. Rev. D **60**, 084006 (1999) [arXiv:hep-th/9903228].
- [49] L. Susskind and E. Witten, arXiv:hep-th/9805114.
- [50] M. Reed and B. Simon, “Methods Of Modern Mathematical Physics. 2. Fourier Analysis, Selfadjointness,” *New York 1975, 361p*
- [51] M. Carreau, E. Fahri, S. Gutmann, P. F. Mende, Ann. Phys. **204** (1990) 186.
- [52] S. Fredenhagen and V. Schomerus, JHEP **0312** (2003) 003 [arXiv:hep-th/0308205].
- [53] C. M. Bender and S. Boettcher, Phys. Rev. Lett. **80**, 5243 (1998) [arXiv:physics/9712001]; C. M. Bender, D. C. Brody and H. F. Jones, eConf **C0306234**, 617 (2003) [Phys. Rev. Lett. **89**, 270401 (2002 ERRAT,92,119902.2004)] [arXiv:quant-ph/0208076].
- [54] L.D. Fadeev and A.A. Slavnov, *Gauge Fields, Introduction to Quantum Theory*, Frontiers in Physics Lecture Notes Series 50, Benjamin Cummings, 1980.
- [55] B. Ratra, Phys. Rev. D **31**, 1931 (1985).
- [56] R. D. Ball, Phys. Rept. **182**, 1 (1989).
- [57] A. J. Tolley and N. Turok, Phys. Rev. D **66**, 106005 (2002) [arXiv:hep-th/0204091].
- [58] I. S. Gradshteyn and I. M. Ryzhik, “Table of Integrals, Series, and Products”, Academic Press, 1994.

- [59] S. R. Coleman and R. Jackiw, *Annals Phys.* **67**, 552 (1971).
- [60] A. Hamilton, D. Kabat, G. Lifschytz and D. A. Lowe, *Phys. Rev. D* **74** (2006) 066009 [arXiv:hep-th/0606141].
- [61] M. E. Peskin and D. V. Schroeder, “An Introduction To Quantum Field Theory,” *Reading, USA: Addison-Wesley (1995) 842 p*
- [62] E. J. Weinberg and A. q. Wu, *Phys. Rev. D* **36** (1987) 2474.